การพัฒนาอุปกรณ์ของไหลจุลภาคชนิดบีบและขยายสำหรับการตรวจจับไมโครฟิลาเรียในเลือด

นายศักดิ์ทิพย์ อู่ทองทรัพย์

วิทยานิพนธ์นี้เป็นส่วนหนึ่งของการศึกษาตามหลักสูตรปริญญาวิศวกรรมศาสตรมหาบัณฑิต
สาขาวิชาวิศวกรรมเครื่องกล ภาควิชาวิศวกรรมเครื่องกล
คณะวิศวกรรมศาสตร์ จุฬาลงกรณ์มหาวิทยาลัย
ปีการศึกษา 2559

A Development of Contraction-Expansion Microfluidic Device for Detecting Microfilaria in Blood

Mr. Saktip Uthongsap

A Thesis Submitted in Partial Fulfillment of the Requirements
for the Degree of Master of Engineering Program in Mechanical Engineering
Department of Mechanical Engineering
Faculty of Engineering
Chulalongkorn University
Academic Year 2016

Thesis Title	A Development of Contraction-Expansion Microfluidic Device for Detecting Microfilaria in Blood
By	Mr. Saktip Uthongsap
Field of Study	Mechanical Engineering
Thesis Advisor	Assistant Professor Alongkorn Pimpin, Ph.D.
Thesis Co-Advisor	Prapruddee Piyaviriyakul, Ph.D.
	Wutthinan Jeamsaksiri, Ph.D.

Accepted by the Faculty of Engineering, Chulalongkorn University in Partial Fulfillment of the Requirements for the Master's Degree

.....Dean of the Faculty of Engineering
(Associate Professor Supot Teachavorasinskun, Ph.D.)

THESIS COMMITTEE

.....Chairman
(Assistant Professor Werayut Srituravanich, Ph.D.)

.....Thesis Advisor
(Assistant Professor Alongkorn Pimpin, Ph.D.)

.....Thesis Co-Advisor
(Prapruddee Piyaviriyakul, Ph.D.)

.....Thesis Co-Advisor
(Wutthinan Jeamsaksiri, Ph.D.)

.....Examiner
(Saran Salakij, Ph.D.)

.....External Examiner
(Mayuree Chanasakulniyom, Ph.D.)

ศักดิ์ทิพย์ อู่ทองทรัพย์ : การพัฒนาอุปกรณ์ของไหลจุลภาคชนิดบีบและขยายสำหรับการตรวจจับไมโครฟิลาเรียในเลือด (A Development of Contraction-Expansion Microfluidic Device for Detecting Microfilaria in Blood) อ.ที่ปรึกษาวิทยานิพนธ์หลัก: ผศ. ดร. อลงกรณ์ พิมพ์พิณ, อ.ที่ปรึกษาวิทยานิพนธ์ร่วม: อ. น.สพ ดร. ประพฤติดี ปิยะวิริยะกุล, ดร. วุฒินันท์ เจียมศักดิ์ศิริ, 99 หน้า.

งานวิจัยนี้มีวัตถุประสงค์เพื่อพัฒนาวิธีการตรวจไมโครฟิลาเรียในเลือดโดยอาศัยช่องทางการไหลขนาดจุลภาค ที่มีลักษณะช่องทางการไหลเพื่อทำการกรอง (Filter) ในเลือดตัวอย่าง จากการทดลองเบื้องต้นพบว่า ปัญหาหลักในการนำชิปไปใช้งาน คือเม็ดเลือดแดงมีจำนวนมาก ส่งผลให้ชิปอุดตันและไม่สามารถมองเห็นไมโครฟิลาเรีย ในส่วนของการวิจัยนี้ได้เลือกนำช่องทางการไหลแบบบีบและขยายมาใช้ในการแก้ปัญหาดังกล่าว ท่อเส้นทางการไหลทั้งหมดมีความลึก 60 ไมโครเมตร โดยมีเส้นทางการไหลชนิดบีบมีความกว้าง 50 ไมโครเมตร ในส่วนที่เป็นท่อขยาย ได้ถูกออกแบบเป็นสองลักษณะคือมีความกว้าง 550 ไมโครเมตร และยาว 500 ไมโครเมตร และมีความกว้าง 550 ไมโครเมตร และยาว 1000 ไมโครเมตร ในแต่ละชิปมีส่วนท่อแบบขยายสามชุดต่ออนุกรมกัน การทดลองเพื่อหาสมรรถนะของชิปทำโดยใช้เม็ดพลาสติกขนาด 5, 10, 15 และ 20 ไมโครเมตร โดยทำการทดลองที่เลขเรย์โนลด์ การไหลในท่อ 5 ค่า คือ 40, 60, 80, 100 และ 120 หลังจากนั้นจึงทำการทดลองโดยใช้เลือดสุนัขที่ผสมกับน้ำเกลือเพื่อหาประสิทธิภาพการแยกไมโครฟิลาเรียของชิป โดยพบว่าชิปสามารถแยก ไมโครฟิลาเรียออกจากเลือดในส่วนของช่องทางการไหลหลักได้ถึง 100 เปอร์เซ็นต์ และไม่พบไมโครฟิลาเรียในส่วนของช่องทางการไหลแยกเลย

ภาควิชา วิศวกรรมเครื่องกล	ลายมือชื่อนิสิต .....
สาขาวิชา วิศวกรรมเครื่องกล	ลายมือชื่อ อ.ที่ปรึกษาหลัก .....
ปีการศึกษา 2559	ลายมือชื่อ อ.ที่ปรึกษาร่วม .....
	ลายมือชื่อ อ.ที่ปรึกษาร่วม .....

5770308921 : MAJOR MECHANICAL ENGINEERING
KEYWORDS: MICROFILARIA / MICROFLUIDIC CHIP / CONTRACTION AND EXPANSION ARRAYS / LAB ON A CHIP

SAKTIP UTHONGSAP: A Development of Contraction-Expansion Microfluidic Device for Detecting Microfilaria in Blood. ADVISOR: ASST. PROF. ALONGKORN PIMPIN, Ph.D., CO-ADVISOR: PRAPRUDDEE PIYAVIRIYAKUL, Ph.D., WUTTHINAN JEAMSAKSIRI, Ph.D., 99 pp.

The objective of this research is to detect the microfilariae in blood by using filtration microfluidic chip. From the preliminary experiment, the main problem is the concentration of red blood cells. These red blood cells clogged and blocked the microfilariae from the observation. In this part of the research, contraction and expansion array was chosen to solve the stated problem. The channel in the chip is 60 μm. The width of contraction and expansion channel is 50 μm. For the length of expansion chambers, there are 500 and 1,000 μm. In each chip, the expansions were connected in series. The experiments were done to determine the efficiency by using polystyrene beads with 4 sizes; 5, 10, 15, and 20 μm. The Reynolds number of 40, 60, 80, 100, and 120 were selected for the experiments. Afterward, the whole blood of the dog together with normal saline solution was injected to determine the separation efficiency of the microfilaria of the chip. The chip could separate 100% of microfilariae to the main outlet.

Department:	Mechanical Engineering	Student's Signature	.....
Field of Study:	Mechanical Engineering	Advisor's Signature	.....
Academic Year:	2016	Co-Advisor's Signature	.....
		Co-Advisor's Signature	.....

ACKNOWLEDGEMENTS

This work has received financial support from Chulalongkorn University through Chulalongkorn Acadamic Advancement into its 2nd century project (Smart Medical Device).

This thesis cannot be accomplished without these people. First I would like to thank Asst. Prof. Alongkorn Pimpin who is the advisor of this thesis, not only provided helpful information in this research, but also cheered me up, when there were troubles during the researching period.

I would like to my gratitude to Asst. Prof. Werayut Srituravanich, who gave useful advises during the meeting sessions.

I would like to express my gratitude toward Dr. Prapruddee Piyaviriyakul and Mrs. Sariya Asawakarn who helped me with biological sample and knowledge. They provided microfilaria in blood sample during the time that the sample was hard to find

I would like to express my gratitude toward the thesis committee that tried to solve the problem that I may not understand clearly. They use their insight in their work field or experience. Their ideas helped me to see the solution of the problem that I faced.

I would like to express my gratitude toward Dr. Wutthinan Jeamsaksiri and Mr. Witsaroot Sripumkhai from Thai Microelectronics Center (TMEC) who manufactured the chip in this research.

Lastly, I would like to thank my friends, lab-mates, and my family who always support and inspire me not only for the research problems, but also other life problems too. Without these people I would not be able to complete this thesis.

Thank you.

CONTENTS

Page

Page

LIST OF FIGURE

LIST OF TABLE

Chapter 1
Introduction

1.1 Background and Statement

Parasite is living creature that lives inside the host. Some of them just live and take the food from the host, but some are also toxic to the host. Most of the parasite's life cycles are relied on a mosquito. Thus, these parasites are quit hard to control and eliminate. Moreover, the rising of the temperature of the earth benefits the parasites, because the growth rate mainly depends on the atmospheric temperature [1, 2]. *Dirofilaria immitis* (heartworm) lives in canine and feline, such as dog, cat, and human. When they are fully grown, heartworm dwells in the heart of host. These parasites breed out a larvae called microfilariae and use mosquito as a vector and incubator during their larvae and microfilariae life-cycles. This makes *D.immitis* a bloodborne disease. Therefore, dogs and cats are wildly infected. This infection does not just affect to the animals healthiness but it could also kill them too. Occasionally, human would get infected by *Dirofilaria immitis.* This worm may not end up in a heart or lung, but it penetrates where else such as brain, skin, eye, and other organs. Treatment of this certain infections is to surgically remove worm adult, where they located. However, microfilaria cannot grow inside human blood, Therefore, heartworm cannot be transmitted person-to-person [3, 4].

These worm were usually growth well in warmer climate. Since the global temperature is rising, the higher temperature shorten the time developing from larva to adult. Therefore, the diseases are found more frequently and broadly than it used to be few decades ago [5].

Nowadays, there are two main heartworm disease detection methods. The first one is by detecting the appearance of adult worm itself such as, physical test, x-ray, antigen test (female worm), and antibody test (male worm). The second method is by detecting microfilariae such as a blood smear test [6] .

However, there are some limitations in using the above techniques. Lately, the microfluidic chips were introduced in biomedical work. By using microfluidic chip to separate other blood components and microfilaria, this not only would promote an easier way to diagnose but also reduce a fault detection from conventional smear method. The technique of microfluidic separation depends on the shape of micro channel. Contraction-expansion array is one of the designs that can sort the particles, based on sizes of the particles in the channel without the requirement of external forces [7].

Other than heartworm disease, there is a lot of parasites and cells, such as tumor cell, that people try to diagnose using microfluidic method. Moreover, there are

numbers of research that not only studied about identifying the parasite, but also tested the chemical or physical properties of them [7-18].

1.2 Motivation

The detection method used nowadays takes long time to examine and depends on many laboratory equipments and specialists. Hence, detecting the dirofilariasis in rural area has been done with difficulty. Providing a laboratory-tools-free method, this should contribute a convenient and mobile method. The less the time used in detecting and analyzing, the more cases detected in a certain time resulting in saving more lives and preventing a further infection.

Even though, the simplest design like filtration can diagnose this microfilaria, but there is a main problem to be solved. The density of red blood cell is primary a concern. If this problem is fixed, the amount of red blood cells entering filter would be decreased and the efficiency of the filter would be promoted.

1.3 Objective and Scope of the research

To design and develop the microfluidic chip using contraction-expansion technique to separate *Dirofilaria immitis* from the blood. The scopes of this research are the following.

1.3.1 To determine the cut-off diameter of the particles those are separated by fabricated channels.
1.3.2 To study the possibility to use contraction-expansion array technique to separate non-spherical and motile organism.

1.4 Research protocols

1.4.1 Review about the designs and mechanisms of microchannel that were used to separate by size-based technique.
1.4.2 Develop the design that is possible to separate the worm from the other blood components.
1.4.3 Experiment on polystyrene beads to determine the cut-off diameter of particles at different Reynolds numbers of the flow.
1.4.4 Experiment on the whole blood sample at selected conditions.
1.4.5 Conclude and discuss on the results.

1.5 Expected benefits

This technique, filtering with a microfluidic chip, does not only provide a detectable method but also the stage of disease, which would be easier than the conventional one for veterinary to decide what diagnostic technique would be used to cure.

Chapter 2
Literature review

2.1 Dirofilaria

Dirofilaria, parasite lives in canine and human, is roundworm genus in Nematoda phylum. One of them is *Dirofilaria immitis*, the cause of heartworm disease. Since the worms have killed numbers of dogs and cats, the attention was extremely risen. *Dirofilaria immitis* usually lives at Pulmonary artery, the vessel delivers blood from heart to lungs, or at right ventricle, bottom right room of the heart in canine, but lives in lungs in human. By using a mosquito as a vertebral host, the parasite can spread wildly throughout the region [2, 5, 19].

2.1.1 Symptom

Dirofilaria immitis is non-toxic parasite even though it is still lethal to the host. Normally, adult worms form a colony, and elongate entire life which can end up to 310 millimeters. With that length, the worm reduces the vessel flow area, going to lungs. Then, heart works harder than usual to deliver the same amount of blood. Consequently, the host will be weak, faint, pant, and even dead, from lacking of oxygen in blood. Even if the heart can pump the blood the same amount as it should, host is risk to get a heart attack or heart failure [3, 20, 21].

2.1.2 Life cycle

Typically, adult worms, live in heart, breed and release microorganism called microfilariae. The larvae flow in blood circulation system waiting a vector, mosquito, to pick up. After they got inside the mosquito, microfilariae relocate from mosquito's midgut pass by hemocoel to Malpighian tubules. In the position for 2 weeks, microfilariae develop two stages from Larvae 1 (L1) to Larvae 3 (L3), infective stage larvae. While mosquito bites the host, any canine or human, L3 infiltrate through the wound and embed in subcutaneous tissue nearby the cut. Three to four days after the infection, L3 mold to L4 then travel to its position, heart. The traveling takes 2-3 months and stops when the worms reach to heart as adults. Three to four months onward, the worms produce another generation of microfilaria, which can live up to 3 years in blood of a living dog. Moreover, the growth rate of larvae in mosquito depends on atmospheric temperature such as, at 27˚C the rate is very fast but there is no development below 14˚C. Normally, female worm can reproduce microfilariae entire life and also be able to live up to 7 years in a dog, and 2-3 years in a cat. Occasionally,

adult worm ends up at eye, brain, and abdominal cavity instead of heart. The life cycle is shown in Figure 1 [2].

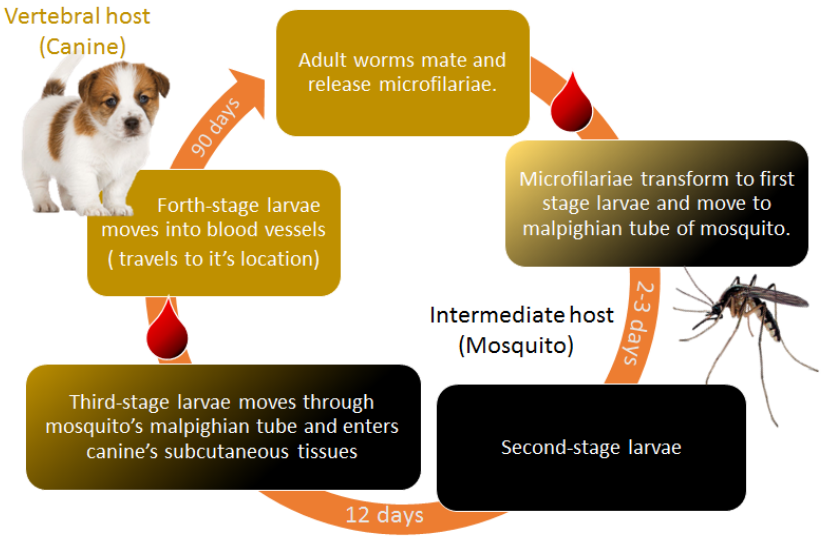

Figure 1 Dirofilaria immitis's life cycle

2.1.3 Morphology of microfilariae

Magnis et al. measured the size of microfilaria of *D. immitis* in 2013 [22]. The result shows that *D.immitis* has 301.77 ± 6.29 µm in length and 6.30 ± 0.26 µm in width. Naturally blood contains red blood cell, white blood cell, platelet and liquid called plasma. Red blood cell has 6-8 µm of diameter. On the other hand, white blood can categorized into many types and the sizes vary from 10-15 µm. In conclusion microfilaria is obviously longer than every blood component. However, the diameter of microfilaria is close to the red blood cell as shown in Figure 2.

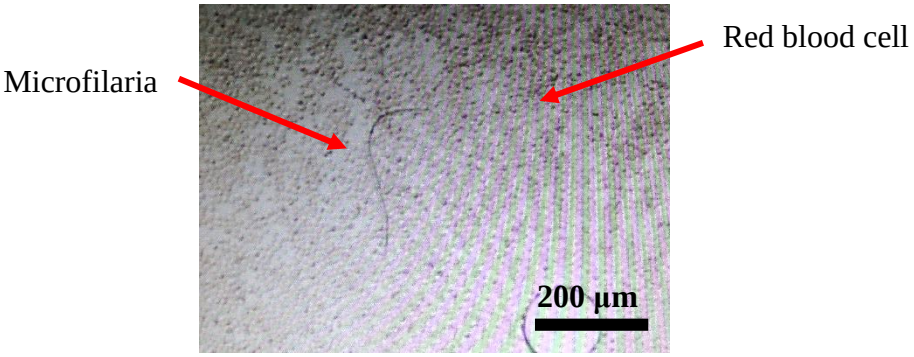

Figure 2 Microfilaria in blood

2.1.4 Detection method

Since this nematode can kill dogs and cats, Dirofilaria needs to be identified to help preventing a further spreading. Detecting the existence of Dirofilaria can be done in three main way; symptom of infection, adult detection, and Microfilariae detection.

Symptom of infection can be observed by physical test. As the indicated symptom in dog can be separated in to three classes, which are class I, asymptomatic; class II, coughing and unusually easily exhausting; class III, anemia, fainting, drained out, and heart failure. In human, the disease tends not to show any identifiable condition. On the other hand, cat shows several conditions that affect with respiratory system more than heart, such as coughing, difficulty to breath, weight loss, vomiting, fainting, and sudden death.

Adult worm lives in a heart. By this reason, detecting the worm can be done by x-ray, angiography or ultrasonography at right ventricle, and antibody.

Lastly, microfilaria can be found in blood of both cats and dogs. There are numbers of traces in blood to be tested, i.e. antigen test, flesh blood smear, modified Knott's test, physically filtration, and so on [6].

2.2 Microfluidic Chip

Nowadays, microfluidic chip has been used for several applications, trapping, detecting, and sorting. These operations can be done by both active and passive way. Active one is the name for techniques, which use field of external force to control particles inside the chip, Dielectrophoresis (Electrical), Magnetophoresis (Magnetic), Acoustophoresis (Sound wave), as only three to be named. Passive one is another way round, this technique uses different designs to control the flow of fluid inside, namely hydrophoresis (Filter), inertial focusing and vortex [7].

The project's target is to create a chip that can be used in rural area, remotely locate far away from laboratory equipment. High throughput is also required. For all the reasons indicated above, passive control is more suitable than the active one.

Passive control of microfluidic provides a various useful purposes. Elizabeth Hulme et al. (2007) successfully trapped *C.elegans* worm for morphological study [23]. By using an array of square cross-sectional area with wedge-shape channel, from 100 μm to 10 μm wide over 5 mm long. In this experiment, they used constant pressure across inlet and outlet, to prevent any damage that may cause to either the chip or the worm. After the injection of worm into the bifurcation worm-trap chip, they found that more than 90% of the channel could trap a single worm with a 100% of the worm is still alive. Moreover, this filtration had no effect on the worm behavior. The passages are shown in Figure 3.

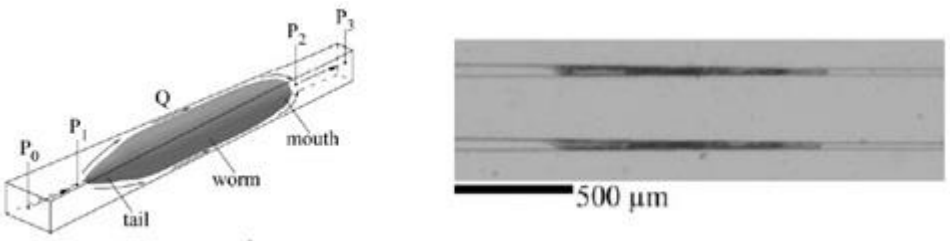

Figure 3 *C.elegans* trap schematic (left) and photo (right) [23]

Beside physical analysis, the worm trapping devices are also used in chemical response too. In 2011, Jinjing Wang et al. tested a neuronal activity upon dynamic chemical stimulation in microfluidic chip [24]. The trapping zone has a shape of comb that can control the flow of main stream to flow back and forth until the target worm is in the focusing zone, which is in between the legs of the comb as shown in Figure 4.

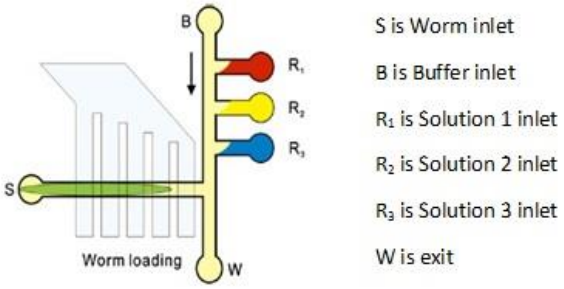

Figure 4 Nematode trapping comb [25]

In 2013, Navid Ghorashian, et al. fabricated a microfluidic chip that could transfer *C.elegans* from 16 reservoirs to the outlet [25]. These wells were controlled by 12 valves. The flow was restricted by main channel flush inlet. From this design, they reported 90% of worm population was transferred from the well within 4.7 seconds. Moreover, they claimed that the chip reduced the bubble problem from the conventional sample switching method. The chip layout is shown in Figure 5.

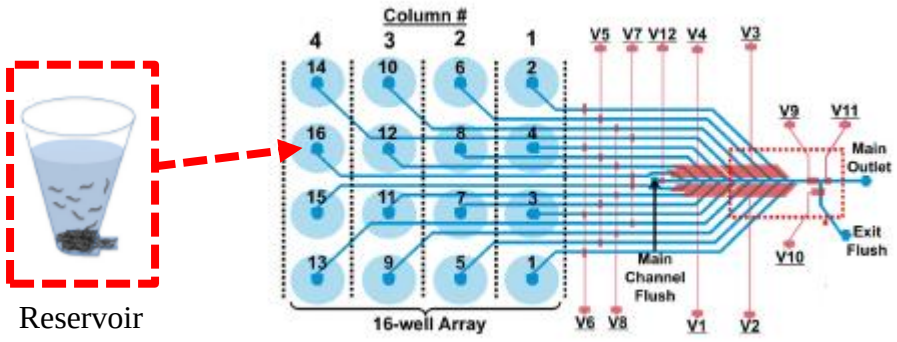

Figure 5 Multiplexer for fast delivery C.elegans from multi wells [24]

In 2015, Do-Hyun Lee et al. introduced microfluidic chip integrating filter and micro well to separate Hela (25 μm cell), 15 μm, and 5 μm microparticle [26]. The chip schematic is shown in Figure 6. They flowed the sample twice, forwardly and backwardly, in order to discrete the particle by the size. Fluid and particles experienced the first filter, 18 μm width channel, which held 25 μm cell. Then, particles which remained were strained by 7 μm gap divided 15 μm and 5 μm. After that, they flowed the fluid backwardly to release the filtered microparticles, 25 and 15 μm. From the design of the channel 25 μm particle was drawn out by the inlet channel, but 15 μm particle were moved to micro-well-channel and trapped individually.

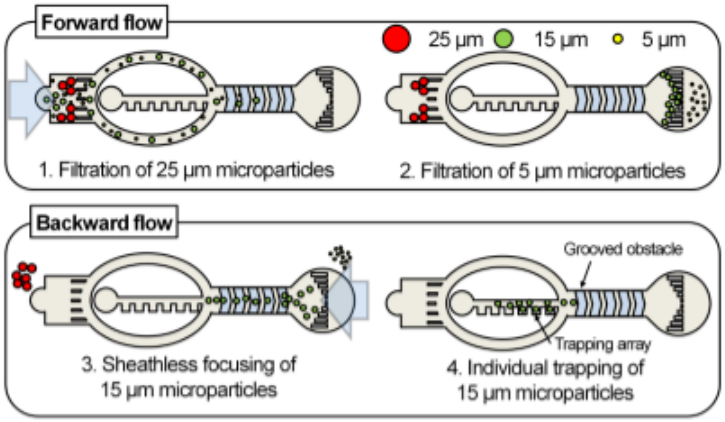

Figure 6 Do-Hyun Lee et al. chip integrating filter and micro well [26]

In 2016, Y. Xiao et al. designed and experimented the chip that was used to detect Schistosomiasis in urine [8]. The chip layout is shown in the Figure 7. They used syringe to drawn out the sample from the chip. The inlet of the chip was connected to the urine reservoir. This chip contains fifteen 25 μm channels in the middle of reservoir and outlet containing the egg of the parasite. The chip gave out 100% efficiency at 300 μl/min and 83% at 3000 μl/min.

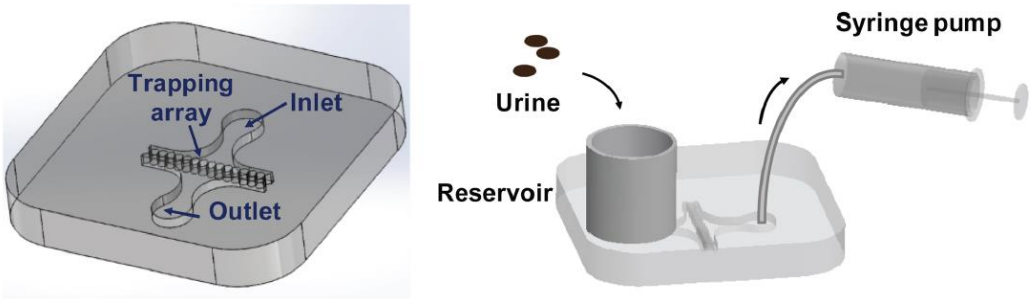

Figure 7 Urogenital filtration chip [7]

2.2.1 Filtration using microcapillary

In 2014, Jingdong Chen et al. separated plasma from red blood cell [27]. They tested 2 designs, straight line filter and square wave structure filter. They found that the chip gave out the better efficiency with grater dilution ratio and smaller filter gap. For straight line filter, they reported the lowest efficiency of filtration is 20% at lowest dilution ratio, 10 times, with biggest gap of the filter, 2 μm. However, they achieved 100% of separation at 20 dilution ratio and 1 μm gap. The structure of the chips is shown in the Figure 8.

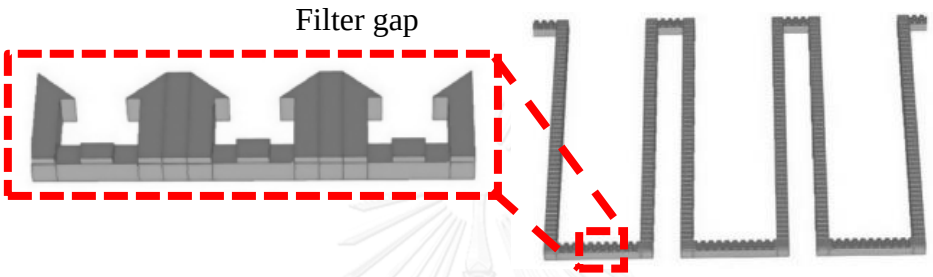

Figure 8 Straight line filter (left) and square wave structure filter (right) [27]

One of the nematode microfluidic filter, shown in Figure 9, has been introduced by Andras J. Laki' et al. (2013). They uses *D. repens*, which is 369.44 ± 10.76 μm length and 8.87 ±0.58 μm width, as a tested subject [28]. They constructed the chips with a wall of twelve different sizes of micro capillary and also varied three flow rates, 0.25, 0.5, and 1.0 ml/h. The efficiency and inhomogeneity are calculated in the function of micro capillary sizes.

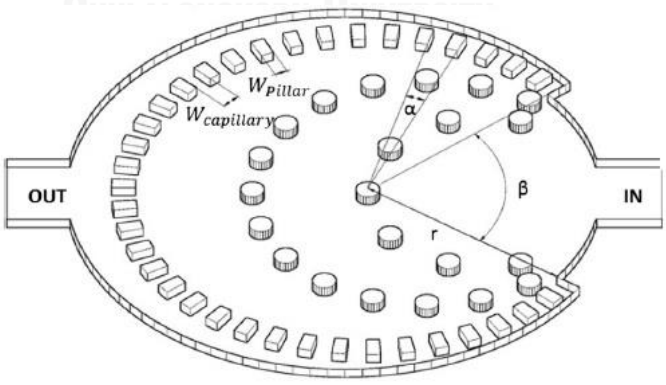

Figure 9 A.J. Laki et al.'s nematode filter [28]

The chip's channel, 20 μm high, contained one inlet and one outlet, which is 400 μm wide. The filtration zone was shaped as cylindrical with 1 mm of diameter. The sizes of micro capillaries are 6.1, 6.8, 7.6, 8.4, 9.2, 10, 10.8, 11.7, 12.6, 13.5, 14.4, and 15.4 μm.

Experimental procedures were divided into five steps. Firstly, they counted number of nematode larvae in the solution (σ_{pre}). Secondly, serological solution was injected into the chip with constant flow rate. Thirdly, deionized water was pumped to hemorrhage the left over red blood cell and to flush it through micro capillaries, which helped to clarify the held microfilariae. Fourthly, they counted the nematode inside the chip ($\sigma_{capture}$). Finally, the number of microfilariae were counted (σ_{post}).

Efficiency of the chip was defined as the number of captured microfilariae divided by the post and captured microfilariae as in Equation 2.1

$$\eta = \frac{\sigma_{capture}}{\sigma_{post} + \sigma_{capture}} \quad (2.1)$$

Inhomogeneity, as expressed in Equation 2.2, is occurred from sedimentation in blood during the experiment, which was described as the different between actual pre-experiment microfilariae and number of overall microfilariae that passed through the chip over an actual pre-experiment microfilariae.

$$IH = \frac{|\sigma_{pre} - (\sigma_{capture} + \sigma_{post})|}{\sigma_{pre}} \quad (2.2)$$

The maximum average efficiency of 1 ml/h is 28% at 6.8 μm, and average inhomogeneity is 3.5%. At 0.5 ml/h, the most effective size is 6.1 μm 56% efficiency with 10.5% inhomogeneity. When the pump was fixed at 0.25 ml/h, the maximum is still at 6.1 μm but the efficiency dropped to 45% together with the variation of inhomogeneity in range of 65-80% depend on capillary width.

In conclusion, the experiments illustrate the relationship between capillary width and efficiency by varying flow rate. The higher flow rate used, the lower efficiency. On the other hand, the inhomogeneity is increased while decreasing the flow rate. The size of micro capillary that gives the relatively high output is smaller than the diameter of microfilaria [28, 29].

Another filter technique was introduced by Sung-Woo Lee et al [30]. Their Filter bend around the inlet channel. They tested on tumor cell and blood cell in whole blood. This channel provided a longer filtration zone. The result showed that they can separate 95% efficiency with 99% purity with 10 μm gap. The chip flow channel is shown in Figure 10.

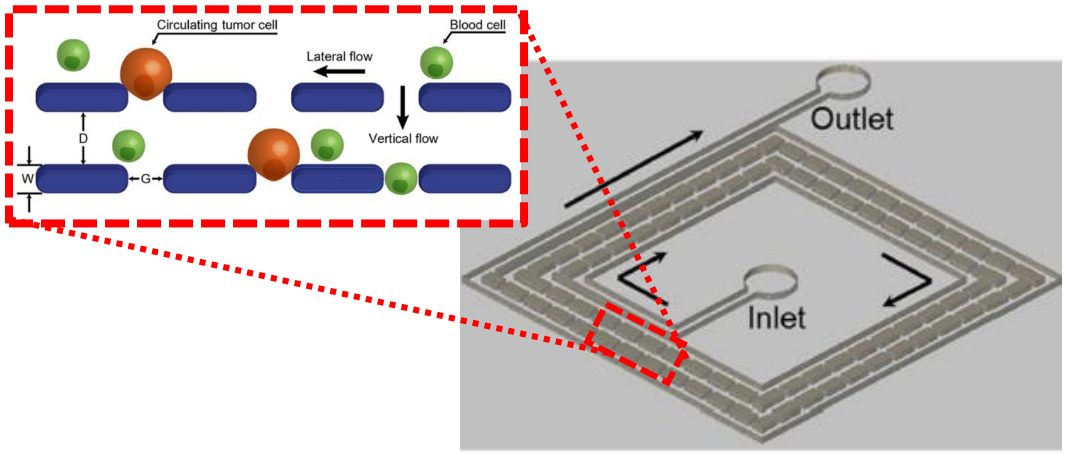

Figure 10 Lateral flow filtration chip [30]

2.2.2 Contraction-Expansion Channel

Contraction and expansion channel, which uses the change of cross sectional area, is the new idea to either trap or sort the particles based on size of the particles. In the flow, there are three forces acting on the particles, which are wall interaction, velocity shear gradient lift, and Dean Drag force [7, 31, 32].

From no-slip condition, fluid's velocity has a shape of parabola, the vertex point at the middle of the channel. For a particle suspended in flowing fluid, velocity of particle is usually not equal to the fluid. Therefore, the relative velocity between the particle and fluid on both sides of particle is not the same. This phenomenon causes the pressure difference, at which the surface on near wall side, the particles experience a higher pressure than another side. From this difference, the particle is lifted away from the wall. This lift force is called wall interaction force (F_W) as stated in Equation 2.3.

$$F_W = C_W \rho V_m^2 \frac{a^6}{D_h^4} \quad (2.3)$$

Velocity shear gradient is a result of curved profile of fluid. Relative velocity between fluid and particle at the position near to the center of the channel is in the direction of a flow, but the direction of the relative velocity near the wall is backward relatively to the flow. By that effect, the fluid generates force, pushing the particle toward the wall (F_L) as shown in Equation 2.4.

$$F_L = C_L \rho V_m^2 \frac{a^3}{D_h} \quad (2.4)$$

From the higher magnitude of velocity shear lift gradient, the equilibrium position in straight channel is located at the middle of each of the side wall as shown in Figure 11. By balancing the lift force and stroke drag, horizontal distance of the particle that moves into the equilibrium position can be determined as the Equation 2.5. It needs to be noted those this two forces are hard to compare, because it is complexly coupled. In laminar flow, the lift coefficient (C_L) is usually equal to 0.5. However, the equations are derived by Asmolov and simplified by Di Carlo [33], as shown in the Equation 2.6 [34].

$$F_L = \frac{\rho V_m^2 a^4}{D_h^2} C_L(Re_C, x_C) \quad (2.5)$$

$$L_{min} = \frac{D_h}{2V_L} V_m = \frac{3\pi\mu D_h^3}{\rho V_m a^3} \quad (2.6)$$

In the contraction area, there is a secondary flow, the flow of fluid in another direction beside the direction of main flow, which generates drag force called Dean Drag force. This force relocates the particle from the original equilibrium position, the position that particles in flow will locate in a steady flow. Dean Drag force magnitude is shown in Equation 2.7.

$$F_D = 3 \pi \mu a (V_{FSF} - V_{PSF}) \quad (2.7)$$

The parameters in Equation 2.3-2.7 are as follows.

F_W	=	Wall interaction force
F_L	=	Velocity shear gradient lift force
F_D	=	Dean Drag force
C_W	=	Lift coefficient of wall interaction
C_L	=	Lift coefficient of velocity shear gradient lift
ρ	=	Density of fluid
μ	=	Fluid viscosity
a	=	Particle diameter
D_h	=	Hydraulic diameter
V_{PSF}	=	Secondary flow velocity of particle
V_{FSF}	=	Secondary flow velocity of fluid
V_m	=	Maximum velocity

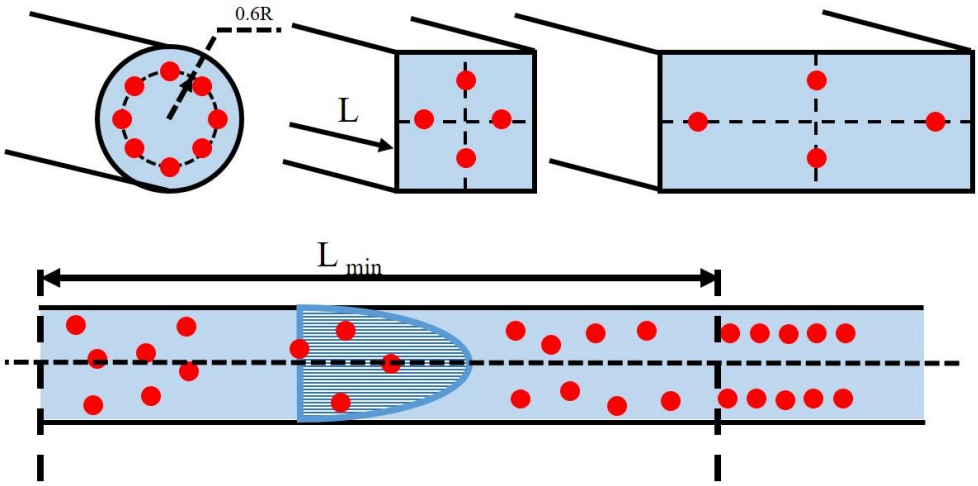

Figure 11 Equilibrium position in channel

In filtration purpose, S. C. Hur et al. (2010) did the experiment of trapping particles with different sizes such as 1 μm, 4.8 μm, and 9.9 μm [33]. From the indicated forces, wall interaction and velocity shear gradient lift force act on the same particle. From Equation 2.8, the magnitude of velocity shear gradient lift is obviously bigger than the wall interaction. With this different, the particles will be pushed to the side of the wall, where the equilibrium positions are. When the flow reaches the expansion area, wall effect is vanished, only velocity shear gradient lift is still acting on the particle. The position of particle in the channel is changed creating a vortex trapping particles that has a diameter bigger than the critical diameter (D_C). The critical diameter is the diameter that separate the particle that which one will flow with the fluid and which one will stuck in the vortex.

By dividing Equation 2.4 with 2.3 (assuming C_L and C_W are equals), the result is

$$\frac{F_L}{F_W} = \frac{W^3}{a^3} \tag{2.8}$$

$$Re_C = \frac{\rho V_m D_h}{\mu}$$

$$Re_P = Re_C \frac{a^2}{D_h^2}$$

where Re_C = Reynolds number of flow
Re_P = Reynolds number of particle

From the experiments, vortex occurs when the Reynolds based on the channel size (Re_c) is equal to 21 and fully developed at 215. At Reynolds number of 215, particles with 1 and 5 μm pass through the expansion area without diffusing out to the

vortex. On the other hand, particles with 10 μm are trapped in the chamber of expansion area. A further experiment was taken, they found that 10 μm particles are trapped when the flow is between the Reynolds numbers of 130 – 240.5, but if the Reynolds number exceeds that range the particle will remain in the flow. It is needed to be noted that for the same diameter of living cell and particle, the D_C should be different causing by the deformability and interaction of cells.

In 2013, J. Zhang et al. used an asymmetrical CEA to sort particles [35]. The expansion chamber is designed into three types, right triangle 45˚ to the chamber, half circle, and dimension. The experiment was done by varying the flow rate between 50 – 700 μm/min. By various flow rate, the flow can be divided into three types, single focusing streak, double focusing streak, and half of the particles focused (vortex), which is preferred in this project. Half of the particles focused creates pattern that contains some particles inside of an expansion area, and can be used as a type of filter.

Each particle has its own equilibrium position. At first, flow in the channel experiences the expansion. In this stage, there is nothing particularly happening inside the flow. When the flow reaches the contraction area, a secondary flow is generated by the fluid particle that force to flow in a smaller channel. At the side wall, near contraction, direction of Dean Drag and velocity shear gradient lift force are opposite to one another. The magnitude of those two forces depend on both the cross sectional position and particle size. This differences result in separation of focusing stream. If Dean Drag beats the velocity shear gradient lift, there is no focusing; the particle circulate as same as the fluid in the cross sectional area. On the contrary, the focusing will take place, if the velocity shear gradient lift force is stronger than Dean Drag force. The higher Reynolds number the flow is, the more obvious the separation will be. Until the Reynolds number is high enough, the particle will be trapped by the vortex in the expansion. Nevertheless, if the Reynolds number of flow is too high, particle moves too fast, the fluid will take all the particle without expanding into an expansion channel. The patterns of focusing from the experiment are shown in Table 1.

Table 1 Reynolds number that gives each type of expansion cavity the pattern [14]

Pattern / Expansion type	Channel Reynolds number range		
	Single focusing	Double focusing	Vortex focusing
Square triangle	0 – 208	208– 249	Re > 249
Half circle	0 – 166	166 – 208	Re > 208
Diamond	0 – 83	83– 124	Re > 124

Xiao Wang, Jian Zhou, and Ian Papautsky approached contraction-expansion arrays in a new way [36]. They presented about the effect of the dimension of the channels on separating condition. They distinguished the flow into 3 parts such as main flow, sheath flow, and vortex, as shown in Figure 12a. There are 3 parameters indicating

the separation of the particles. The first one is a distance from equilibrium position and wall (d_p). This distance mainly depends on the size of the particle, the bigger it gets the further it will be from the wall. The second parameter is a distance from the point that start to separate from the main flow (sheath d_b). The final one is defined as a distance traveled by the particle from the equilibrium position to the expansion ($d_m = d_p - d_b$). If d_m is too far, the particle will not be able to move to the sheath flow. The point that starts to separate to the sheath flow (d_b) depends on Reynolds number of the main channel. They experimented d_b by varying the Reynolds number of the flow as shown in Figure 12b. Nonetheless, d_p is not only based on the size of the particle but also the Reynolds number of the flow too. Therefore, each d_p must be obtained only by experiment. The Figure 12c shows the relationship of the Reynolds number of the flow on d_p.

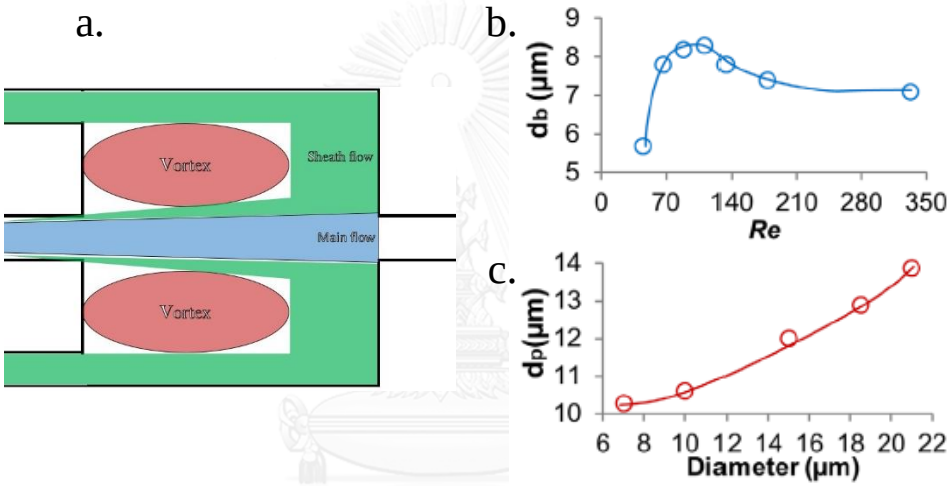

Figure 12 (a) Section of the flow in an expansion unit, (b) relationship between d_b and Reynolds number of the flow, and (c) relationship between d_p and diameter of the particle [36]

In 2015, Xiao Wang fabricated an array of expansions unit as shown in Figure 13 [37]. In the chip, the second inlet of the expansion unit contains a lower flow rate than the first expansion. They investigated the separation diameter (cut-off diameter) of each unit. The results are shown in Table 2.

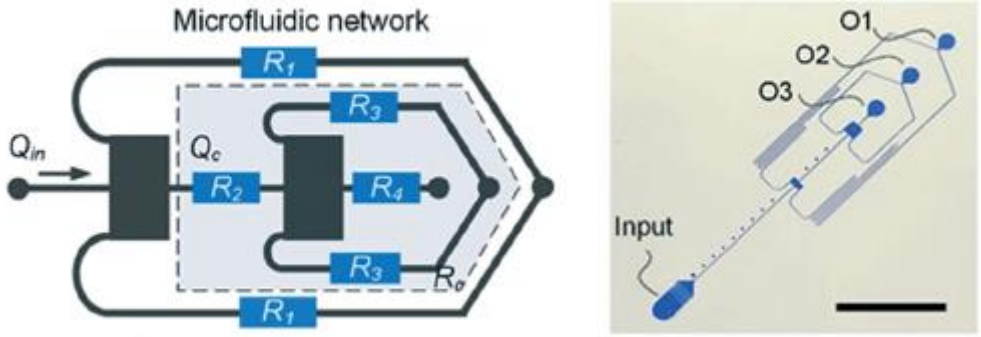

Figure 13 Multimodal micro particle sorter [37]

Table 2 Result of Multimodal microparticle sorter

Qin [ml/min]	R1/Rc	Cut-off diameter [μm]	Qc [ml/min]	R3/R4	Cut-off diameter [μm]
0.525	4	> 20	0.35	4.9	15 - 18.5
0.525	5.5	> 21	0.385	11	20
0.500	5.5	> 24	0.37	11	21

In 2016, X.Wang and I.Papautsky reported that they were successfully separated particles with three different sizes, RBC, 18 μm bead, and 23 μm bead, from each other [38, 39]. They fabricated contraction and expansion channel chip which its contraction channel is 50 μm wide and 70 μm tall. There are two identical expansion channels which are 500 μm wide, 500 μm long, and 70 μm tall as shown in Figure 14. The secondary outlet resistances are 14 and 10 times higher than the main outlet in the first and second chamber, respectively. At the beginning, the whole solution, containing all three sizes particles, was flown at 190 μL/min (Re = 53.4). The first expansion chamber separates RBC away from 18 and 23 μm beads by letting RBC to flow through the main outlet, yet drawn the beads to the secondary outlet. After being flown to secondary outlet from the first loop, the flow was accelerated to 115 μL/min (Re = 32.3) by buffer inlet. In the second expansion chamber, 18 and 23 μm were isolated apart from each other. This results in filtering three different sizes of particles by using two expansion chambers.

Figure 14 Wang and I. Papuatsky microfluidic chip design [38, 39]

2.3 Conclusion

From the literatures, microfilaria is longer than the blood cell. This should provide the advantage of separation of the particle size. More than that, there are abundant techniques that had been used to separate the particles. However, the number of the research about microfilaria is still limited. The filtration is a common technique to capture the specific particle based on size. The main problem is the density of red blood cell, which is much higher than the density of the worm. Therefore, the primary target is to separate red blood cells out, to enhance the performance of the filtration technique.

Chapter 3
Filter experiment

3.1 Filter chip

For the filtration chip, the concept of designing was to filter microfilaria without hemorrhage the red blood cell. Therefore, the device should be able to separate a red blood cell while deliver microfilaria to the microcapillaries wall zone. In the first experiment, the simple configuration is chosen.

Hele-Shaw Equation (Equation 3.1) is used to design the chip. Shear stress and pressure drop in an incompressible, steady, Newtonian, and between two flat plates flow could be approximated. Shear stress, τ_W, is calculated at the bottom wall as [40].

$$\tau_W = \frac{6\mu}{h}\overline{V} \qquad (3.1)$$

where h = height of the channel
μ = Viscosity of fluid
$\overline{V}$ = Local velocity of fluid particle

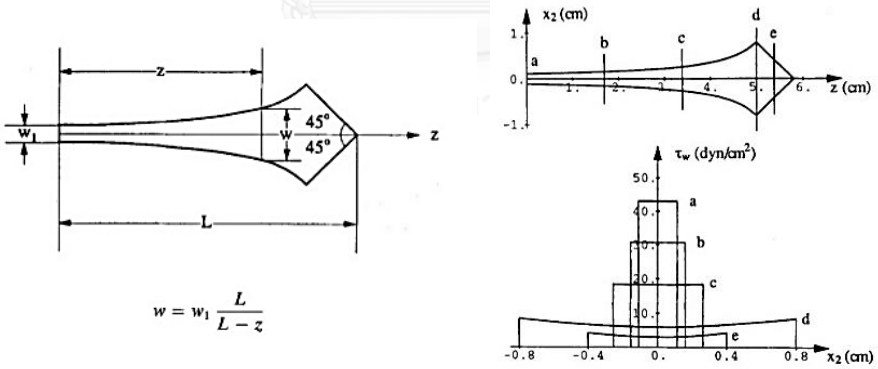

Figure 15 Channel dimension and shear stress across each cross sectional area [40]

The channel is shown in Figure 15. Shear stress is linearly distributed with decreasing from inlet to outlet. From the calculation, shear stress from the wall is almost the same as the center of the channel.

In our previous experiment design, the chip was shown in Figure 16. The inlet channels were designed in rectangular channel with two sizes, which are 200 μm and

500 μm. From the different dimension but the same flow rate, velocities of fluid are varied and could be observed.

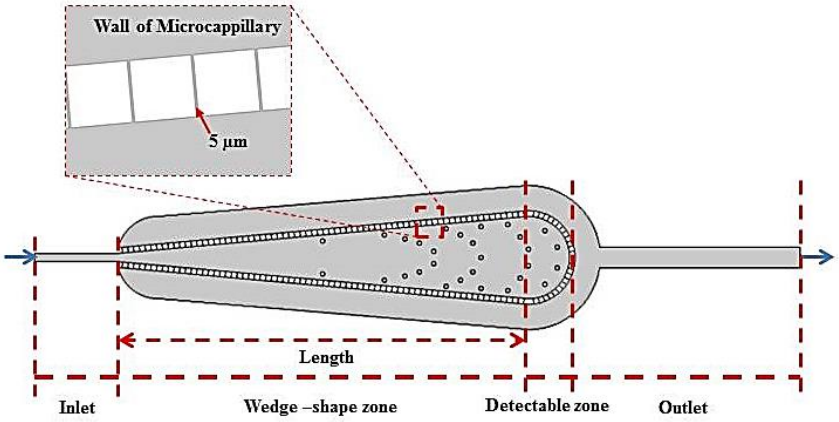

Figure 16 Nematode filtering chip

Wedge-shaped zone is next to the inlet and functions as a red blood cell drainer zone, left out the microfilariae to flow to the next zone. This wedge shape provides constant shear stress across the cross sectional of the flow. At first, we expected that this constancy would prevent the dismissing of wall interaction force, push the microfilariae through the microcapillaries. By differentiating the length of this zone, the effect of slope to the efficiency could be observed. The length are 10 and 20 mm.

After the blood traveled through the slope, the remaining blood components will experience the cylindrical detectable zone. For the ease of identification, this zone is designed to contain the microfilariae inside 1 mm diameter of vertical cylindrical shape zone.

Microcapillaries form together as a wall separates the red blood cell, white blood cell, and plasma away from the microfilariae. Microcapillaries are 5 μm gap, which are smaller than RBC (6-8 μm), WBC (10-14 μm), and microfilaria (6-6.5 μm). Finally, the outlet, 500 μm rectangular channel, drains the solution out from the chip.

3.2 Simulation

According to this study, COMSOL 5.0 was used to calculate and simulate the flow. Water is selected as a liquid substance. The velocity and pressure drop inside the chip were calculated in a condition of 2.0 ml/h. For 200 μm inlet, mean velocity is 0.028 m/s, while 500 μm inlet has a mean velocity of 0.011 m/s. For the pressure drop, the main effect comes from the length of wedge-shaped zone. 10 mm and 20 mm generate 0.6 kPa and 0.3 kPa, respectively. The simulation results are shown in Figure 17.

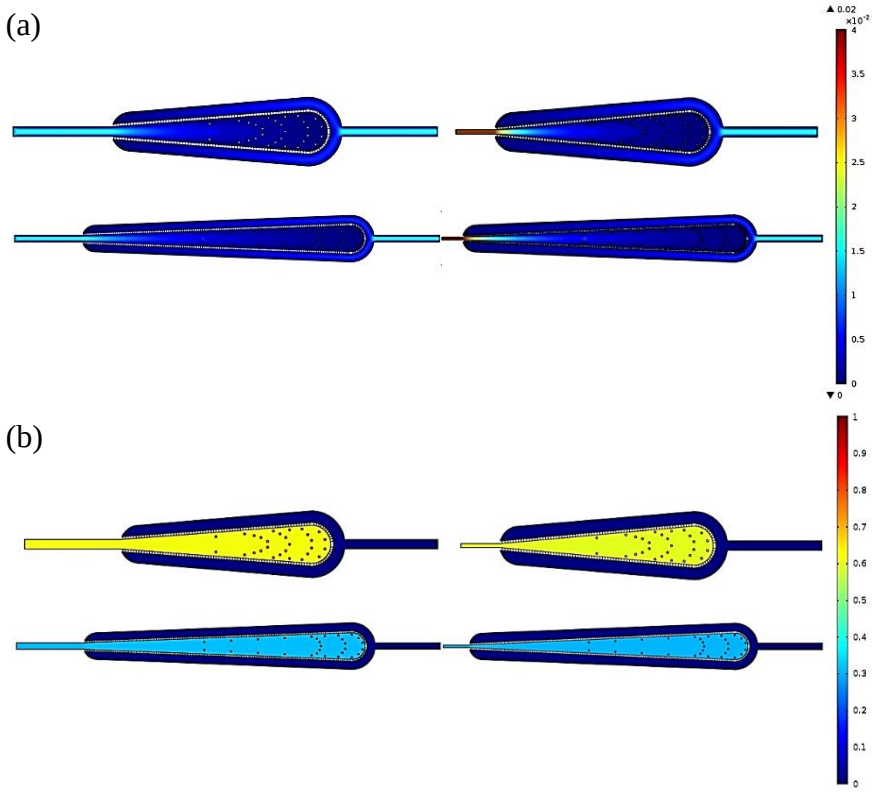

Figure 17 2-D simulation of (a) velocity contour and (b) pressure contour

3.3 Fabrication of Chip

Micro channel was manufactured by casting a Polydimethylsiloxane (PDMS) in a mold, which was patterned by using photolithography on a silicon wafer.

When pouring PDMS down the mold, there are bubbles trapped inside the solution. Therefore, the PDMS liquid was vacuumed inside the chamber. Later, the chip was heated, to vaporized the liquid substance, and harden, form as a flexible solid. By doing these step with different but compatible mold, two PDMS can bond together with oxygen plasma creating a micro channel.

After the PDMS channels were casted, there are three steps left to be done, cleaning the surfaces, treating the surfaces, and bonding PDMS with glass slide or other PDMS to form a channel.

In a normal environment, there are particles both organic and non-organic floating in the air. Therefore, before bonding the channels, there must be a cleaning process to make sure that there would be nothing blocking the channel. With this size of channel, even the small dust could block the channel and ruin the chip.

Cleaning PDMS can be done by injecting deionized water first. Then, it needed to be cleaned with isopropanol, to wash out the organic substances. After that, deionized water was injected to clean the isopropanol that still remain in the channel. As soon as

the second deionized water washed the alcohol out, Nitrogen gas was blown to dry the chip before the water would vapor and leave the watermark. Noted that, it is necessary that this whole processes were done in the hood with proper air suction.

Glass slide has its own surface treatment procedures. First, Piranha cleaning was done by putting a glass slide in a mixture between five sixth of Sulfuric acid and one sixth of Hydrogen peroxide for 30 minutes. Then, the glass slide was cleaned with deionized water to wash out the Piranha solution. After that, Acetone were used to clean the remaining non-organic matters that may still remain on the slide. Next, Isopropanol responsible for an organic particles, and deionized water to clean out the alcohol. Finally, blowing nitrogen gas was done to dry the glass slide before the liquid dry by itself and leave the mark on the slide. The cleaning procedures are shown in Figure 18.

After cleaning all the surfaces, the surfaces of both PDMS and glass slide were treated by oxygen plasma for two minutes. Oxygen plasma not only removes organics but also chemically treats the surface to ready for bonding too.

Until this step, all the channel wall were ready to be bonded. Both PDMS and glass slide were clamped together. In this step, it was needed to be sure that there is no bubble that left in an area that is not a channel. Finally for a stronger bonding, the bonded chips were left on the heating plate for 90 minutes at 75˚C.

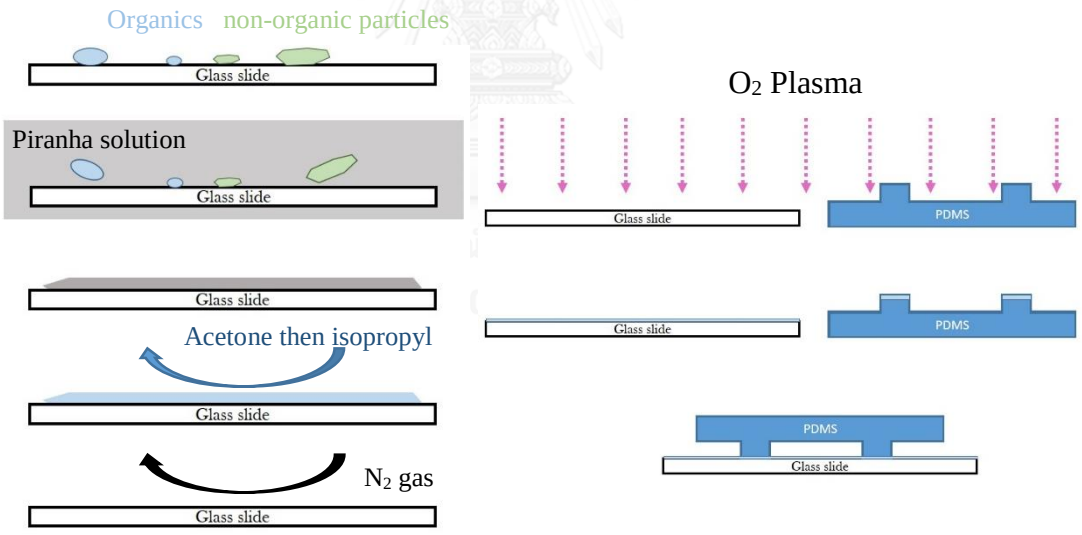

Figure 18 Glass slide cleaning process (left) and Oxygen plasma bonding (right)

3.4 Experiments

Firstly, the microfilariae in 10 µl sample were counted by fresh blood smear test (N_{total}). Secondly, the 0.1 ml blood samples were diluted into three ratios, blood to normal saline solution, 1:1, 1:5, and 1:10. After that, solutions were injected with constant flow rate at 2.0 ml/h. Later, the microfilariae inside the chip were counted ($N_{Capture}$). Finally, the efficiencies were determined by Equation 3.2

$$\eta = \frac{N_{Capture}}{N_{Total}}. \quad (3.2)$$

The experiment was conducted starting by draining out to count for microfilaria. After that, blood sample was diluted into the ratio stated above. Then the diluted sample was loaded into the syringe of 1 ml. Next, the silicon tubes with connectors were connected to the chip, the inlet size was connected to the syringe, and the outlet was placed in the tube. While the sample was injected, the experiment was observed real-time by microscope that connected to the computer. After 1 ml of blood was injected, the pump was stopped. The microfilaria inside the filter was counted after everything stop. The schematic of the experiment is shown in the Figure 19.

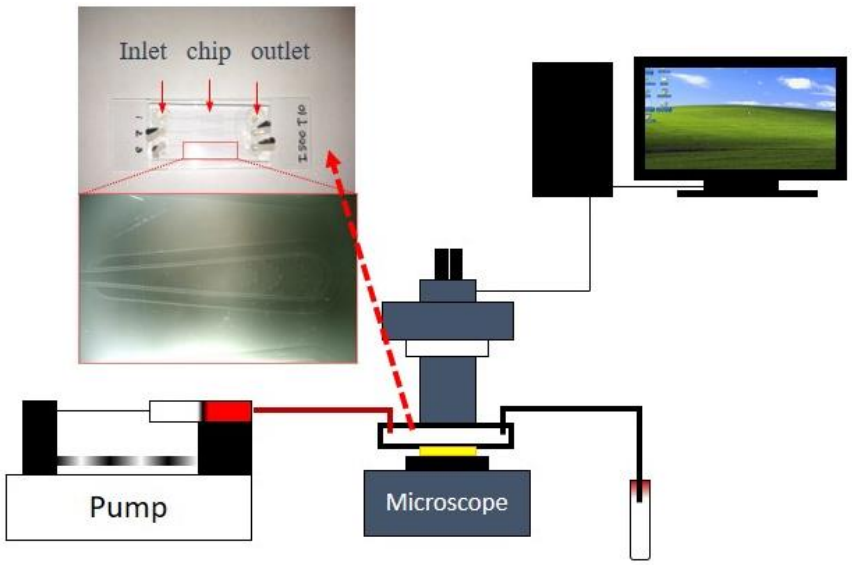

Figure 19 Schematic of the experiment

In 1:1 case, the solution is too thick to observe both while the experiment and counting. Then, pure water was injected to rinse remaining red blood cell. Red blood cells were hemorrhaged and form together as the flow continues. Even though, the microfilariae were still uncountable as shown in Figure 20.

For 1:5, after the injection, Chip, Inlet of 200 μm wide with 10 mm long, Inlet of 500 μm wide with 10 long and 20 mm, contained 11, 8, and 56 microfilariae, respectively. The experiments are shown in the Figure 20.

In the ratio of 1:10, the chips, 10 mm long with the inlet with 200 and 500 μm wide, trapped 4 and 2 microfilariae, respectively. However, in some of the experiments, the chip was broken as shown in Figure 21.

From preliminary experiment, it demonstrated that pumping water after the blood seemed to be a poor decision. Blood ratio should be greater than 1:10. Most of microfilariae were found in wedge-shape zone at which we do not intend to detect. This incident may occurred from the side wall effect from inner side of outer wall. However,

the chip with 500 µm wide inlet and 20 mm long is the most promising. Since it granted the most efficiency at 12%, so the further experiment was made.

The second experiment was done by using the chip with 500 µm wide inlet and 20 mm long with two flow rates, 2.0 ml/h and 0.5 ml/h, fixing blood ratio at 1:25 as shown in Figure 22. Since finding blood sample was quite hard at that time, so the experiment was done with low repetition. Before doing an experiment, microfilariae were counted as 15 microfilariae in 1 ml sample.

The average number of nematode decreased from 5 to 2 when the flow rate was decreased from 2 to 0.5 ml/h. This occurred from the sedimentation in the syringe while doing an experiment.

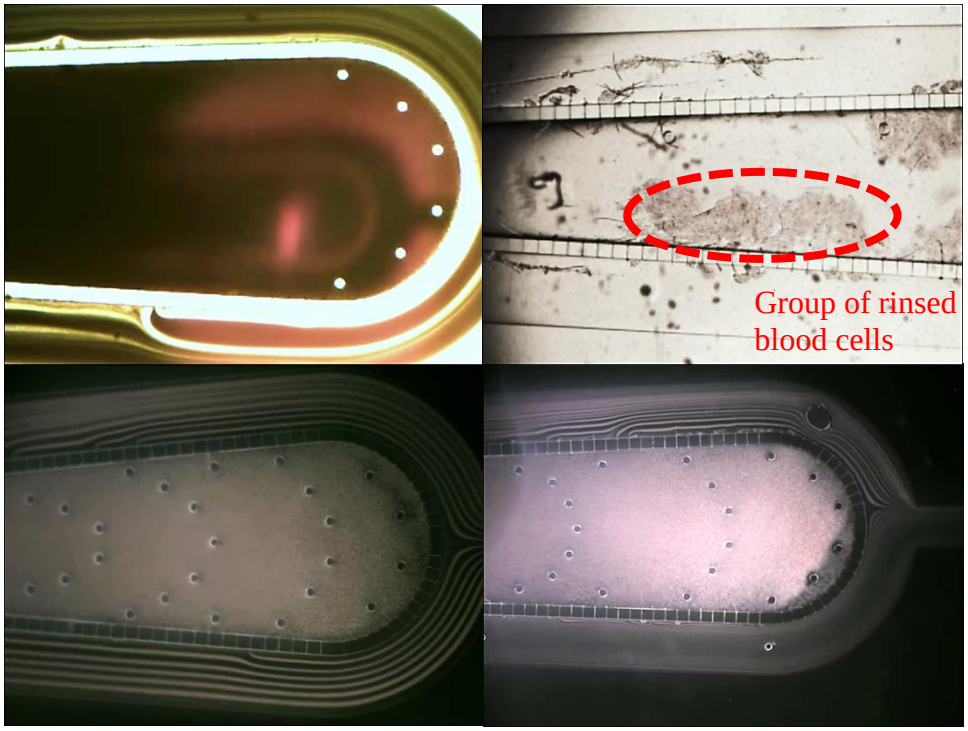

Figure 20 Cylindrical zone of 1:1 experiment (top left), wedge shaped zone after injecting pure water of 1:1 experiment (top right), Cylindrical zone of 1:5 experiment (bottom left) Cylindrical zone of 1:10 experiment (bottom right)

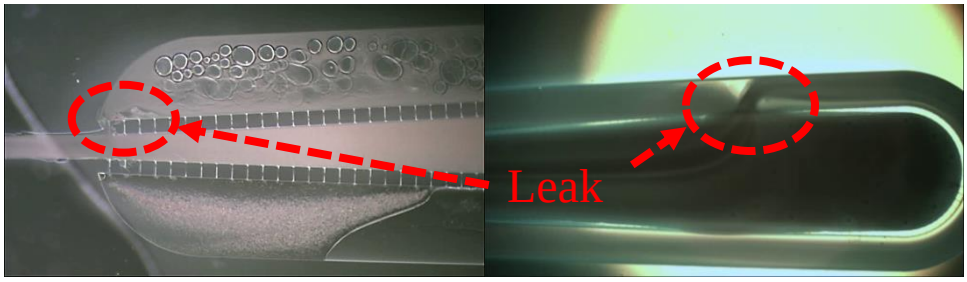

Figure 21 Damage at micro capillaries wall

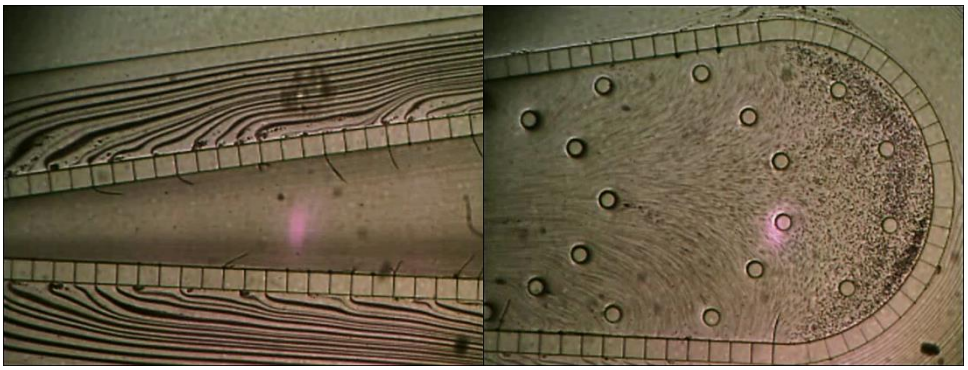

Figure 22 Overview of 1:25 experiment

3.5 Conclusion

The chips were designed to filter out the microfilaria from the whole blood. Since the micro capillaries were chosen, the filter area could be increased by expanding the length of the wall area, still the microfilaria should mainly be focused at the end of the chip, and blood cell should pass through the wall in the first section. Considering, the major force, acts on particles, in the channel is velocity shear lift gradient, which is caused by velocity gradient in the lateral direction. Therefore the shape of Hele-Shaw equation was chosen at the entrance to flatten the shape of flow profile. But due to the fabrication limitations, the shape was changed to the linear wedge shape.

There are two separated experiments. One is to find the suitable ratio between blood and normal saline solution. The ratio at 1:1, 1:5, and 1:10 were selected. In 1:1 ratio, the sample contained too much blood cells and blocked the light from microscope. Therefore, pure water was injected to rinse all the remaining blood cells, but it did not work well. Water could not reach to the end of the filter (cylindrical zone) and left out the group of rinsed blood cells blocking the micro capillaries. For 1:5 and 1:10, the blood samples were still too dense and hard to observe the microfilaria. Even though, the chip with 500 μm wide inlet with 2 mm cylindrical diameter represent the relatively high efficiency. A further development is needed.

The second experiment was to observe the effect of flow rate to the efficiency of the separation. In this experiment, 0.5 and 2 ml/h flow rates were used. The inlet sample is the same. The result shows that the higher flow rate provided the higher efficiency and also the deviation. This due to the sedimentation of the sample and the pressure across the micro capillaries, respectively. The lower flow rate took longer examination time for the same quantity of the sample. Thus, there was a time for the sedimentation for blood component in the case slow flow rate is chosen. On the other hand, the high pressure across microcapillaries occurs if the high flow rate is chosen. The pressure across the micro capillaries pushes the particle through the wall. This

resulting in the slipping of the microfilaria through the wall in to the outlet. Therefore, the optimal flow rate should be found before the real implementation.

From results, it can be concluded for the following points. The first one is too much blood cells in the sample could clog inside the filter and decrease the flow area, resulting in a higher pressure and finally chip's damages. The second point is the shape of linear wedge shape promotes the jet profile in the channel as shown in Figure 17a. This jet stream pushes particles to both side of the wall, only little amount of sample reached to the end. The result shows, the smaller slope, 500 wide inlet and 2 mm cylindrical diameter, obtains the better efficiency. The slower the flow rate is, the higher the sedimentation is. The higher the flow rate is, the lower the wall effectiveness is.

Chapter 4
Contraction and Expansion Array

As the result of the preliminary experiment, there are two main problems that need to be solved. The filter configuration does not bring the particles to the end of the chip. This problem could be solved by changing the design of the filter. The second problem is the dense of blood cells that clogged the channels and caused the damage to the chip. It should be noted that, this problem cannot be solved by diluting the whole blood, because time would take longer to inject the same amount of blood. The longer it takes, the more missing particle would be.

4.1 Approached solution

From the problem stated above, the main problem seems to be the dense of blood cells. Therefore, there must be one part of the device draws out the blood components from microfilaria before entering the detection zone. This particular zone will be called blood cells draining zone. This zone must capable of separating or sorting the particles based on the size of the particles. For simplicity for using the chip, passive technique (no external force) is selected. From all the criteria, the inertia size based sorting using contraction and expansion channel is chosen.

In the channel, velocity shear lift gradient not only seems to be a dominated force, but also depends on the size of the particles too. These brings advantages in the term of separation. With the suitable dimension, contraction and expansion arrays (CEA) can roughly separate microfilariae and red blood cell. Therefore, the chip must contain CEA as the first part of the filtration. After coarse filtration, one portion of blood sample should remain only blood component. While the microfilariae will be separated into another way. Consequently, the portion that contains microfilariae will pass through the filtration zone.

Our chip has 60 μm high and 50 μm wide for the main channel similar to the study of Wang and Papautsky whose dimension is 70 x 50 μm^2. It was designed to be integrated with micro capillaries with 5 μm wide. With this small capillary, it is also one limitation that makes us use 60 μm high microchannel.

In an expansion chamber, this structure affects to the sheath flow directly so this means that the length of the chamber influences to the separation efficiency. Therefore, two lengths of the expansion chamber were chosen to compare for the separating efficiency. The chambers are 500 μm and 1000 μm long with 550 μm wide for both length as shown in Figure 23.

The resistance of both main channel and secondary channel also affect to the pattern of the sheath flow. From the reviews the ratio between the resistances of

secondary channel to the resistance of main channel were assigned as 14 times. In this project, the length of main channel is selected to be 2,000 μm from the channel so the total length of secondary channel from each chamber is 48,000 μm long. Since the channel is limited in a certain space, we decided to bend the secondary channels as shown in the Figure 24.

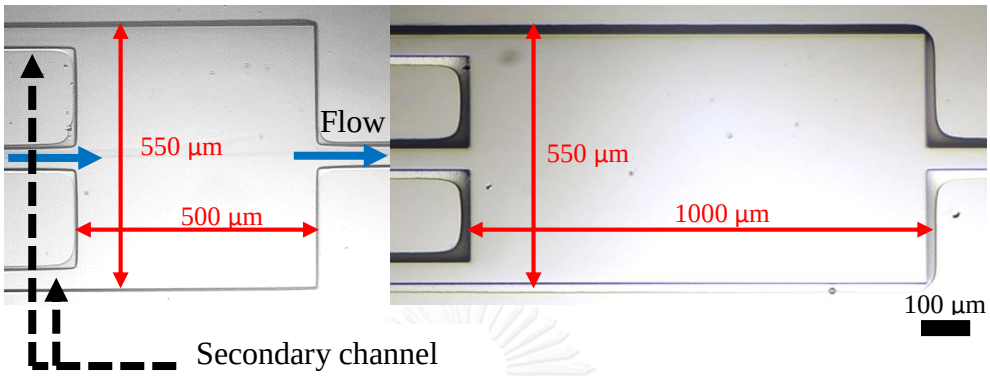

Figure 23 Dimension of Expansion with 500 μm long (left) and 1,000 μm long (right)

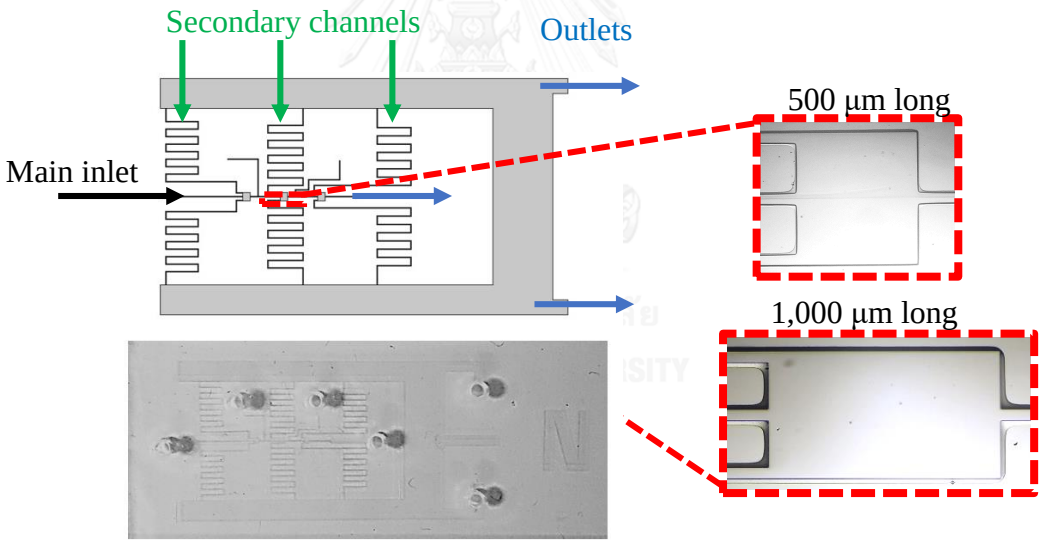

Figure 24 An overview of Contraction and Expansion arrays chip

4.2 Flow simulations

Simulation is a numerical method for solving equations. The principle of this technique is to calculate the value from point to point, these points are called meshes. By constraining all of the boundary conditions, the equation can be solved. In this project, COMSOL 5.2 was used to calculate and predict the flow. The total chip is 27,000 μm long and 16,000 μm wide. The outlet of the main and secondary channels that connected to each expansion are 2,000 and 28,000 μm long as shown in Figure 25a.

4.2.1 Mesh validation

To be able to confirm the solution from the simulations, the mesh validation must be analyzed. The mesh analysis in this project is done by reducing the mesh sizes. If the calculation results are converged into one value, the simulations are reliable.

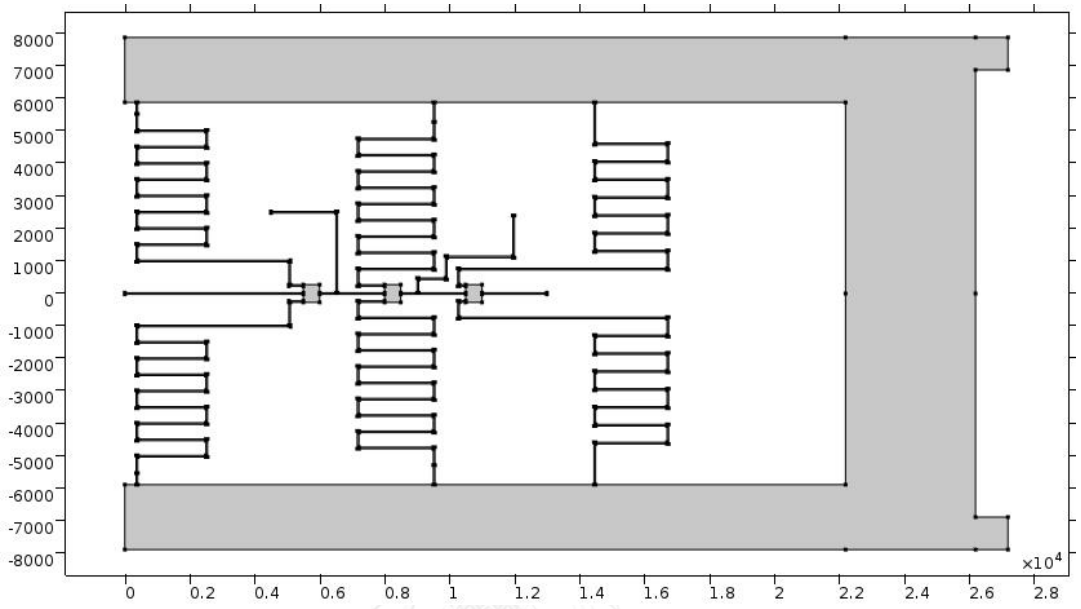

(a)

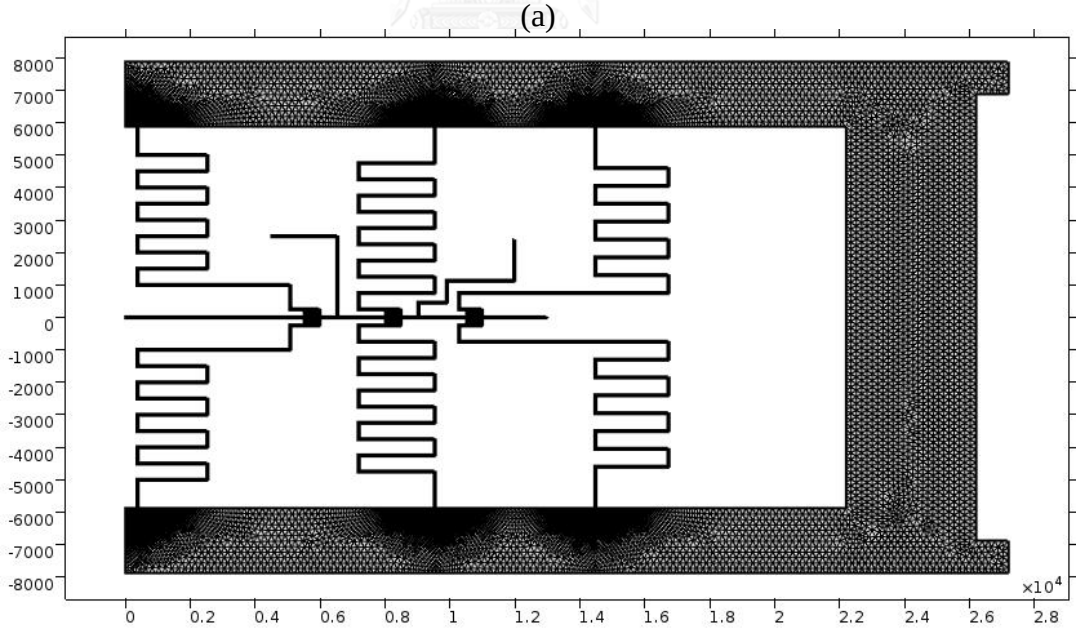

(b)

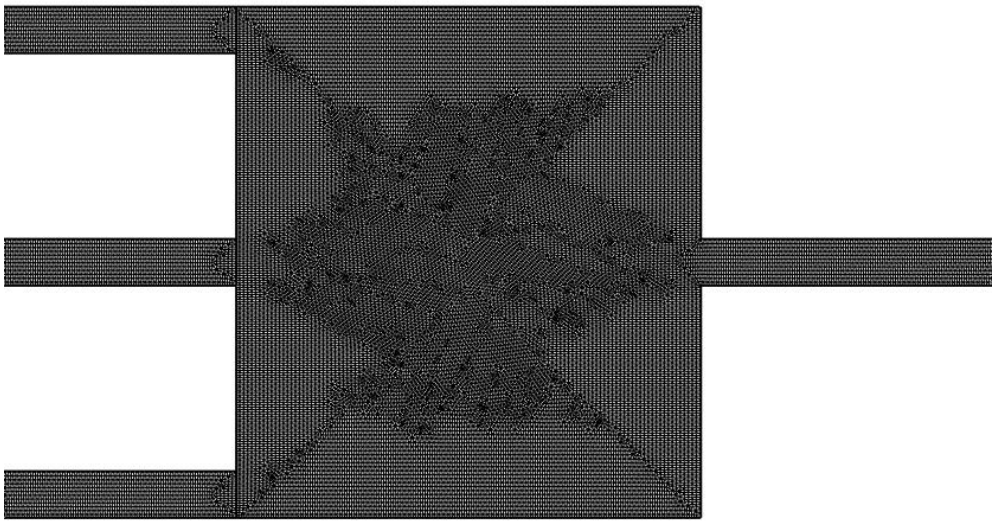

(c)

Figure 25 (a) Channel's overview in COMSOL, (b) Meshing of the channel and (c) Mesh of the expansion channel of N-type

From the above procedure, meshing conditions for this simulation are in Table 3. After meshing was done, the next step is to fix the properties of the flow. In this simulation, pure water properties were used, density is 998.2 kg/m^3 and viscosity is 0.001 kg/m s. The simulations were set as the following conditions, the inlet main flow velocity was set as stated in the Table 4 and the outlet is zero pressure (atmospheric pressure).

Table 3 Meshing condition

Maximum element size (μm)	106
Minimum element size (μm)	0.315
Maximum element growth rate	1.05
Curvature factor	0.2
Resolution of narrow regions	1
Number of degrees of freedom solved	1,543,572

Table 4 Experimental conditions

Reynolds number	Main flow rate [ml/h]	Main flow velocity [m/s]	Sheath flow rate [ml/h]	Sheath flow velocity [m/s]
40	6.63	0.79	2.30	0.28
60	9.94	1.19	3.48	0.41
80	13.26	1.58	4.62	0.55
100	16.57	1.98	5.76	0.69
120	19.89	2.37	6.90	0.83

Since this simulation is in 2 dimension, this flow rate can be determined as an area flow rate [m^2/s]. This parameter can be developed into volume flow rate by multiplying with the height of the channel. After the calculations were finished, the velocity flow fields were plotted for every channel of all Reynolds numbers for both types of the chip and are shown in the Figure 26 and 27. The vortex zone looks similar between both types of the expansions. The chip with 1,000 μm long has a longer distance from inlet to the recirculation of the fluid than that with 500 μm long. In each type, the pattern of the flow of every Reynolds numbers are the same. The only difference is the magnitude of the velocity. The area flow rates per unit height from the simulation are shown in Table 5 and 6.

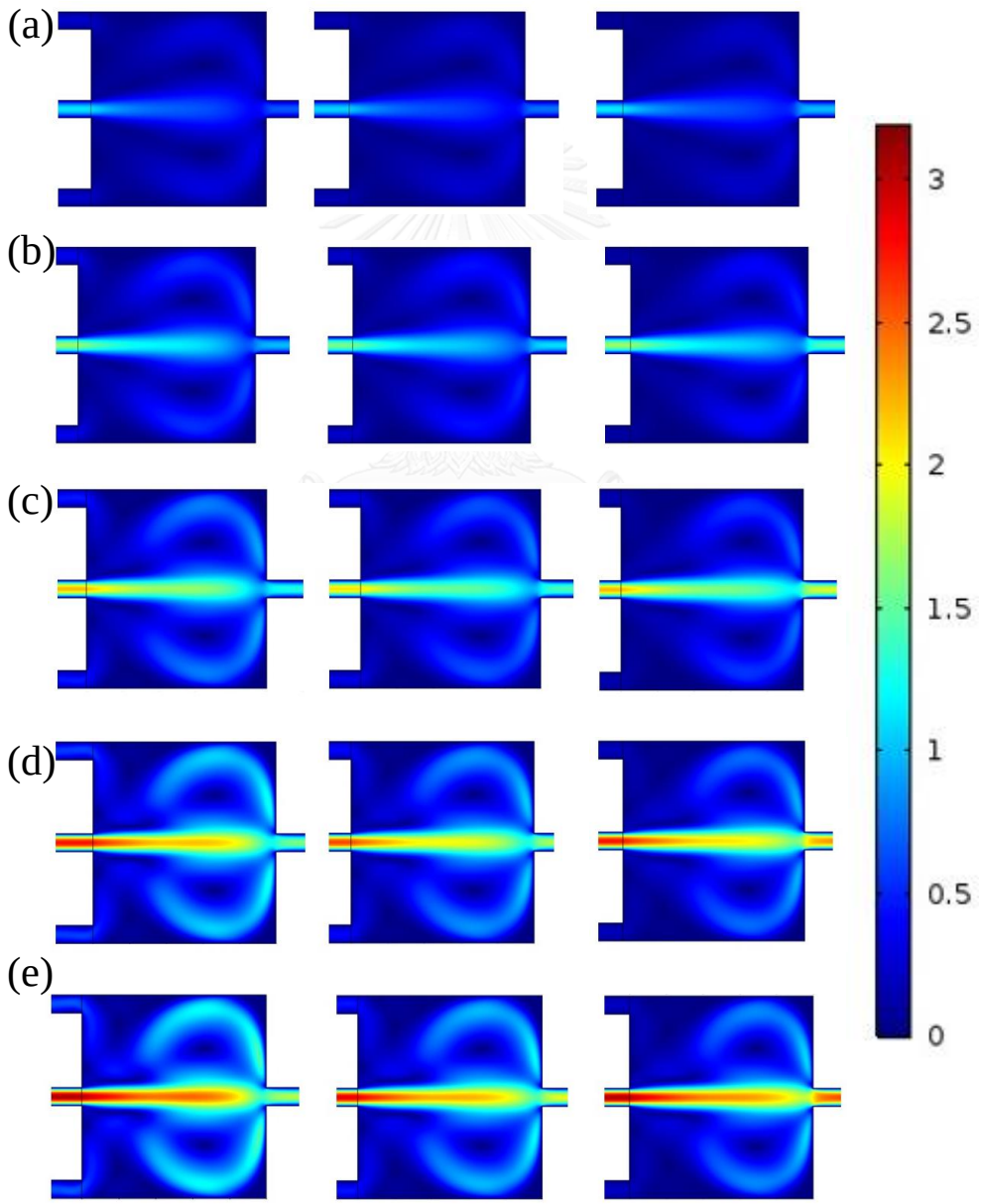

Figure 26 Velocity profile (m/s) in an expansion chamber of 500 μm long models at (a) 40, (b) 60, (c) 80, (d) 100, and (e) 120.

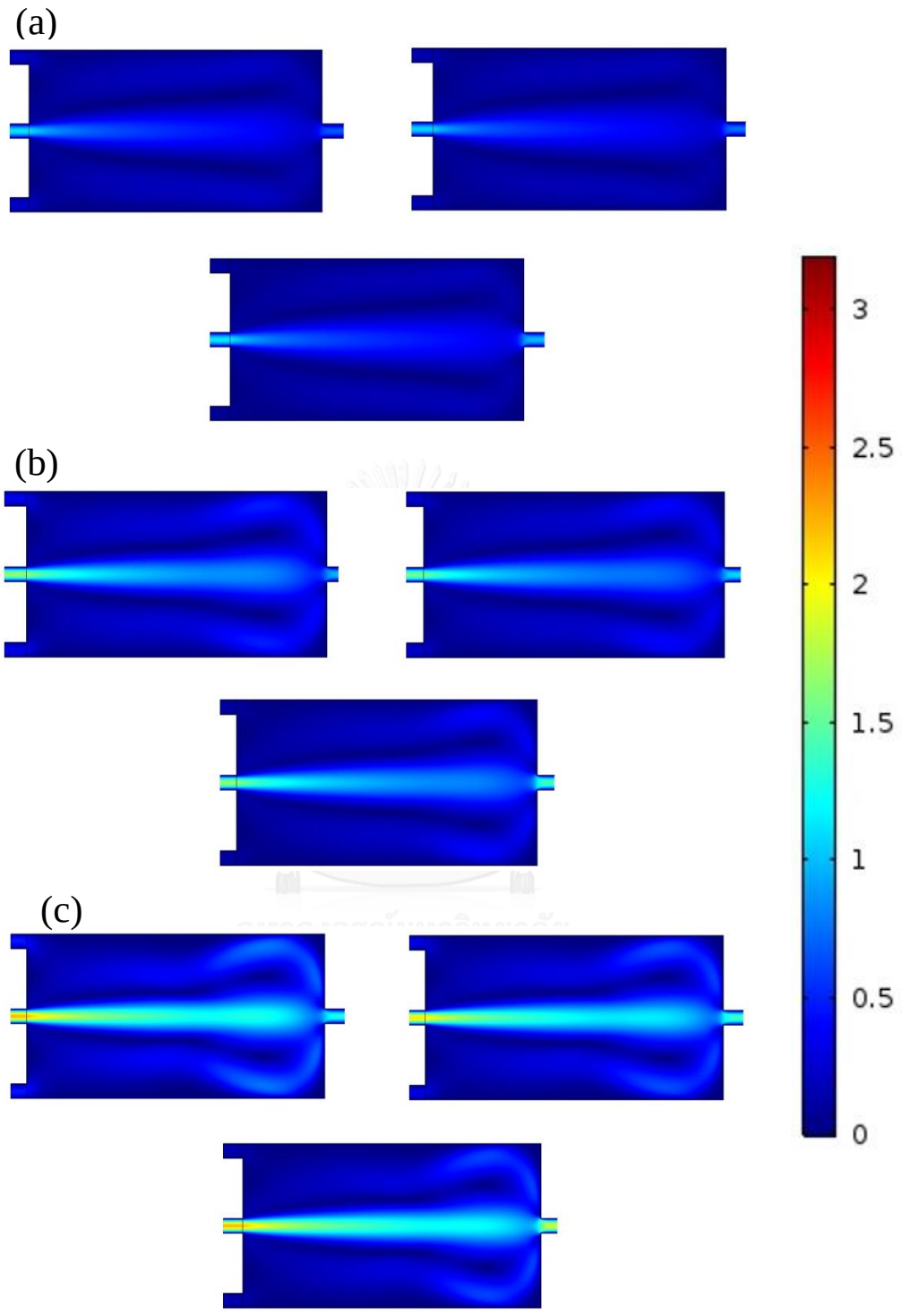
(a)
(b)
(c)
3
2.5
2
1.5
1
0.5
0

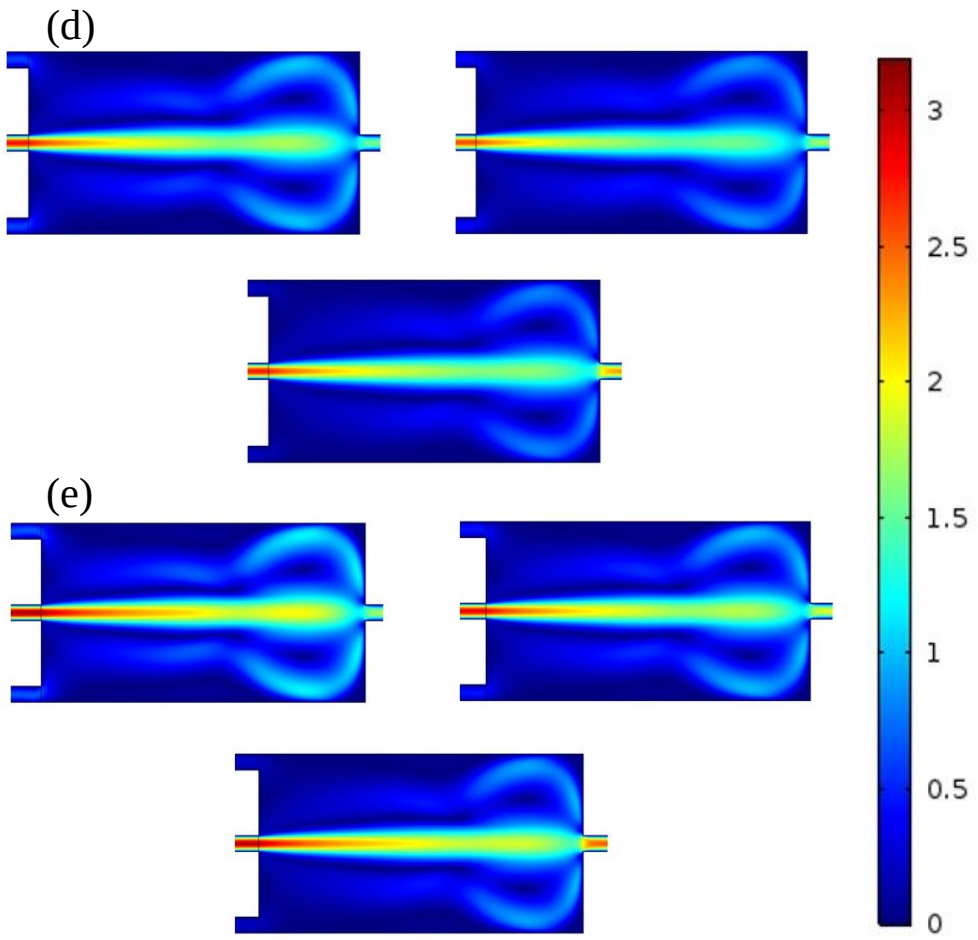

Figure 27 Velocity profile (m/s) in an expansion chamber of 1,000 μm long models at (a) 40, (b) 60, (c) 80, (d) 100, and (e) 120.

Table 5 Area flow rate of the chip with 500 μm long expansion chamber

500 μm long expansion	Area flow rate [m^2/s]				
	Re = 40	Re = 60	Re = 80	Re = 100	Re = 120
Inlet	3.80×10^{-5}	5.65×10^{-5}	7.51×10^{-5}	9.41×10^{-5}	1.05×10^{-4}
Upper secondary 1	7.76×10^{-6}	1.17×10^{-5}	1.59×10^{-5}	2.02×10^{-5}	2.26×10^{-5}
Lower secondary 1	7.76×10^{-6}	1.17×10^{-5}	1.59×10^{-5}	2.02×10^{-5}	2.26×10^{-5}
Upper secondary 2	5.35×10^{-6}	8.04×10^{-6}	1.09×10^{-5}	1.38×10^{-5}	1.54×10^{-5}
Lower secondary 2	5.35×10^{-6}	8.05×10^{-6}	1.09×10^{-5}	1.38×10^{-5}	1.54×10^{-5}
Upper secondary 3	2.53×10^{-6}	3.76×10^{-6}	5.02×10^{-6}	6.31×10^{-6}	7.02×10^{-6}
Lower secondary 3	2.53×10^{-6}	3.76×10^{-6}	5.03×10^{-6}	6.31×10^{-6}	7.03×10^{-6}
Total Secondary	3.13×10^{-5}	4.71×10^{-5}	6.35×10^{-5}	8.05×10^{-5}	9.01×10^{-5}
Inlet to secondary	2.34×10^{-5}	3.53×10^{-5}	4.76×10^{-5}	6.04×10^{-5}	6.77×10^{-5}
Main outlet	3.38×10^{-5}	4.96×10^{-5}	6.55×10^{-5}	8.15×10^{-5}	9.04×10^{-5}
Inlet to main outlet	1.46×10^{-5}	2.13×10^{-5}	2.75×10^{-5}	3.36×10^{-5}	3.68×10^{-5}
Sheath flow	1.60×10^{-5}	2.32×10^{-5}	3.08×10^{-5}	3.75×10^{-5}	4.15×10^{-5}

Inlet in 2nd Expansion	3.85 x 10^{-5}	5.62 x 10^{-5}	7.42 x 10^{-5}	9.13 x 10^{-5}	1.01 x 10^{-4}
% Inlet 2nd Expansion/Inlet	101 %	99 %	99 %	97 %	96 %
Inlet in 3rd Expansion	4.38 x 10^{-5}	6.33 x 10^{-5}	8.33 x 10^{-5}	1.01 x 10^{-4}	1.11 x 10^{-4}
% Inlet 3rd Expansion/Inlet	115 %	112 %	111 %	108 %	107 %
$\%V_{\text{inlet to secondary}}$	62 %	62 %	63 %	64 %	65 %
$\%V_{\text{inlet to main outlet}}$	38 %	38 %	37 %	36 %	35 %

Table 6 Area flow rate of the chip with 1,000 μm long expansion chamber

1,000 μm long expansion	Area flow rate [m^2/s]				
	Re = 40	Re = 60	Re = 80	Re = 100	Re = 120
Inlet	3.80 x 10^{-5}	5.65 x 10^{-5}	7.51 x 10^{-5}	9.41 x 10^{-5}	1.05 x 10^{-4}
Upper secondary 1	7.80 x 10^{-6}	1.18 x 10^{-5}	1.59 x 10^{-5}	2.02 x 10^{-5}	2.27 x 10^{-5}
Lower secondary 1	7.80 x 10^{-6}	1.18 x 10^{-5}	1.59 x 10^{-5}	2.03 x 10^{-5}	2.27 x 10^{-5}
Upper secondary 2	5.37 x 10^{-6}	8.09 x 10^{-6}	1.09 x 10^{-5}	1.39 x 10^{-5}	1.56 x 10^{-5}
Lower secondary 2	5.37 x 10^{-6}	8.10 x 10^{-6}	1.09 x 10^{-5}	1.39 x 10^{-5}	1.56 x 10^{-5}
Upper secondary 3	2.54 x 10^{-6}	3.79 x 10^{-6}	5.08 x 10^{-6}	6.40 x 10^{-6}	7.14 x 10^{-6}
Lower secondary 3	2.54 x 10^{-6}	3.79 x 10^{-6}	5.08 x 10^{-6}	6.40 x 10^{-6}	7.14 x 10^{-6}
Total Secondary	3.14 x 10^{-5}	4.73 x 10^{-5}	6.39 x 10^{-5}	8.11 x 10^{-5}	9.08 x 10^{-5}
Inlet to secondary	2.35 x 10^{-5}	3.55 x 10^{-5}	4.79 x 10^{-5}	6.08 x 10^{-5}	6.81 x 10^{-5}
Main outlet	3.36 x 10^{-5}	4.92 x 10^{-5}	6.48 x 10^{-5}	8.04 x 10^{-5}	8.90 x 10^{-5}
Inlet to main outlet	1.45 x 10^{-5}	2.11 x 10^{-5}	2.72 x 10^{-5}	3.32 x 10^{-5}	3.64 x 10^{-5}
Sheath flow	1.60E-05	2.32E-05	3.08E-05	3.75E-05	4.15 x 10^{-5}
Inlet in 2nd Expansion	3.56 x 10^{-5}	5.26 x 10^{-5}	6.93 x 10^{-5}	8.63 x 10^{-5}	1.01 x 10^{-4}
% Inlet 2nd Expansion/Inlet	101 %	99 %	99 %	97 %	96 %
Inlet in 3rd Expansion	3.81 x 10^{-5}	5.61 x 10^{-5}	7.36 x 10^{-5}	9.12 x 10^{-5}	1.11 x 10^{-4}
% Inlet 3rd Expansion/Inlet	115 %	112 %	111 %	107 %	106 %
$\%V_{\text{inlet to secondary}}$	62 %	63 %	64 %	65 %	65 %
$\%V_{\text{inlet to main outlet}}$	38 %	37 %	36 %	35 %	35 %

4.3 Conclusion

To solve the problem stated in chapter 3, the contraction expansion array is selected to separate the smaller particle or red blood cells, to main outlet and delivered bigger particle or microfilaria to the secondary outlets. The channel was fabricated as 50 μm high throughout the chip. The contraction channel and secondary channel were designed as 50 μm wide. The expansion zone was designed as 550 μm wide with 500 μm and 1,000 μm long.

To be able to predict the result, computational simulation was selected. This technique provides a velocity profile and flow rate of every channels in the chip. The velocity profile for each type is similar. For 500 μm long expansion, the vortices took nearly 75% of the channel area, but the magnitude was different. The longer expansion channel, the vortices took about 42% of the total expansion area. Furthermore, the area flow rates per unit height of the chip were shown in Table 5 and 6.

Chapter 5
Experimental Procedure and Sample Preparation

5.1 Goals

This experiment would be done to determine the relationship between the Reynolds numbers of the flow on the separation efficiency (η) as shown in Equation 5.1, the missing percentage (λ) as shown in Equation 5.2, and the separation factor of the expansion (X) as shown in Equation 5.3 and 5.4. In these experiments, polystyrene beads of 5, 10, 15, and 20 μm were chosen. The Reynolds number that were selected are 40, 60, 80, 100, and 120.

$$\eta = \frac{N_m \text{ or } N_s}{N_{control}} \times 100 \qquad (5.1)$$

$$\lambda = \frac{N_{control} - (N_m + N_s)}{N_{Control}} \times 100 \qquad (5.2)$$

where $N_{Control}$ = Number of beads at inlet (or control)
N_m = Number of beads in main outlet
N_s = Number of beads in secondary outlet

Efficiency of the separation (η) represents the overall ratio of each particle size at each outlet compare with the control sample. The missing percentage (λ) demonstrates the missing portion of the particle inside the chip.

Furthermore, the efficiency only represented the overall performance of all expansions. For a better understanding, the sorted out portion between main and secondary outlet of a single expansion must be determined. By assuming that the ratio of the number of beads that left at the secondary exit is equal to X as shown in the Figure 28, the numbers of bead, exited from the main and secondary outlet, are shown in Equation 5.3 and 5.4, respectively.

$$N_m = (1-X)^2(1-2X)N_{Control}$$

$$= (-2X^3 + 5X^2 - 4X + 1)\, N_{Control} \qquad (5.3)$$

$$N_s = (2X^3 - 5X^2 + 4X)\, N_{Control} \qquad (5.4)$$

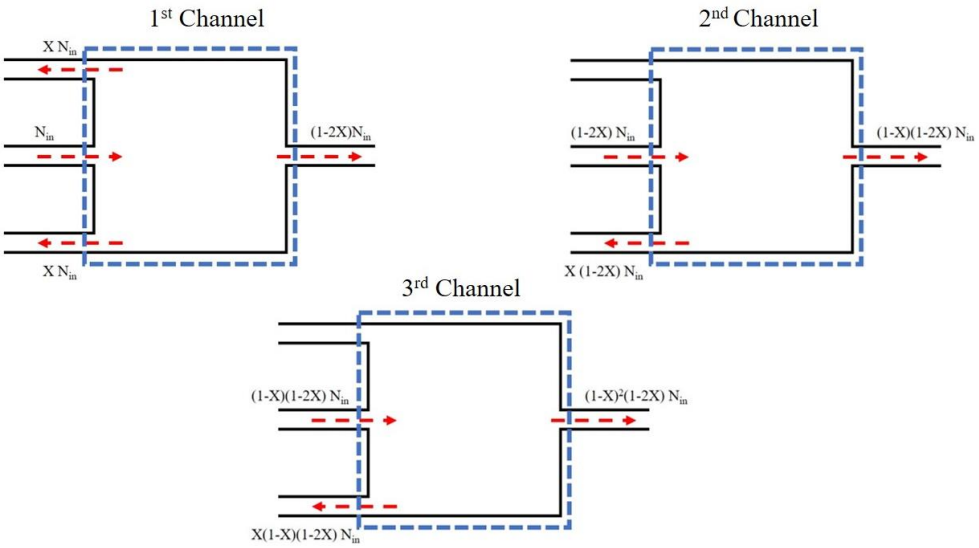

Figure 28 The separation model of the expansion units

5.2 Solution preparation and Experiment setup

From the pioneer experiment, the concentration that presented a low standard deviation, should be 10^6 bead/ml. This resulted in the clogging in the main entrance by the beads as shown in Figure 29. It is needed to be noted that the main channel is only 50 μm, thus the 20 μm bead took about 40% of the channel cross sectional area by only a single bead.

Meanwhile the sample was injected into the chip, there are an appearance of the unknown particles inside the channel as shown in Figure 30. The particle not only blocked the channel, but also gathering the upcoming bead in the flow and totally barricade the channel. Then, the experiments must be stopped.

Other than the pointy long particles, there are small groups that was suspected to be a PDMS fraction from puncturing process as shown in the Figure 31. This particle also blocked the channel and started the bead blocking.

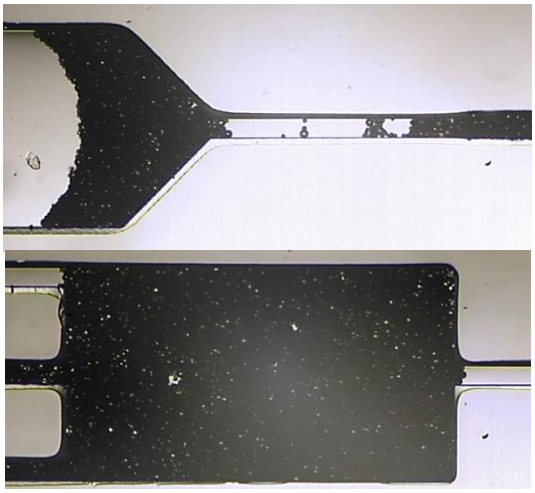

Figure 29 Bead clogging in main inlet (top) and in an expansion unit (below)

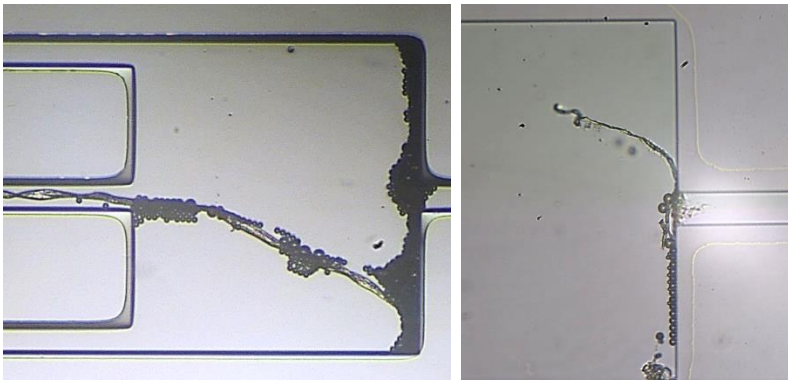

Figure 30 Unknown particle found in an expansion unit

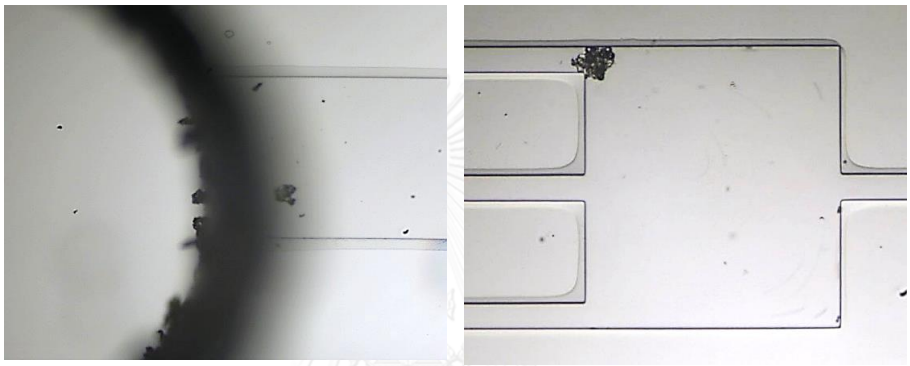

Figure 31 PDMS fraction from puncturing process

With beads clogging problems were found, the ideas of fabricating the chip was changed. The clamping mechanism was selected the clamp is shown in Figure 32. The idea is to be able to clean the blocking bead inside the channel and to be able to reuse the chip again. However the clamp did not work out so well. There was a leakage of the fluid from the channel no matter how tight the chip was clamped. Therefore the clamp mechanism was revoked. Then, the bead problem was fixed by filtration of the bead solution before entering the chip, and by reducing the bead concentration of the big particles.

Figure 32 Mechanical clamping mechanism component

First of all, deionized water was filtered by cellophane paper with 20-25 μm pore size to eliminate the contaminate particles in water. Later, cellophane paper was replaced by cell strainer. Polystyrene beads were shaken by bio-shaker for 2 minutes. From previous experiment and the instruction of hemocytometer, the number of particle should be minimum at 50 and not exceed 200 beads per 0.001 x 0.001 m^2 grid. If the beads are too low, the standard deviation would be too high. If the beads are too dense, the beads usually stuck inside the channel and block the flow. Thus, the beads solution volumes that suspended to 40 ml of water are; 30 μl of 5 μm, 150 μl of 10 μm beads, 400 μl of 15 μm, and 450 μl of 20 μm beads. After all the beads were added to the solution, a drop of tween, surface tension reductant, was added and mixed by bio-shaker.

After the solution is ready, it would be loaded into 2 syringes. These two syringes were placed on a micro pump, one was connected to the inlet of the chip, another to the control experiment tube. There must be a controlled sample because polystyrene beads usually sediment inside the syringe rather than flowing into the experiment kits. This leads to the missing of the beads. Thus, the controlled sample represent the beads that actually flow into the chip. Other than main inlet, there are sheath flow inlet, which were filled with filtered colour mixed deionized water. On the outlet sides, both main outlet and secondary outlet were connected with separated experiment tube. Figure 33 shows the experimental setup.

The experiment starts by the following procedure. First, the deionized water was filtered by cell strainer with 40 μm pore size, and this water would be used throughout the experiment. Second, the water was split into two portion, add colour into one then filtered it again. Third, silicon tubes were cleaned by 70% alcohol rinsing the dust on the outside, injected by filtered deionized water to clean the inside of the tube, and was gently plugged in to the chip one by one. Fourth, the filtered deionized water and coloured filtered deionized water, loaded in syringes, were injected with the Reynolds of the flow that would be used for both main inlet and sheath inlet. Meanwhile the filtered deionized water was injecting, the beads was shook and mixed, in the ratio stated above, together with filtered deionized water and few drops of 20% tween. Fifth, shook and filtered the mixture 3 to 4 times. Sixth, the sample were loaded into two syringes, control and sample. Seventh, the syringes were swiftly switched from filtered deionized water to the sample in pump 1, and control syringe were placed next to the sample. Finally, the silicon tubes were put from the outlet into the control, main, and secondary tubes. Noted that during the experiment the chip was real-time observed by microscope connected to computer.

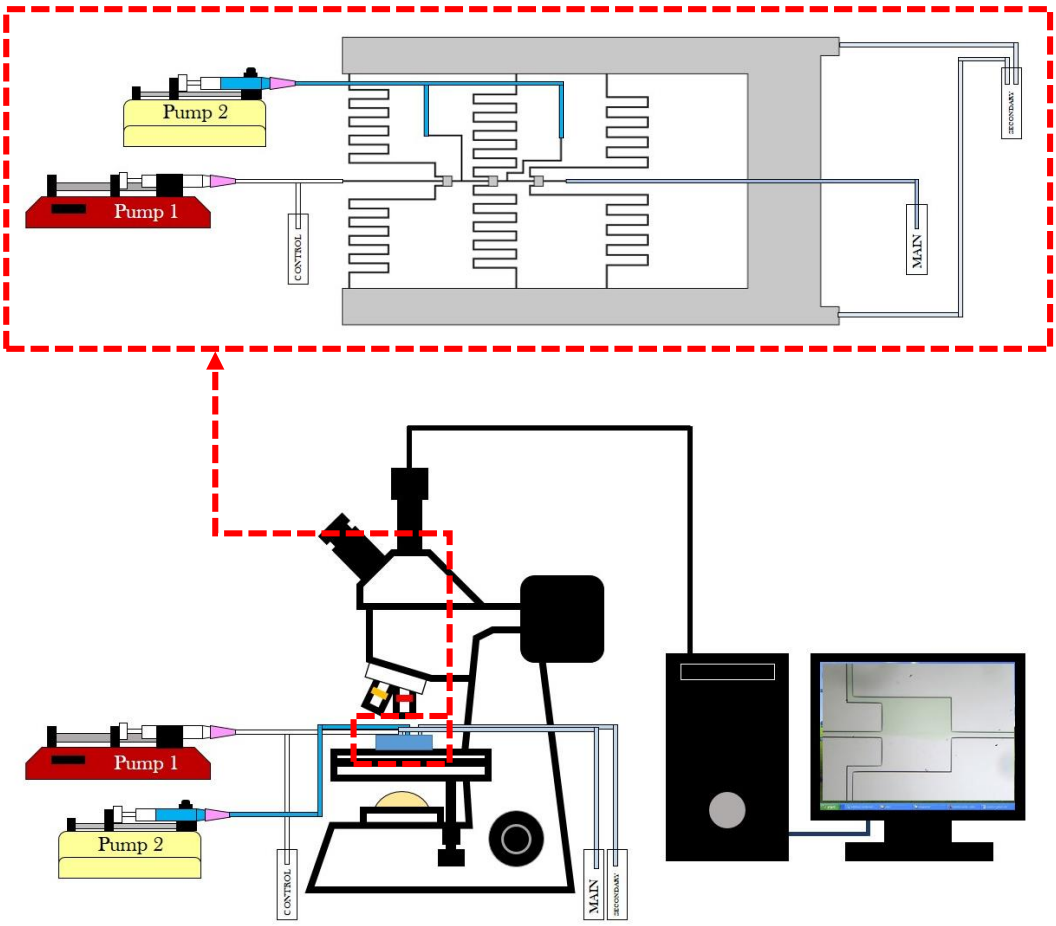

Figure 33 Schematic of the experiment

In these experiments, 10 ml syringes, 15.2 mm of diameter, were selected to inject the fluid into the chip. The flow rate of micro-pumps were set as shown in Table 7 according to the simulation results in the previous chapter. The sample was injected only 3 ml for each experiment.

Table 7 Flow condition of the experiment

Reynolds number	Pump 1 flow rate [ml/h]	Pump 2 flow rate [ml/h]
40	6.63	2.28
60	9.94	3.48
80	13.26	4.62
100	16.57	5.76
120	19.89	6.9

After the solution was injected to the chip. Controlled sample, main outlet, and secondary outlet were drawn at the amount of 10 µl to count the concentration in hemocytometer for three times each. The beads inside hemocytometer were captured as a photo, and to be counted later.

To clean the remained beads inside the chip, the chip would be flushed with filtered deionized water for 5 ml. Before the experimental conditions could be obtained as stated above, there are several efforts. The first time that the contaminated particle was seen, it was believed that the deionized water was not clean enough. Therefore, the deionized water was filtered by cellophane paper with 20 -25 µm pored size before suspended the beads. Despite, there are still contaminated particle left. After that, the process was changed. The beads were suspended in deionized water and tween. Then, the mixed solution was filtered by cell strainer with 40 µm pored size. There were still some contaminated particle left, but it was smaller than the previous procedure. Furthermore, the bead were no longer clogged in the channel.

5.3 Determining the number of particles

The chip contains two sheath flow inlets to make up the lost flow rate from secondary channel. So, the flowed volume must be used to interpret the number of the beads. It should be noted that the solution from main and secondary outlets would be mixed with colour from sheath inlets. The volume of main outlet and the volume of the secondary outlet are shown in Figure 34. These volumes are essential, because they would be used for calculation for the number of the beads. Counting by hemoceytometer, the efficiency of the separations must be determined by the number of beads. Therefore, the number of beads was calculated by Equation 5.5-5.7.

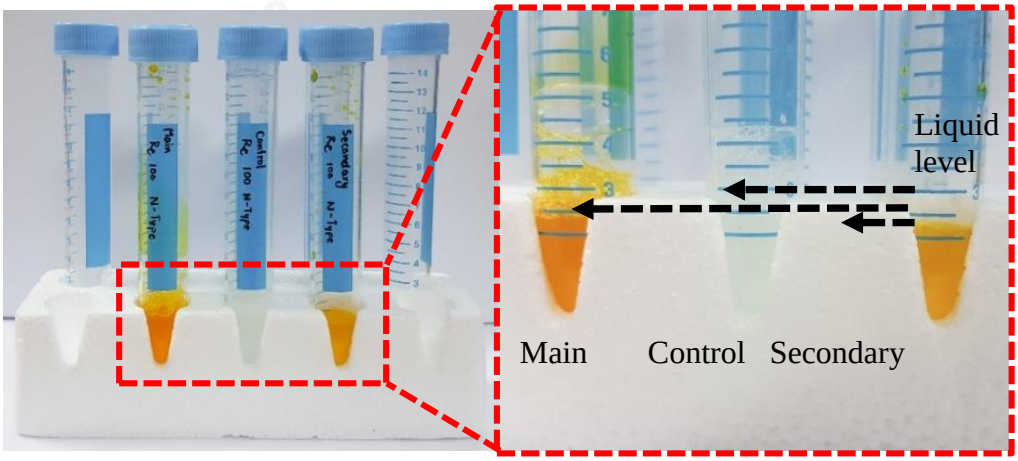

Figure 34 Volumes of inlet and outlets

$$N_{control}\,[bead] = C_{control}\left[\frac{bead}{mm^2}\right] x\ 10^4\left[\frac{mm^2}{ml}\right] x\ V_{control}[ml] \quad (5.5)$$

$$N_m[bead] = C_m\left[\frac{bead}{mm^2}\right] x\ 10^4\left[\frac{mm^2}{ml}\right]\ x\ (V_m)\ [ml] \quad (5.6)$$

$$N_s[bead] = C_s\left[\frac{bead}{mm^2}\right] x\ 10^4\left[\frac{mm^2}{ml}\right]\ x\ (V_s)\ [ml] \quad (5.7)$$

where
$C_{control}$ = Concentration of bead in control sample
C_m = Concentration of bead in main outlet sample
C_s = Concentration of bead in secondary outlet sample
V_c = Volume of control sample from the experiment
V_m = Volume of main outlet sample from the experiment
V_s = Volume of secondary outlet sample from the experiment

5.7 Conclusion

The main target of the experiment is to obtain the efficiency of the separation for each outlet, main and secondary, for each case of the Reynolds number. By varying the Reynolds number of the flow, the outcome was expected to be distinctive. The different would provide the most suitable condition to separate particles based on the size of the particles.

At first, the procedures of the experiment must be obtained. The main problem is the long pointy unable to identified particle blocked the channel and ruined the whole chips. Then, the clamping mechanism was took place but did not worked out. The cellophane filter was introduced to filter the dust that may found in the sample. Still, the cellophane did not distinguish all of the particle, but reduce the chance to find them. After that, cell strainer was selected to filter the sample, containing beads with all sizes. The unidentified object that found in the channel was reduced, only a very small size was found. Finally, the experimental method was acquired as stated previously.

After the experiment, hemocytometer was selected to identify the concentration of the particle in all the outlet, control, main, and secondary. After that the number of particles at each location is calculated using the liquid volume at each outlet and inlet, and the efficiency as well as other index is calculated.

Chapter 6
Beads Experiment Results

6.1 Expansion channel with 500 μm long

6.1.1 Flow pattern in expansion channel

While the beads were injected into the chip, the pictures of the flow were taken. These beads travel continuously and captured as a streamline of the beads as represented in Figure 35. The vortex area is bigger as the Reynolds number of the flow is increased, and starts to take over all of the expansion chamber at Reynolds number of 80. Since the flow in the channel is laminar, main inlet would not mix with sheath inlets. Thus, most of the beads, remain in the lower half of the main flow, would only flow to the lower secondary channels of the second and third expansion chamber. Comparing streamline of the beads with the velocity field in Figure 26 in Chapter 4, the bead moved across the fluid streamline, and this would be happened due to the effect of velocity-gradient lift forces.

(a)

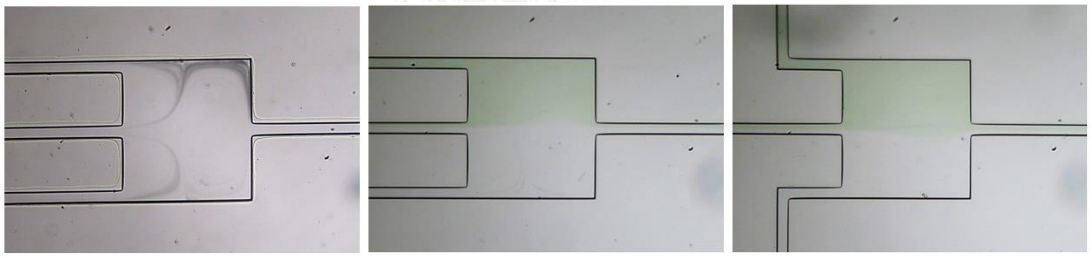

(b)

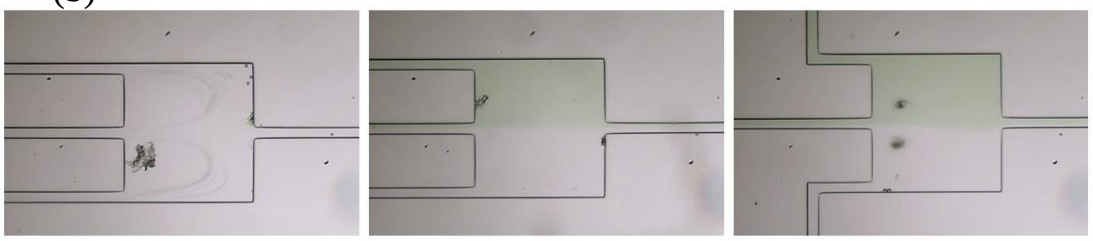

(c)

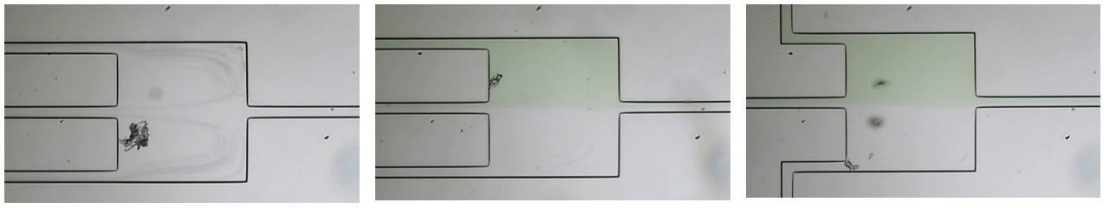

(d)

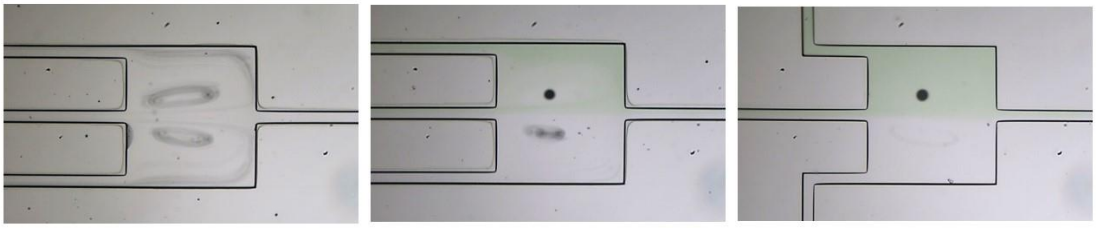

(e)

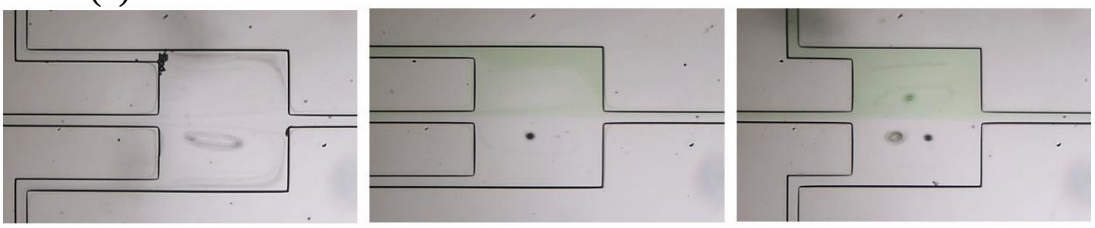

Figure 35 Flow pattern of 1st, 2nd, and 3rd channel at Reynolds number of (a) 40, (b) 60, (c) 80, (d) 100, and (e) 120.

The control sample were counted as 5 μm bead was suspended in the range between 8.7 x 10^5 to 2.01 x 10^6 bead/ml, 10 μm was counted from 1.04 x 10^6 to 2.62 x 10^6 bead/ml, 15 μm was counted from 1.25 x 10^5 to 8.25 x 10^5 bead/ml, and 20 μm was counted from 0 to 1.97 x 10^5 bead/ml. The raw data of the experiments are shown in Figure 36. The experiments were done for all beads at Reynolds numbers between 40 - 120. Three tests were repeated for all cases

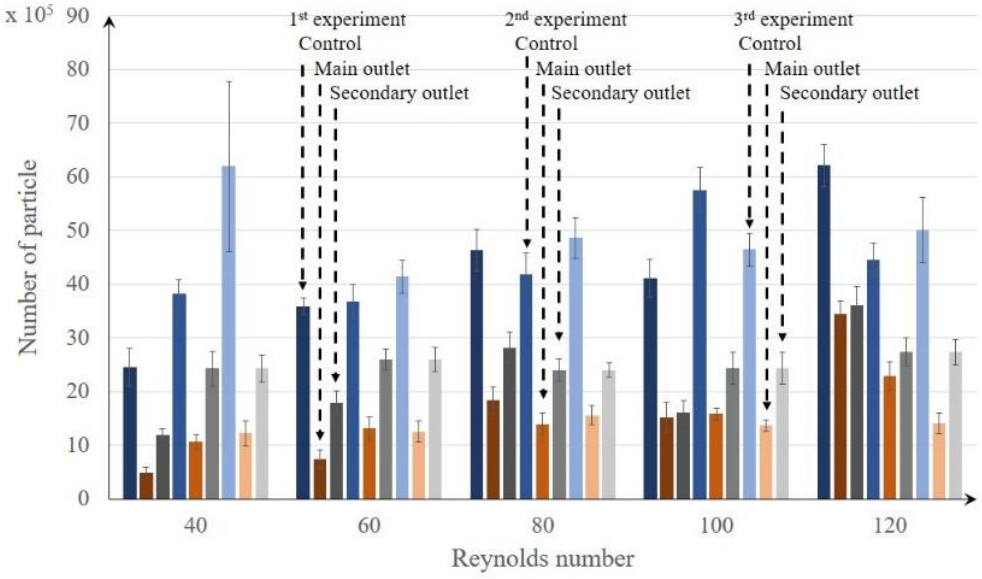

(a)

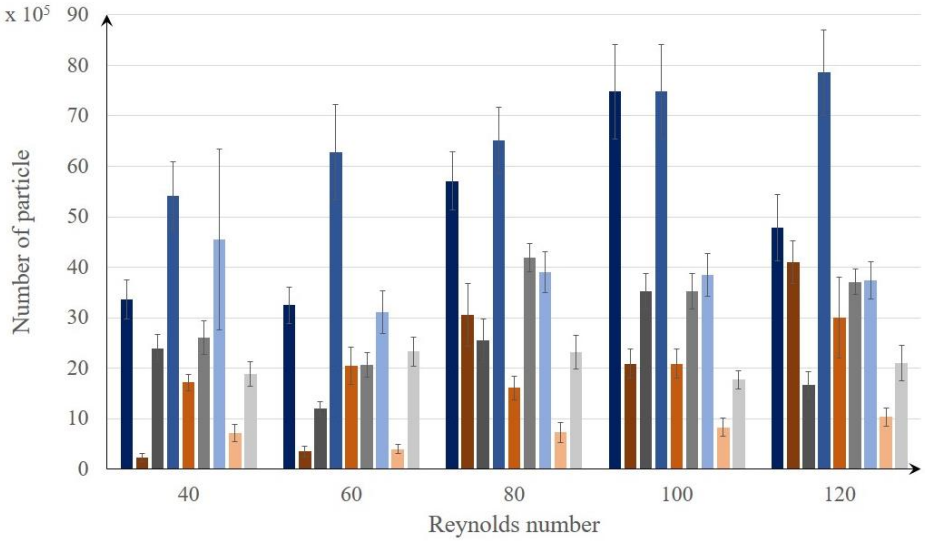

(b)

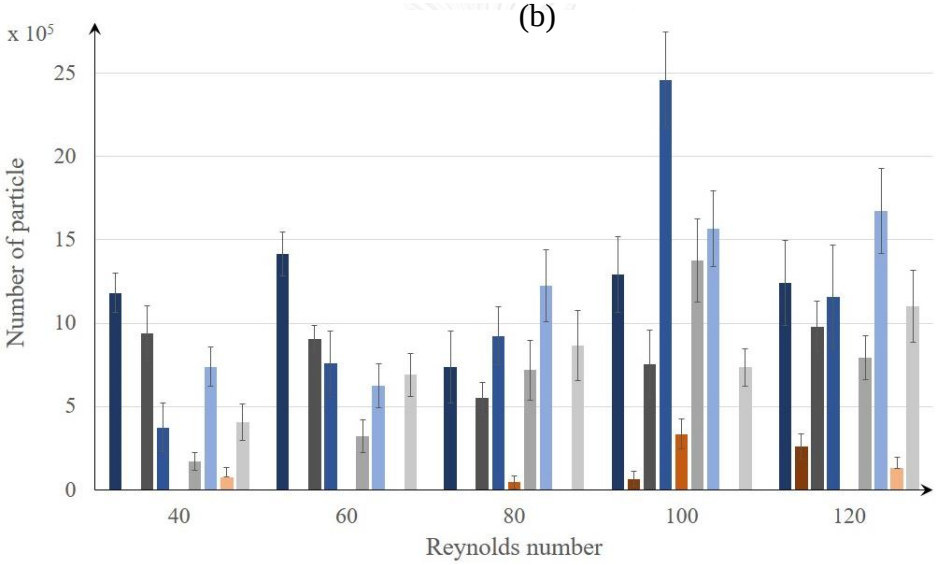

(c)

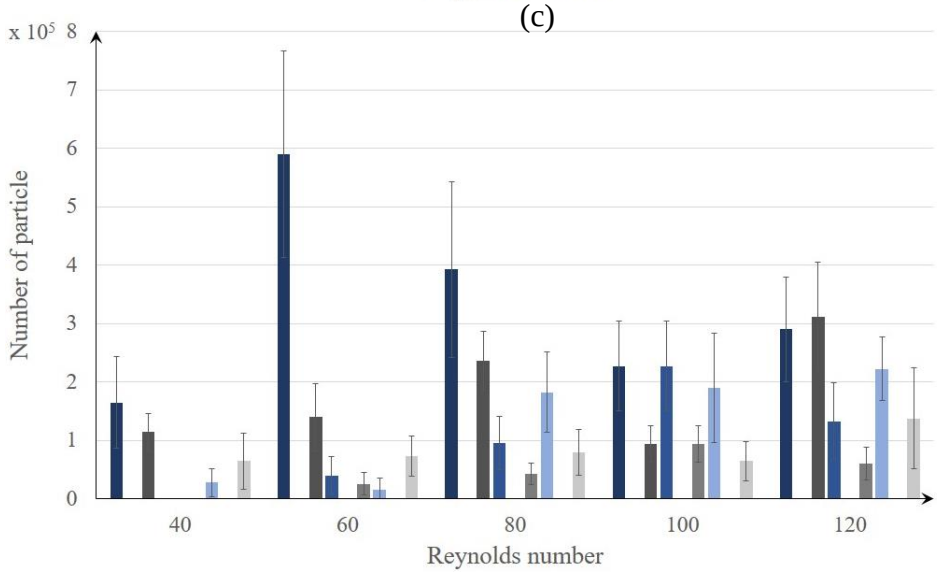

(d)

Figure 36 Raw data of the experiment of (a) 5, (b) 10, (c) 15, and (d) 20 μm bead

6.1.2 Separation efficiency (η)

The efficiencies were obtained by calculating the efficiency of each experiment using equation 5.1, then averaged them as the efficiency of separation of the experiment. The result is shown in Figure 37. Error bar was calculated from the standard deviation between three experiments.

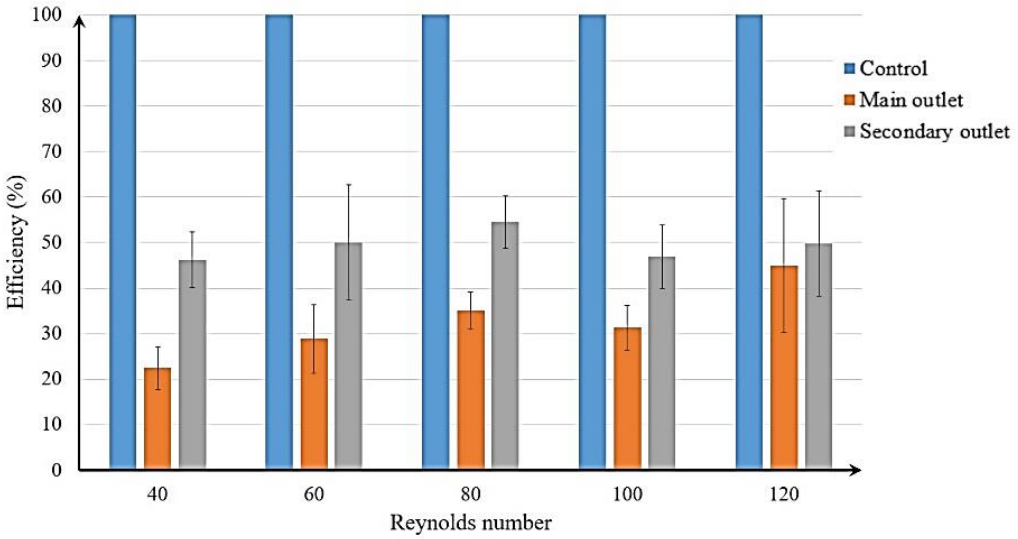

(a)

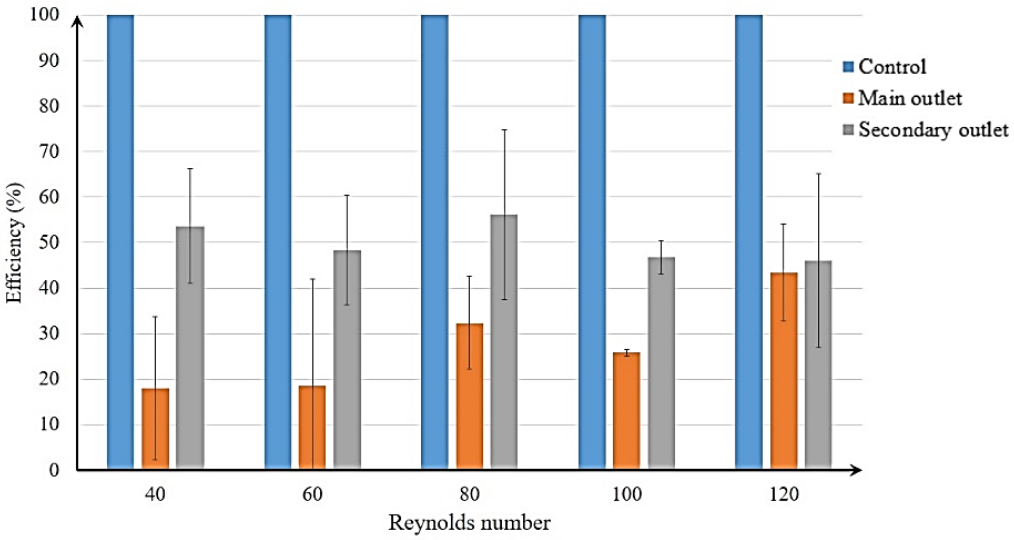

(b)

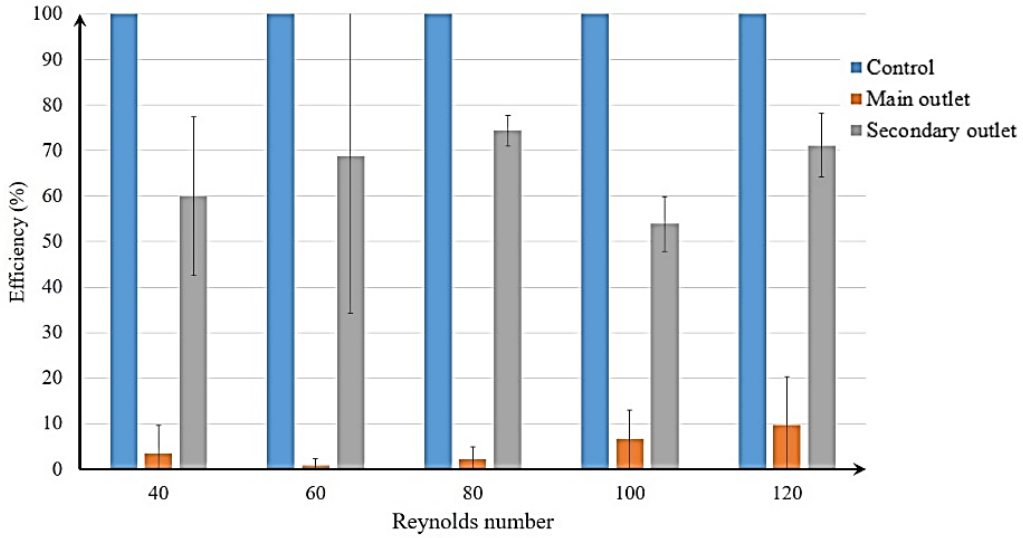

(c)

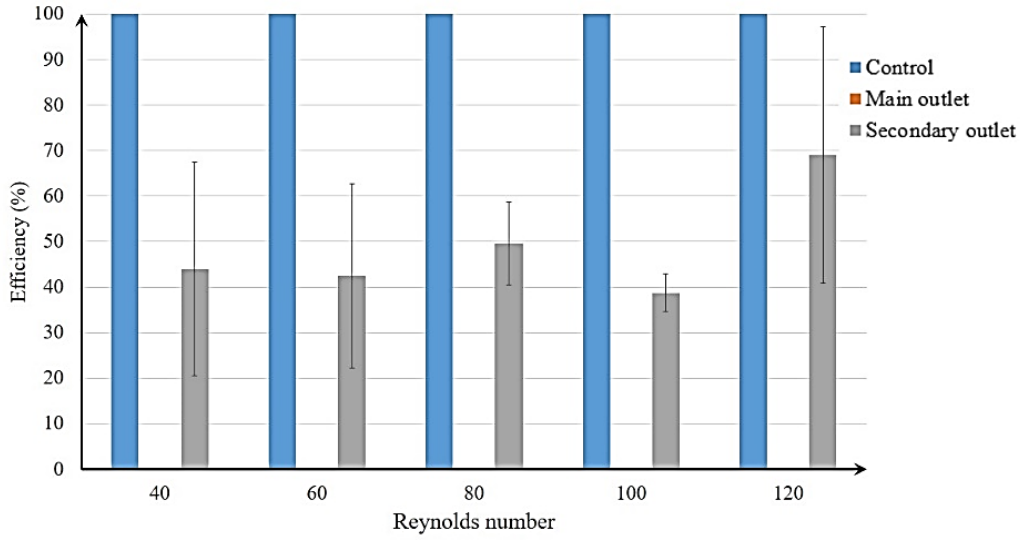

(d)

Figure 37 The separation efficiency of (a) 5, (b) 10, (c) 15, and (d) 20 μm bead of different Reynolds numbers

From Figure 37, the appearance of all beads at main outlet increases when the Reynolds number increases except the beads of 20 μm. On the other hand, the efficiency at the secondary outlet does not change much for every size of beads in the range of Reynolds number. The beads with 5 μm exist the most in main outlet at Reynolds

number of 120 with 45% efficiency, and appeared in the secondary outlet at nearly the same efficiency, around 45-55%, at every Reynolds number.

In case of 10 μm bead, the highest efficiency of the main outlet and secondary outlet are at Reynolds number of 120 at 43% and at Reynolds number of 80 at 55%, respectively. For 15 μm, Reynolds number of 120 provided 10%, the highest efficiency of separation at main outlet.

Nevertheless, there were no 20 μm bead turn up in the main outlet, and show up the most at Reynolds number of 120 with 69% at secondary outlet. However, the standard deviation is very high at due to experimentation of low concentration.

6.1.3 Missing percentage (λ)

Figure 38 represented the percentage of missing bead. In every Reynolds number, the bead with 20 μm disappeared the most comparing to other sizes. The lower Reynolds number it is, the higher missing percentage it gets for all beads.

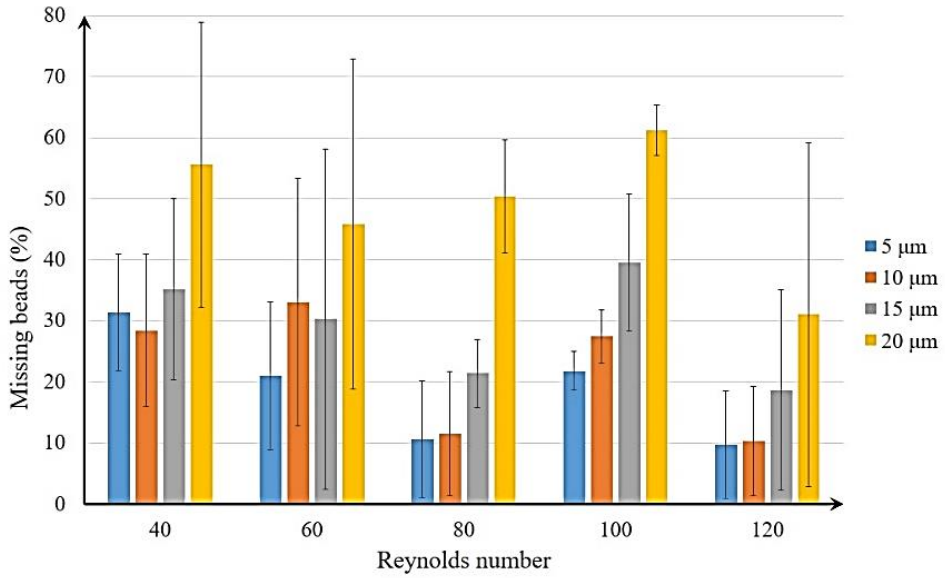

Figure 38 The missing percentage of the beads at different Reynolds numbers

6.1.4 Separation factor (X)

From Figure 39, it can be seen that the separation factor of every particle sizes decreases when the Reynolds number of the channel increases. For 20 μm bead, the separation factor is about 0.49 for all cases, which would imply that beads were entirely drawn out to the secondary channel at the first unit of expansion. The increasing of the Reynolds number of the channel results in the increment of drag force; therefore, the beads tend to be pushed out into main outlet as the separation factors were decreased. In all cases of Reynolds number of the flow, the velocity shear lift gradient force that acted on the bigger bead such as 15 and 20 μm, was higher than the drag force as the separation factors were relatively high.

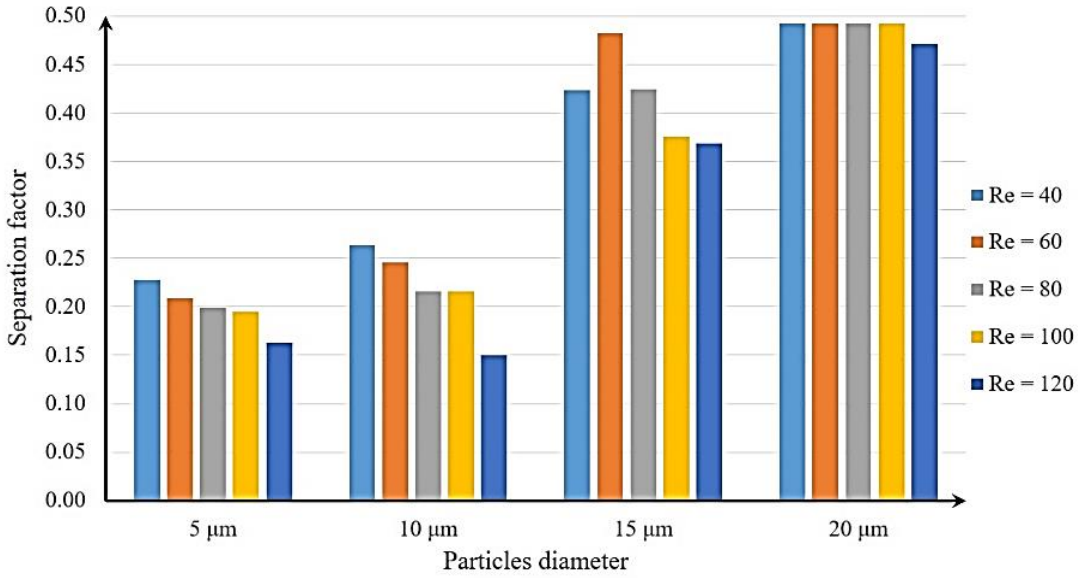

Figure 39 The separation factor of the beads at different Reynolds number

6.2 Expansion channel with 1,000 µm long

6.2.1 Flow pattern in expansion channel

As same as 500 µm long expansion channel, beads flow cross the streamline of fluid comparing to the simulation in Figure 27 in Chapter 4. Secondary flow area were increasing while the Reynolds number increased. The vortex starts to form at the Reynolds number of 80. The faster the flow is, the larger the vortex is. The flow patterns are shown in Figure 40.

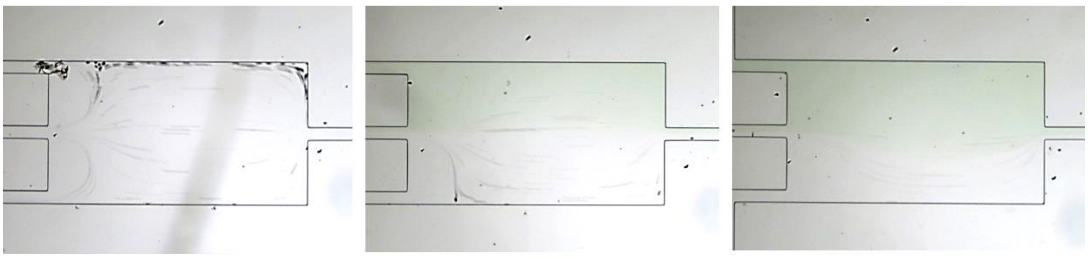

(a)

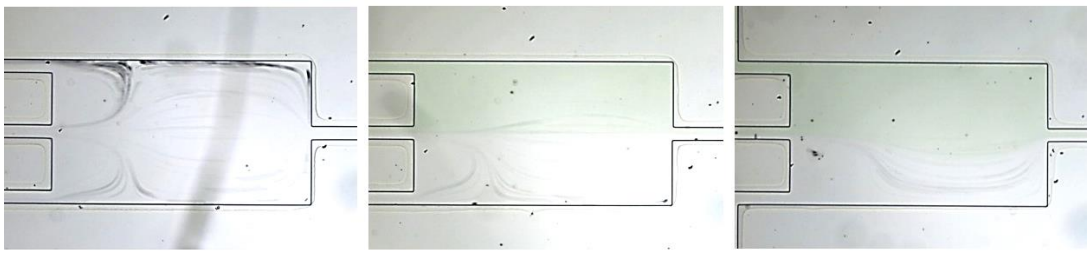

(b)

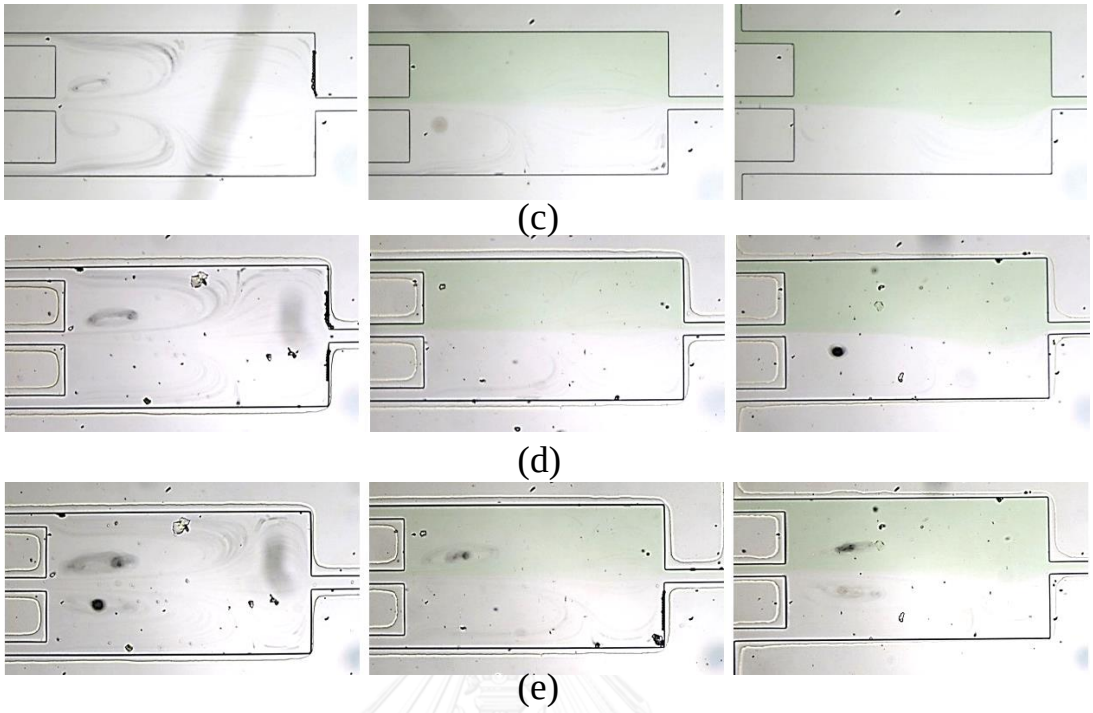

Figure 40 Flow pattern of 1st, 2nd, and 3rd channel of Reynolds number of (a) 40, (b) 60, (c) 80, (d) 100, and (e) 120.

The control sample were counted as 5 μm bead was suspended in the range between 3.94 x 10^6 to 8.37 x 10^6 bead/ml, 10 μm was counted from 2.1 x 10^6 to 5.28 x 10^6 bead/ml, 15 μm was counted from 5.48 x 10^5 to 1.89 x 10^6 bead/ml, and 20 μm was counted from 0 to 4.64 x 10^5 bead/ml. The raw data of the experiments are shown in Figure 36. The experiments were done for all beads at Reynolds numbers between 40 - 120. Three tests were repeated for all cases.

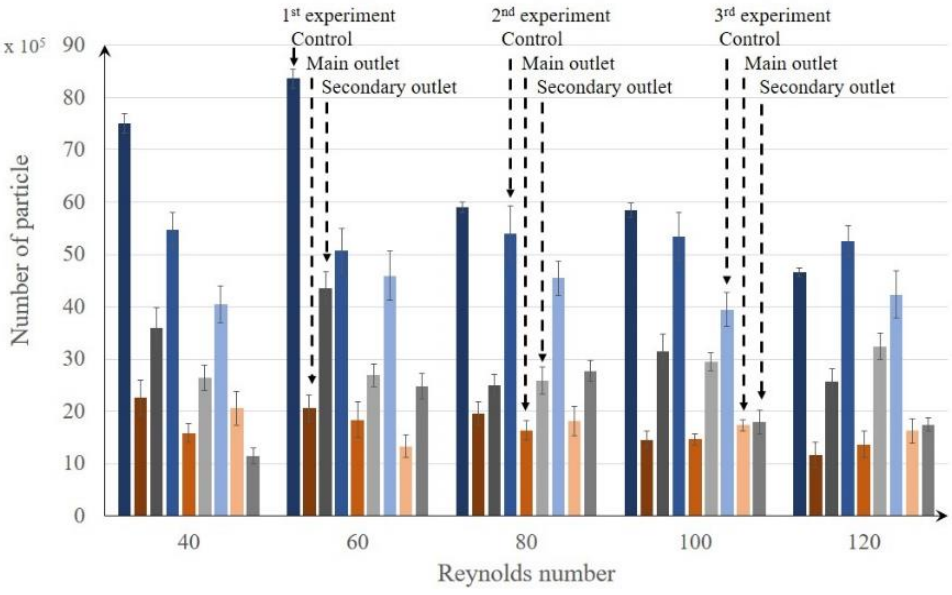

(a)

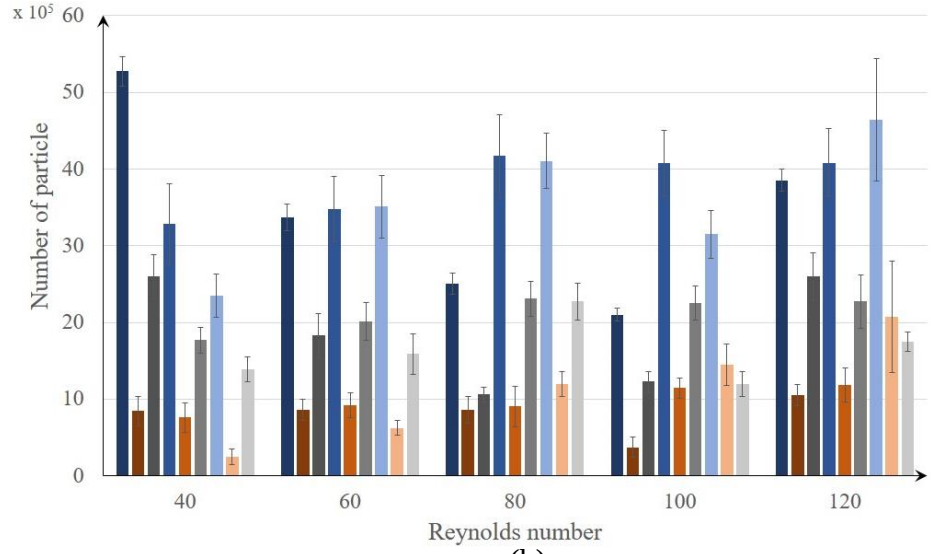

(b)

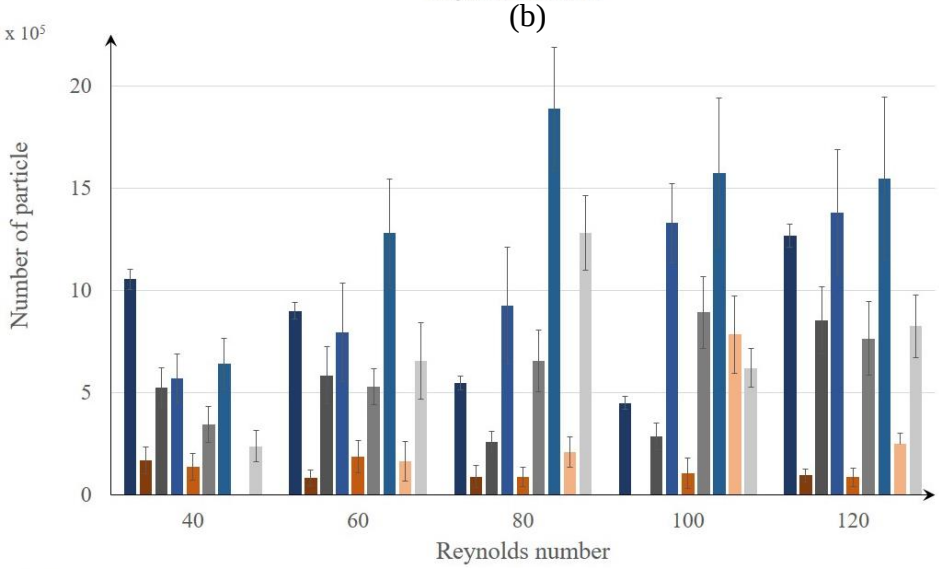

(c)

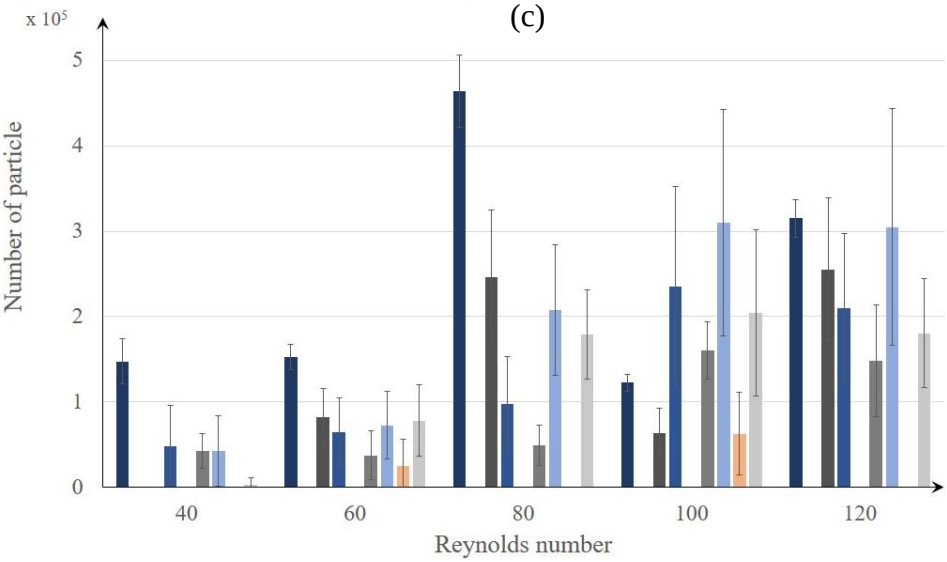

(d)

Figure 41Raw data of the experiment of (a) 5, (b) 10, (c) 15, and (d) 20 μm bead

6.2.2 Separation efficiency (η)

From Figure 42, the beads at secondary outlet does not change much for every Reynolds number of the channel except for the beads with 20 μm. The beads with 5 μm appeared the most in the main outlet at Reynolds number of 40 with 37% efficiency, and exist in the secondary outlet at nearly the same efficiency, about 50% efficiency at every cases of the flow

For the beads with 10 μm, the separation efficiency of main outlet increases when the Reynolds number increases. The highest separation efficiency of main outlet is 34% at the Reynolds number of 120, but the separation efficiency of the secondary outlets are almost the same at 50% of every Reynolds numbers. In case of 15 μm, Reynolds number of 100 provided 19% separation efficiency at the main outlet, which is the highest efficiency.

Moreover, the beads with 20 μm were found at the main outlet at the Reynolds number of 60 for 12% of separation efficiency, and has the highest separation efficiency at 70% at secondary outlet. Nevertheless, this low concentration experiment affects the standard deviation to be high.

Comparing between the expansion with 500 μm long and 1,000 μm long, the length does not have an obvious influence on the separation efficiency on a small beads with 5 and 10 μm. Other than that, the beads with 20 μm appeared at the secondary outlet since the Reynolds number of 40 of the expansion channel with 1,000 μm long. This is implies that the drag force of the expansion with 1,000 μm long has stronger effects than the expansion channel with 500 μm long.

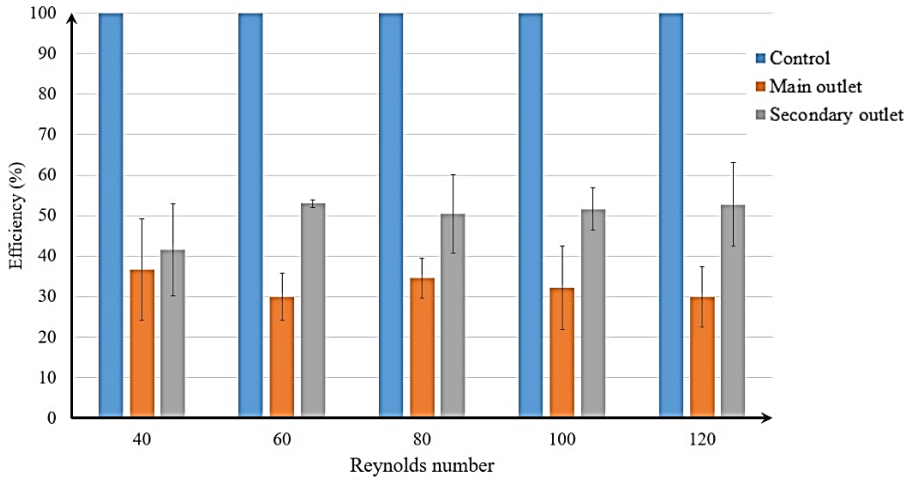

(a)

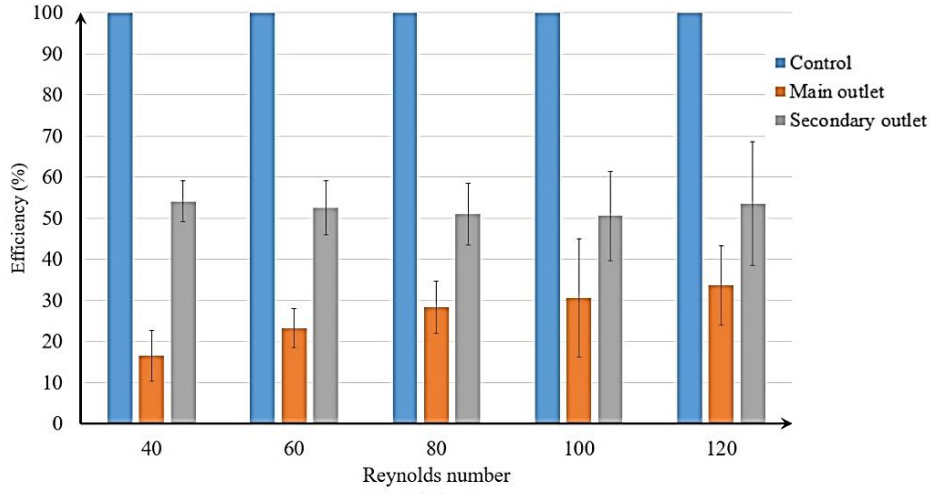

(b)

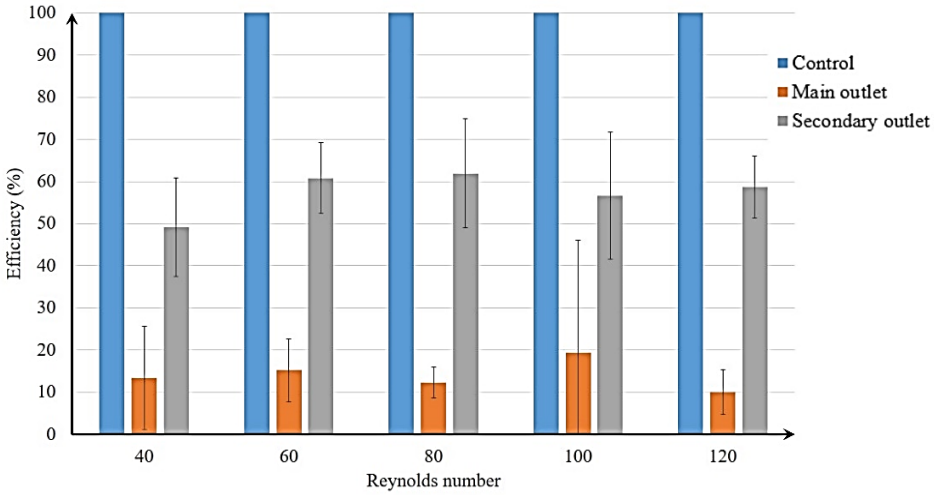

(c)

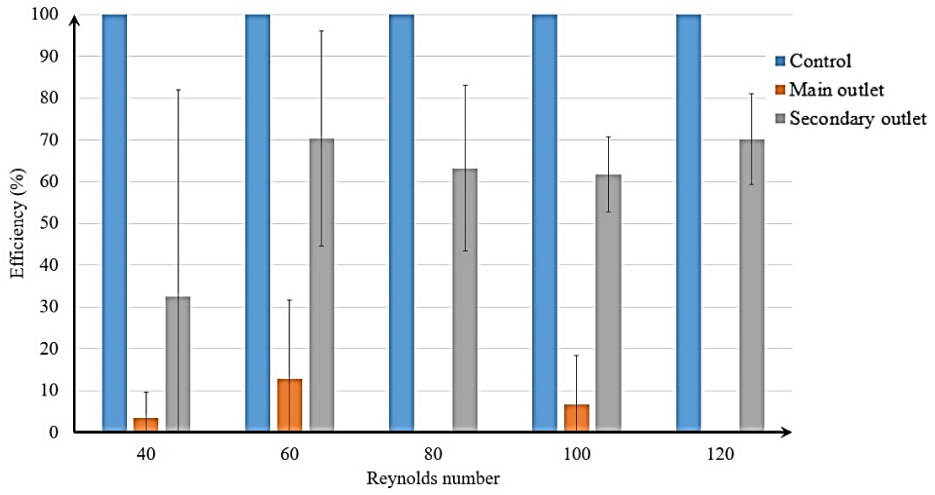

(d)

Figure 42 The separation efficiency of (a) 5, (b) 10, (c) 15, and (d) 20 μm bead of a different Reynolds numbers

6.2.3 Missing percentage (λ)

From Figure 43, the missing percentage is lower with the higher Reynolds number of the flow. Most of the flow rate, the beads with 20 μm seems to be missing more than other sizes. This is similar to the experiments with the expansion of 500 μm long.

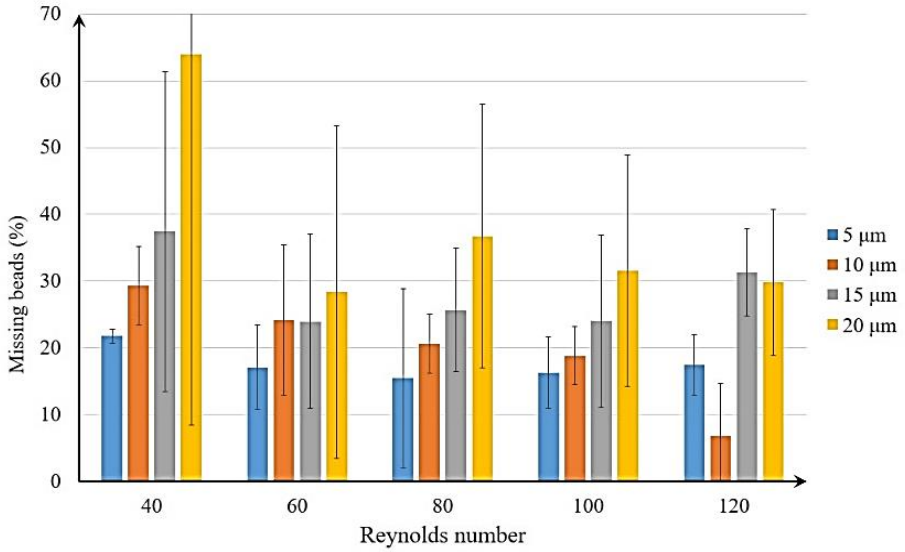

Figure 43 The missing percentage of the beads at different Reynolds numbers

6.2.4 Separation factor (X)

The separation factor of every sizes of the particle tends to increase as the Reynolds number of the flow increase as shown in Figure 44. The tendency is opposite to that with 500 μm long expansion chamber. At higher Reynolds number, the vortex grew bigger and prevented the back-flow to the main channel. The effects of the increment of Reynolds number on the magnitude of drag force were small comparing to the expansion with 500 μm long.

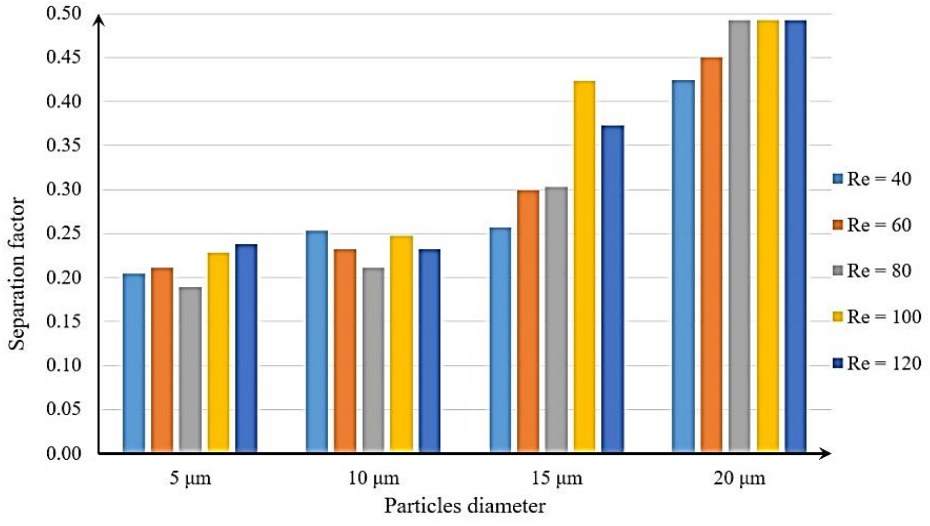

Figure 44 The separation factor of the beads at different Reynolds number

6.3 Sedimentation

While the pump injecting the sample, there were some beads those do not move inspected. This implied that there was sedimentation inside the chip at the big secondary outlet as shown in Figure 45. This sedimentation affected to the efficiency of the separation, mostly by reducing the efficiency of the secondary outlet. Moreover, the sedimentation did not only took place in the chip, but also exist in the silicon tube and other kit of the experiment too.

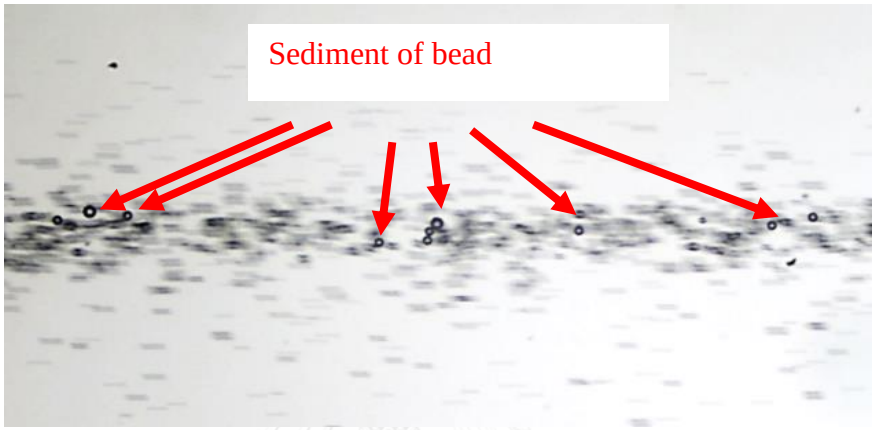

Figure 45 The sedimentation of the bead

6.4 Conclusion

The velocity of the flow of the channel increased as the Reynolds number increased, and the vortex had the size comparable to the expansion at Reynolds number of 80 for the expansion chamber with 500 μm long. On the other hand, the vortex area in expansion chamber with 1,000 μm long can still be increased in the experimented range of Reynolds number. As the flow exceed that certain Reynolds number, the size of vortex still increases, and occupied the area of the flow of the secondary channel.

Most of the efficiency of the separation for both main and secondary outlet of the small beads, 5 and 10 μm, are around 30% – 50% at every Reynolds number for both expansion channel length. On the contrary, the big beads, 15 and 20 μm were mostly separated to the secondary channel.

For the expansion channel with 500 μm long, the higher Reynolds number it gets the lower separation factor. On the contrary, the higher Reynolds number of the expansion channel with 1,000 μm long it has the higher separation factor. Therefore, the separation factor could be improved by lowering the Reynolds number in expansion channel with 500 μm long, and raising the Reynolds number in expansion channel with 1,000 μm long.

The missing of the beads mostly occurred in the secondary channel since at the big channel, connecting each secondary channel, the flow is very slow. This results in the sedimentation of the beads. Other than that, after the particle flow through out from

the chip, there was a silicone tube leading the sample to the tube connected. So this means that the sample, passed through the chip, has more possibility to be lost.

The selected condition for the next experiment with whole blood is the flow with Reynolds number of 80 in the expansion channel with 500 μm long. The microfilariae were predicted as a big particles, which would be separated to the secondary channel.

Chapter 7
Whole Blood Experiment

7.1 Sample preparation

The experiment was done with the same procedures for polystyrene bead, but deionized water was replaced by normal saline solution to prevent the lysing of blood cell. At first, whole blood sample was diluted with normal saline solution with the ratio of 1 to 20. Then the experiment was done with the Reynolds number of 80 with the expansion chamber with 500 μm long. After that, control sample and those collected at both outlets were counted by hemocytometer. It is clear that the number of microfilaria in the sample was very low in the blood sample (less than 1 microfilaria per 10 μl of blood) in which it is very hard to find microfilaria in the hemocytometer. The picture of cell in hemocytometer are shown in Figure 46. Therefore, the procedure was changed. The whole blood had been spun by centrifuge at 3000 rpm, to increase the concentration microfilaria and blood cell. Later, the bottom portion of the sample in the tube was drawn by micropipette and diluted with normal saline solution. Therefore, the sample contained more microfilaria and probably fewer blood cell. After the experiment, 10 μl sample was injected in hemocytometer and counted in all area of it, since the number of microfilaria is too less to be counted by the grid.

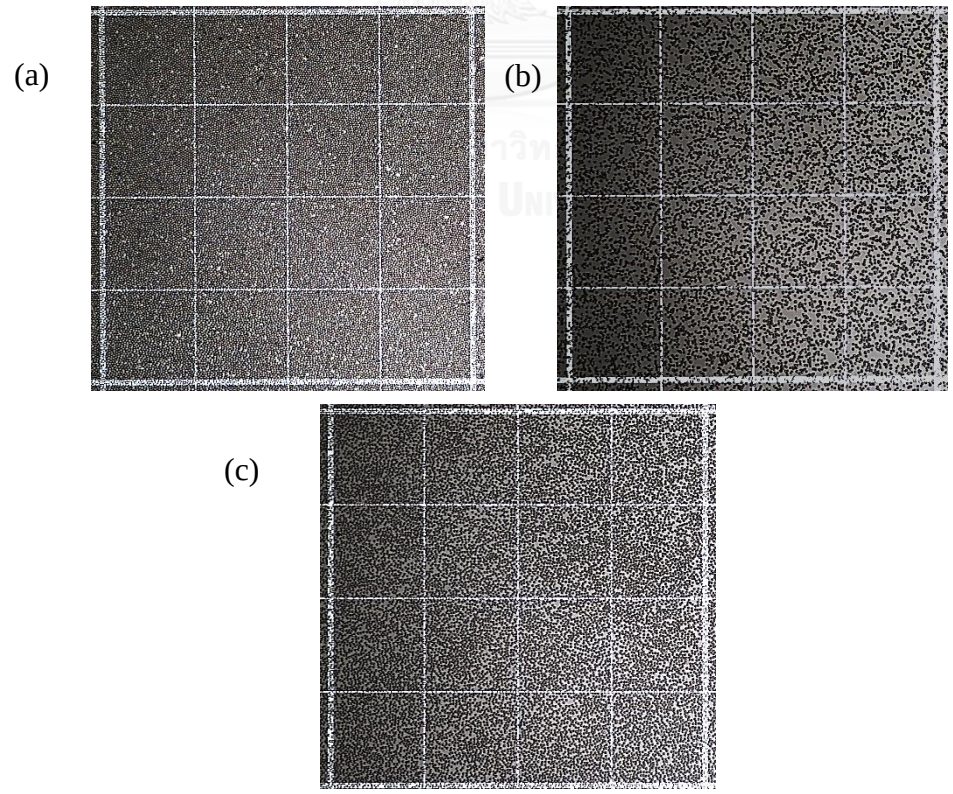

Figure 46 (a) Control sample, (b) Main outlet, and (c) Secondary outlet.

7.2 Results

7.2.1 Flow patterns in expansion channel

Flow pattern inside the channel are similar to the flow of the bead experiment in Chapter 5.

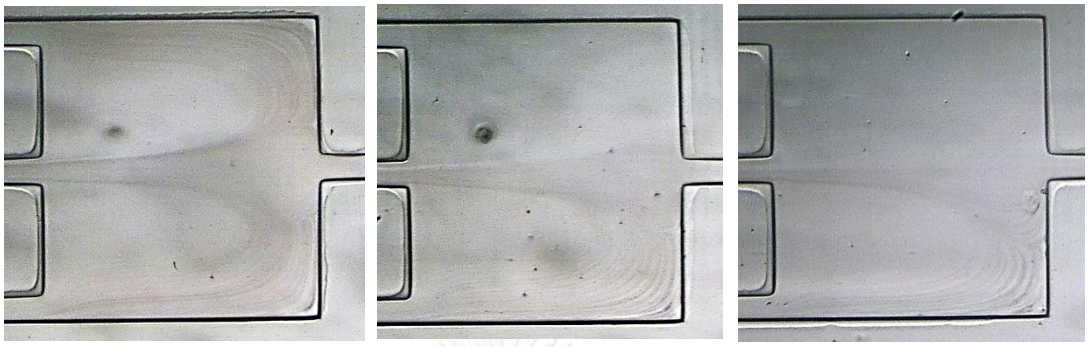

Figure 47 Flow pattern of the 1st, 2nd, and 3rd, channel of blood experiment

7.2.2 Separation percentage of the worm

The experiment was repeated twice. The worms were surprisingly drawn out to the main outlet. Furthermore, there is no microfilaria found at secondary outlet. The average number of microfilaria in controlled sample and secondary outlet are 9.33 and 11.67 ± 1.41 worms per 10 μl, respectively.

Microfilaria acts unlikely to beads in the fluid flow. To be more precise, the microfilaria would flow out at the secondary channel if it behave like a big particle. On the other hand, the microfilaria would be separated to both outlets. If the microfilaria act as a small particle.

From the result, this may be the result of the alignment of the worm in the channel. In addition, the worm is more than four times longer than the width of the channel. Together with, the velocity of the main channel is 1.58 m/s. With all factors, the worm acted unlike the particle, and passed to the main outlet.

7.3 Conclusion

The whole blood sample was tested in the Reynolds number of 80. The blood cell concentration was too thick to be able to observe the microfilaria. Furthermore, there were not a lot of microfilaria. Therefore, the blood was centrifuged to condense the concentration of the microfilaria and to dilute the blood cell.

After the experiment, the result represents that all of the microfilariae were pushed through the main outlet. The concentration of the microfilaria was also increased. Thus, the contration-expansion channel not only 100% separated the microfilaria to the main outlet, but also decreased the concentration of blood cell in the sample too.

Chapter 8
Conclusion

This project studied and developed the separation of microfilaria from the blood by using a microfluidic. The separation method based on the difference of the sizes of the particles, blood cells and microfilaria. The filtration is the simple technique to capture the specific object based on its size. However, the previous study reported problem of the high density of red blood cells that is much higher than the microfilaria. To develop the high efficiency of the separation, the main target should be a separating blood cells out before the employment of filters to detect microfilaria.

The filtering chips using microcapillaries as a wall were fabricated based on the shape of Hele-Shaw equation. The red blood cell should pass through the capillaries, while microfilaria should be kept inside and flow directly to the end of the chip. There were four types of the channel, inlet width of 200 and 500 μm and channel length of 10 and 20 mm. The first experiment was done by varying the ratio of dilution between blood and normal saline solution into 1 to 1, 1 to 10 and 1 to 15. In every cases of the experiment blood samples were flowed at 2.0 ml/h. The main problem is the concentration of red blood cells, which block all the microcapillaries. By this blocking, the pressure across the wall was risen by the decreasing of the flow area. This increment of the pressure broke the bonding between the PDMS layers. Other than that, in the case of 1:1 ratio case, the water was injected in to the channel to lyse and flush blood cells. The result was not as expected, the red blood cell lysed, stick with other hemorrhage blood cells and completely blocked the channel. Accordingly, the next experiment was done by varying the flow rate into two flow rates, which are 2 ml/h and 0.5 ml/h. In this case the sample was diluted with 1 to 25. The efficiency of the separation is decreased by lowering the flow rate from 33% to 13%, because of the sedimentation of particles in the syringe while the sample was injected. However, the problem with blood cells is still remained. The main problem that should be focused on is the density of the blood cell in whole blood sample.

From the results, it can be concluded into two points. The first one is that there is too much blood cells in the sample. These cell clogged inside the filter and decreased the flow area of the fluid, resulting in a higher pressure and finally caused the damage to the chip. The second point is the shape of microcapillaries wall, this shape promotes the jet profile in the channel. The jet profile pushes particles to both side of the wall, only little amount of sample reached to the end of the chip. The highest efficiency occurred in the chip with 500 wide inlet and 20 mm long channel. The results showed that the higher the flow rate and dilution ratio is, the higher efficiency of separation would be.

Therefore, there must be a mechanism that draws out the blood cell before entering the filtration zone. This part of the device should bringt only microfilaria and

some remained red blood cell to the detection zone. With the criteria, Contraction-Expansion arrays chip was selected to coarsely separate the blood cell and microfilaria. The contraction connected each three expansions in series together. There are two secondary channels connected on both sides, top and below, of the expansion. Each secondary channel is connected to the secondary outlet of the chip. The channel works by separating the particles by their size. The big particle would leave the expansion by secondary channels. On the other hand, small particle would exit the expansion channel by the main outlet.

Contraction and Expansion arrays were fabricated. The channel is 60 μm deep. The contraction channel is 50 μm wide. The expansion channel was designed into two types, 500 μm long and 550 μm wide and 1000 μm long and 550 μm wide. The ratio of the resistance of the channel between secondary channel and main channel is fixed at 14 times.

After that, the simulation was done using COMSOL 5.2. The flow simulations were achieved in five Reynolds numbers such as 40, 60, 80, 100, and 120. Flow area and velocity profile were determined. The volume flow rate separates to each outlet is almost the same for all conditions. Velocity profile changes as the flow rate changes. However, both of the information did not represent the separation efficiency. Thus, the experiment must be done with the polystyrene beads as the particle. Red blood cells, white blood cells, and microfilaria were replaced by 5 μm, 10-15 μm, and 20 μm beads, respectively.

In preliminary experiments, there were problems such as the clogging of the beads, the contaminated particles that blocked the channel. At first, the clamping mechanism was selected to replace the bonding. By not bonding with plasma, the PDMS can be separated and cleaned. With the configuration of the channel, clamping was not suitable, the fluid and particles leaked out of the chip. After that, the filtering was chosen to filter the contaminated particles out of the sample before injected to the channel. After using the cell strainer with pore size of 40 μm to filter the groups of beads or the contaminated particle, there was only very small particle found in the channel, which would not blocked the channel while doing the experimnets.

All Reynolds number were done three times each of the experiment. After the flow, 10 μl was examined from each sample; control, main outlet, and secondary outlet. The results showed that small beads such as 5 and 10 μm, had an efficiency of separation around 30% at main outlet and 50% at the secondary outlet for both expansion channel lengths. On the other hand, beads with 15 and 20 μm were mostly separated to the secondary outlet. The expansion channel with 1,000 μm long showed higher percentage of big particle, moved to the main outlet, than the expansion channel with 500 μm long. The missing percentage is higher for the bigger beads than the smaller ones in every cases of the Reynolds number. Not only for the size of the particle, the missing percentage is higher when the Reynolds number of the flow is lower. The separation factor of 5, 10, and 15 μm in the expansion with 500 μm long was decreased

when the Reynolds number of the flow increased. On the contrary, the separation factor of beads in the expansion with 1,000 μm long was increased with the higher Reynolds number. For the beads with 20 μm, the separation factors are almost the same. The beads with 20 μm were almost entirely sorted into the secondary channels for all experiments. It could be concluded that the separation factors for beads could be improved by decreasing the Reynolds number of the flow in the expansion channel with 500 μm long, and by increasing the Reynolds number in the expansion channel with 1,000 μm long. From the hypothesis, the microfilaria was predicted to behave similar to a large spherical bead. Therefore, the conditions of the flow should separate the small bead to the main outlet and the big particle to secondary channel were selected for the separating of microfilariae. In conclusion, the expansion channel with 500 μm long at Reynolds number of 80 was selected to be used with the whole blood experiment.

For the blood experiment, the blood sample was diluted with normal saline solution, with the ratio 1 to 20. In preliminary experiments, both outlets showed that there are too many red blood cells that made the detection of the microfilaria difficult. Thus, the blood sample was centrifuged at 3,000 rpm for 10 minute. Then, 500 μl at the bottom of the sample was drawn out and diluted with the normal saline solution with the ratio of 1:20. From the whole blood experiment, the number of microfilaria is too little to be seen in a gridline in hemocytometer. Therefore, the counting procedure was changed from the number of microfilaria per square millimeter to number of microfilaria per 10 μml of the sample. The result came out surprisingly as the chip can separate 100% of microfilaria successfully at the main outlet. It could be concluded that microfilaria did not flow and act like particles. Moreover, the concentration of the microfilaria is slightly increased. This design shows that contraction-expansion arrays can be used to coarsely separate the microfilaria from the blood before entering detection zone, and the filter must be placed at the main outlet.

REFERENCES

[1] W. James and C. Bill, "Global Warming's Increasingly Visible Impact Environment defense," pp. 1-43, 2005.

[2] C. f. D. C. a. Prevention. (2012, November 30, 2015). *Biology - Life Cycle of D. immitis*. Available: http://www.cdc.gov/parasites/dirofilariasis/biology_d_immitis.html

[3] D. F. S. E. Staff. (2007, November 30, 2015). *Heartworm (Dirofilaria immitis) Infection & Prevention in Dogs*. Available: http://www.peteducation.com/article.cfm?c=2+2096&aid=743

[4] e. a. Sathaporn Jittapalapong, "Prevalence of Heartworm Infection of Stray Dogs and Cats in Bangkok Metropolitan," *Kasetsart University Library/Learning Center (KULC),* 2003.

[5] J. W. McCall, C. Genchi, L. H. Kramer, J. Guerrero, and L. Venco, "Chapter 4 Heartworm Disease in Animals and Humans," vol. 66, pp. 193-285, 2008.

[6] A. H. MOODY and P. L. CHIODINI, "Methods for the detection of blood parasites," *Clin. Lab. Haem,* 2000.

[7] J. M. Martel and M. Toner, "Inertial focusing in microfluidics," *Annu Rev Biomed Eng,* vol. 16, pp. 371-96, Jul 11 2014.

[8] X. Yuan, L. Yi, H. Michael, L. Joseph, and W. Pak Kin, "A Microfiltration Device for Urogenital Schistosomiasis Diagnostics," *PLoS One,* 2016.

[9] M. Cornaglia, L. Mouchiroud, A. Marette, S. Narasimhan, T. Lehnert, V. Jovaisaite, *et al.*, "An automated microfluidic platform for C. elegans embryo arraying, phenotyping, and long-term live imaging," *Sci Rep,* vol. 5, p. 10192, May 07 2015.

[10] H. Bridle, B. Miller, and M. P. Desmulliez, "Application of microfluidics in waterborne pathogen monitoring: a review," *Water Res,* vol. 55, pp. 256-71, May 15 2014.

[11] X. Wang, R. Hu, A. Ge, L. Hu, S. Wang, X. Feng, *et al.*, "Highly efficient microfluidic sorting device for synchronizing developmental stages of C. elegans based on deflecting electrotaxis," *Lab Chip,* vol. 15, pp. 2513-21, Jun 7 2015.

[12] M. Zhan, Y. Cho, and H. Lu, "Automatic Long-term Microfluidic Platform for Individual tracking of Healthspan and Longevity of Caenorhabditis Elegans," *19th International Conference on Miniaturized System for Chemistry and Life Sciences,* 2015.

[13] V. Nock, A. Tayagui, and A. Garrill, "Elastomeric Micropillar Arrays for The Study of Protrusive Forces in Hyphal Invasion," *19th International Conference on Miniaturized System for Chemistry and Life Sciences,* 2015.

[14] T. Huang, C. P. Jia, Y. Jun, W. J. Sun, W. T. Wang, H. L. Zhang, *et al.*, "Highly sensitive enumeration of circulating tumor cells in lung cancer patients using a size-based filtration microfluidic chip," *Biosens Bioelectron,* vol. 51, pp. 213-8, Jan 15 2014.

[15] T. Masuda, M. Niimi, H. Nakanishi, Y. Yamanishi, and F. Arai, "Cancer cell separator using size-dependent filtration in microfluidic chip," *Sensors and Actuators B: Chemical,* vol. 185, pp. 245-251, 2013.

[16] T. Kobayashi and S. Konishi, "Microfluidic chip with serially connected filters for improvement of collection efficiency in blood plasma separation," *Sensors and Actuators B: Chemical,* vol. 161, pp. 1176-1183, 2012.
[17] A. Sin, S. K. Murthy, A. Revzin, R. G. Tompkins, and M. Toner, "Enrichment using antibody-coated microfluidic chambers in shear flow: model mixtures of human lymphocytes," *Biotechnol Bioeng,* vol. 91, pp. 816-26, Sep 30 2005.
[18] D. Lange, C. W. Storment, C. A. Conley, and G. T. A. Kovacs, "A microfluidic shadow imaging system for the study of the nematode Caenorhabditis elegans in space," *Sensors and Actuators B: Chemical,* vol. 107, pp. 904-914, 2005.
[19] M. Corporation, "Vector-Borne-Diseases," pp. 1-16, 2009.
[20] P. A. M. A. Rani, P. J. Irwin, M. Gatne, G. T. Coleman, and R. J. Traub, "Canine vector-borne diseases in India: a review of the literature and identification of existing knowledge gaps," *Parasites & Vectors,* 2010.
[21] P. Shearer, "Heartworm Disease," *BARK Putting Knowledge into Practice,* pp. 1-16, 2011.
[22] M. e. al., "Morphometric analyses of canine blood microfilariae isolated by the Knott's test enables Dirofilaria immitis and D. repens species-specific and Acanthocheilonema (syn. Dipetalonema) genus-specific diagnosis," *Parasites & Vectors,* pp. 1-5, 2013.
[23] S. E. Hulme, S. S. Shevkoplyas, J. Apfeld, W. Fontana, and G. M. Whitesides, "A microfabricated array of clamps for immobilizing and imaging C. elegans," *Lab Chip,* vol. 7, pp. 1515-23, Nov 2007.
[24] J. Wang, X. Feng, W. Du, and B. F. Liu, "Microfluidic worm-chip for in vivo analysis of neuronal activity upon dynamic chemical stimulations," *Anal Chim Acta,* vol. 701, pp. 23-8, Sep 2 2011.
[25] N. Ghorashian, S. K. Gokce, S. X. Guo, W. N. Everett, and A. Ben-Yakar, "An automated microfluidic multiplexer for fast delivery of C. elegans populations from multiwells," *PLoS One,* vol. 8, p. e74480, 2013.
[26] X. L. Do-Hyun Lee, and Abraham P. Lee, "An Integrated Microfluidic Platform For Size-Selective Single-Cell Trapping," *19th International Conference on Miniaturized System for Chemistry and Life Sciences,* p. 3, October 25-29, 2015 2015.
[27] J. Chen, D. Chen, T. Yuan, X. Chen, Y. Xie, H. Fu, *et al.*, "Blood plasma separation microfluidic chip with gradual filtration," *Microelectronic Engineering,* vol. 128, pp. 36-41, 2014.
[28] A. J. Laki, G. Z. Nagy, K. Ivan, O. Jacso, E. Fok, and P. Civera, "Integrated microcapillary system for microfluidic parasite analysis," *IEEE Xplore Digital Library,* 2013.
[29] A. J. Laki, K. Iván, É. Fok, and P. Civera, "Filtration of Nematodes using an Integrated Microcapillary System," *BioNanoScience,* vol. 4, pp. 338-348, 2014.
[30] S. W. Lee, K. A. Hyun, S. I. Kim, J. Y. Kang, and H. I. Jung, "Continuous enrichment of circulating tumor cells using a microfluidic lateral flow filtration chip," *J Chromatogr A,* vol. 1377, pp. 100-5, Jan 16 2015.
[31] M. G. C. Lee, S. Park, J. K., "Inertial separation in a contraction-expansion array microchannel," *J Chromatogr A,* vol. 1218, pp. 4138-43, Jul 8 2011.

[32] M. G. Lee, J. H. Shin, S. Choi, and J.-K. Park, "Enhanced blood plasma separation by modulation of inertial lift force," *Sensors and Actuators B: Chemical,* vol. 190, pp. 311-317, 2014.

[33] S. C. Hur, A. J. Mach, and D. Di Carlo, "High-throughput size-based rare cell enrichment using microscale vortices," *Biomicrofluidics,* vol. 5, p. 22206, Jun 2011.

[34] T. M. Geislinger and T. Franke, "Hydrodynamic lift of vesicles and red blood cells in flow--from Fahraeus & Lindqvist to microfluidic cell sorting," *Adv Colloid Interface Sci,* vol. 208, pp. 161-76, Jun 2014.

[35] J. Z. e. al., "Inertial focusing in a straight channel with asymmetrical expansion-contraction cavity arrays using two secondary flows," *Journal of Micromechanics and Microengineering,* pp. 1-13, 2013.

[36] X. Wang, J. Zhou, and I. Papautsky, "Vortex-aided inertial microfluidic device for continuous particle separation with high size-selectivity, efficiency, and purity," *Biomicrofluidics,* vol. 7, 2013.

[37] X. Wang and I. Papautsky, "Size-based microfluidic multimodal microparticle sorter," *Lab Chip,* vol. 15, pp. 1350-9, Mar 7 2015.

[38] X. W. a. I. Papuatsky, "Inertial Microfluidic Vortex Sorter for Cotinuous Isolation of Rare Cells From Blood With 15,000X Enhanced Purity," *19th International Conference on Miniaturized System for Chemistry and Life Sciences,* p. 3, October 25-29, 2015 2015.

[39] X. Wang, X. Yang, and I. Papautsky, "An integrated inertial microfluidic vortex sorter for tunable sorting and purification of cells," *Technology,* vol. 04, pp. 88-97, 2016.

[40] S. U. e. al., "Design and Construction of a Linear Shear Stress Flow Chamber," *Annals of Biomedical Engineering,* vol. Vol. 21, pp. pp. 77-83, 1993.

APPENDIX

APPENDIX

The expansion channel with 500 μm long at Re = 40

Control

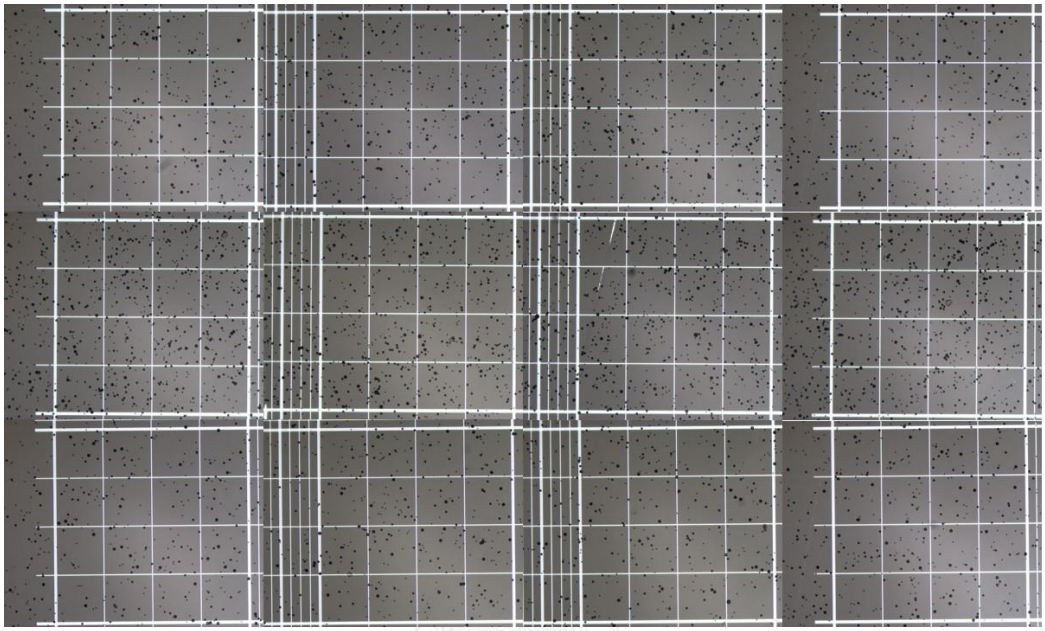

Main outlet

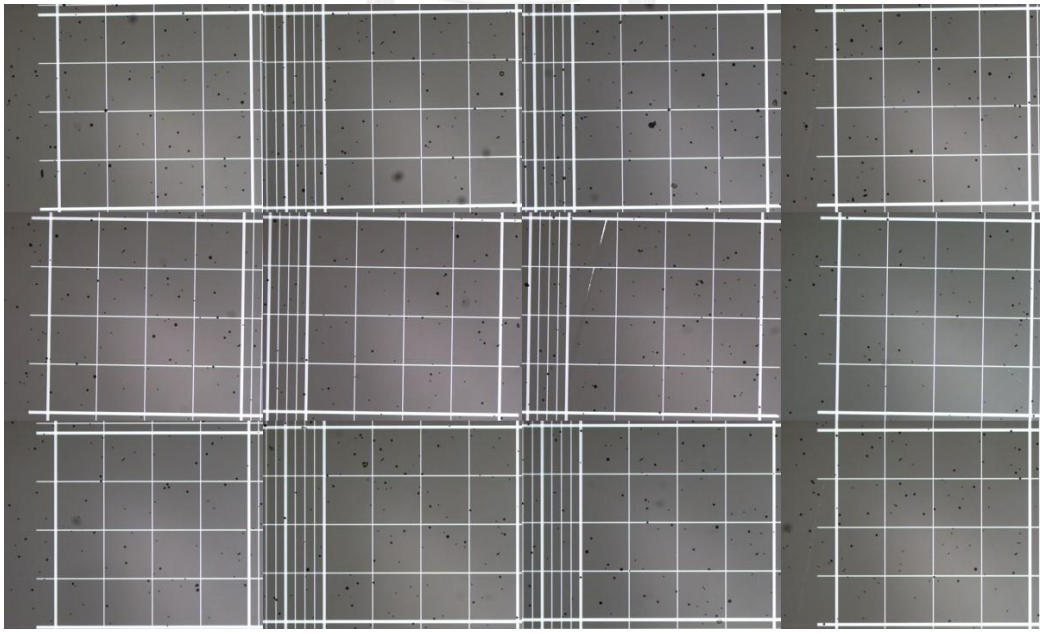

Secondary outlet

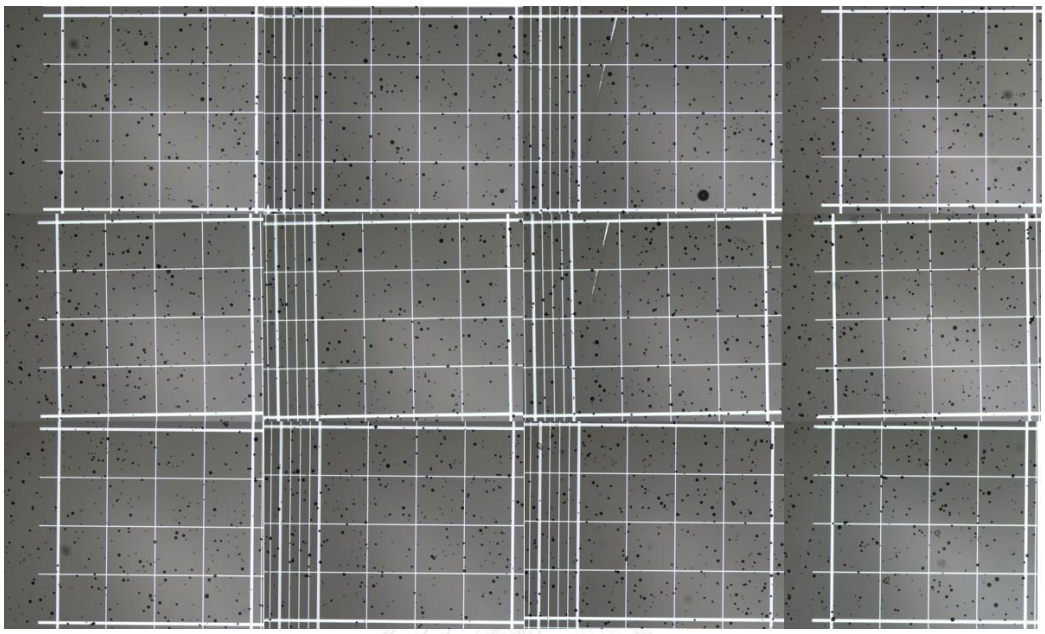

The expansion channel with 500 μm long at Re = 60

Control

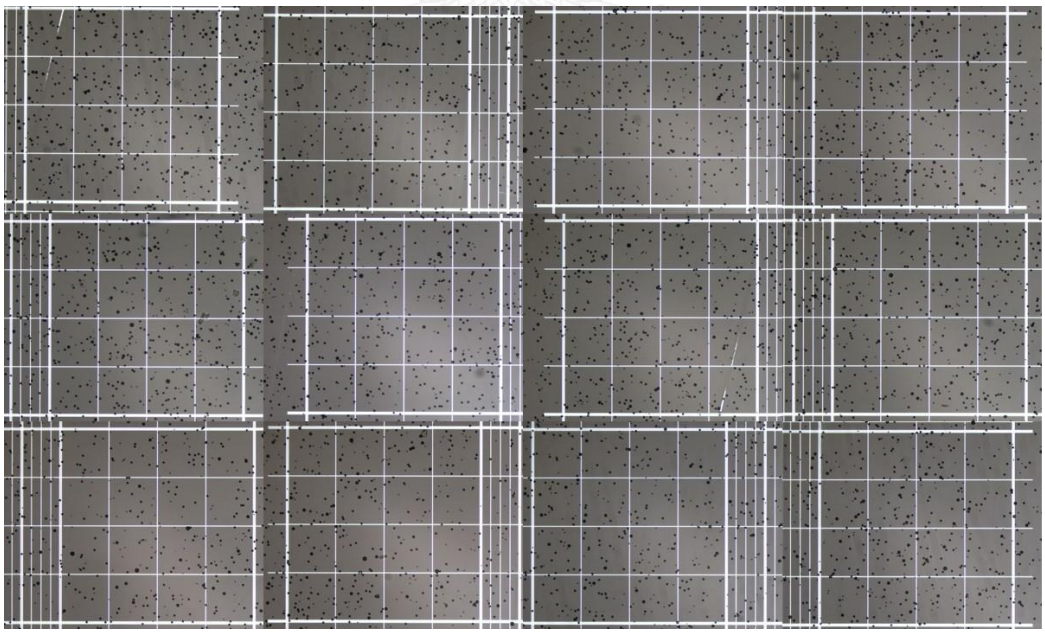

Main outlet

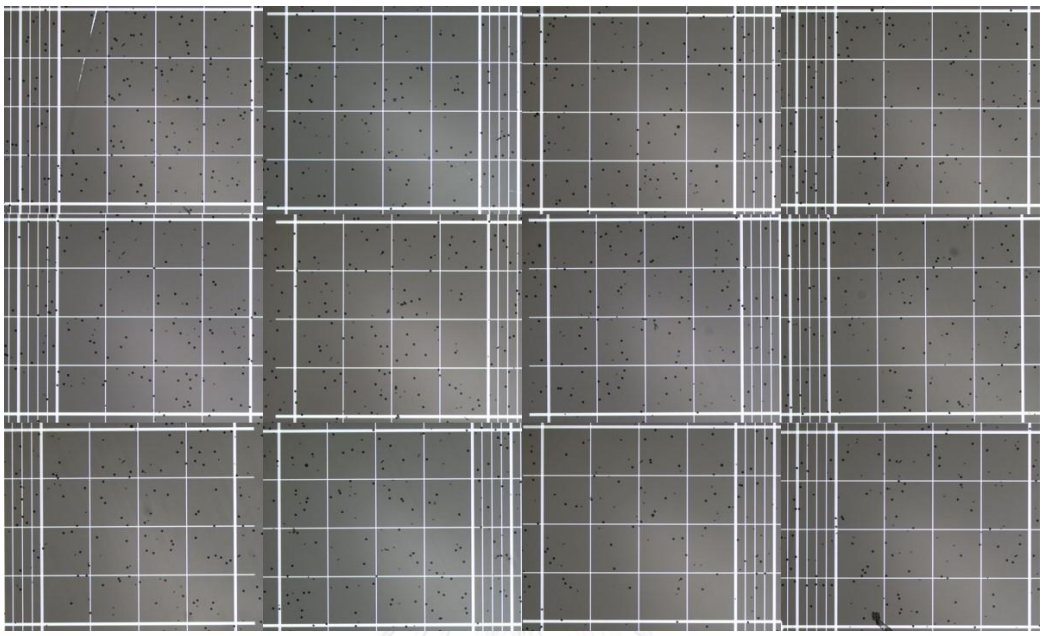

Secondary outlet

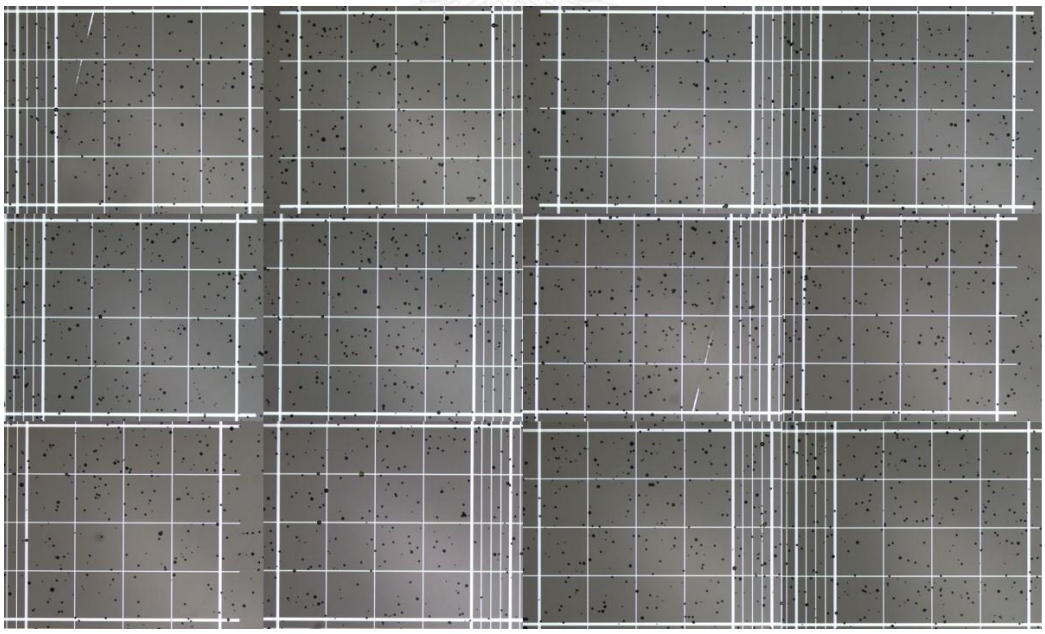

The expansion channel with 500 μm long at Re = 80

Control

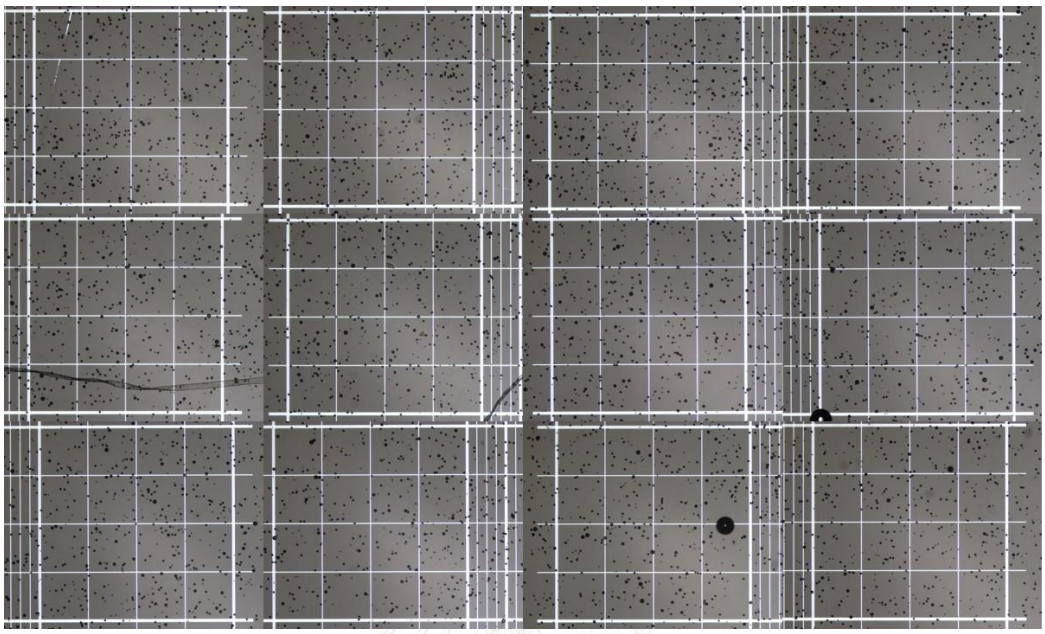

Main outlet

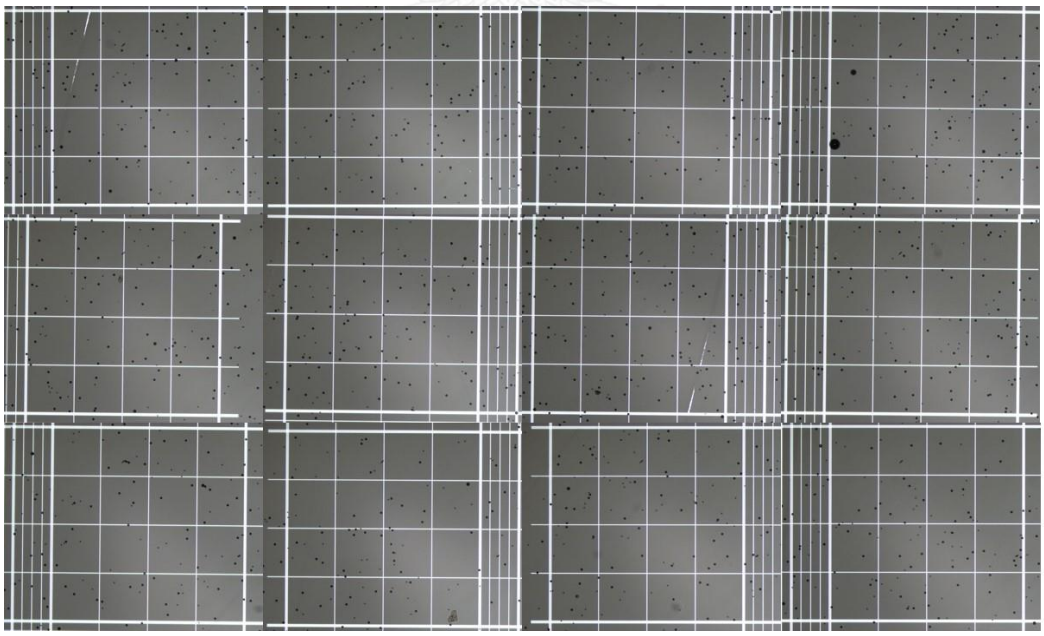

Secondary outlet

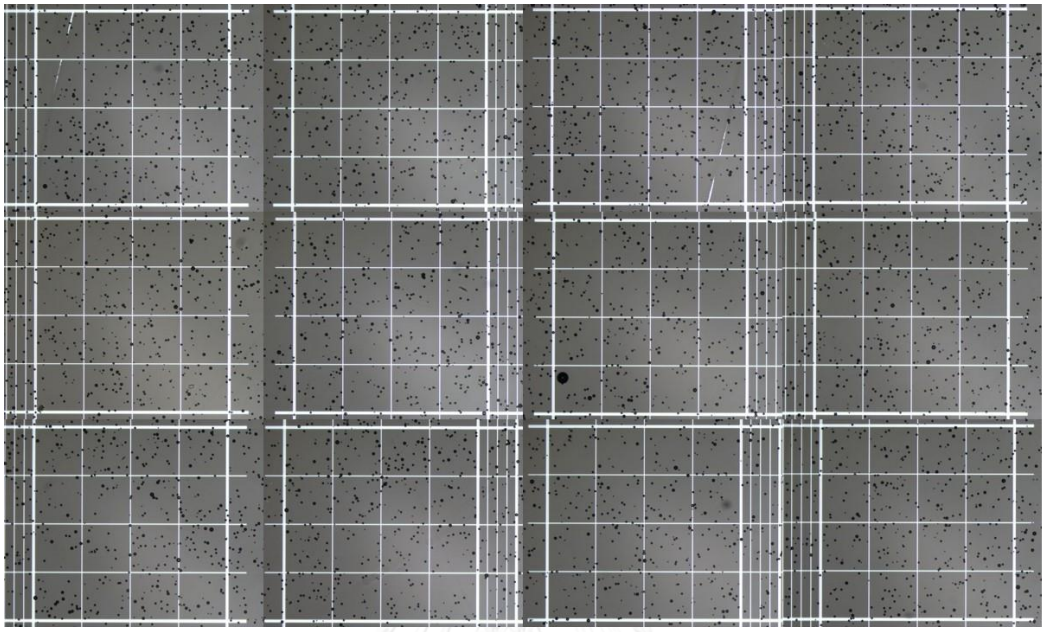

The expansion channel with 500 μm long at Re = 100

Control

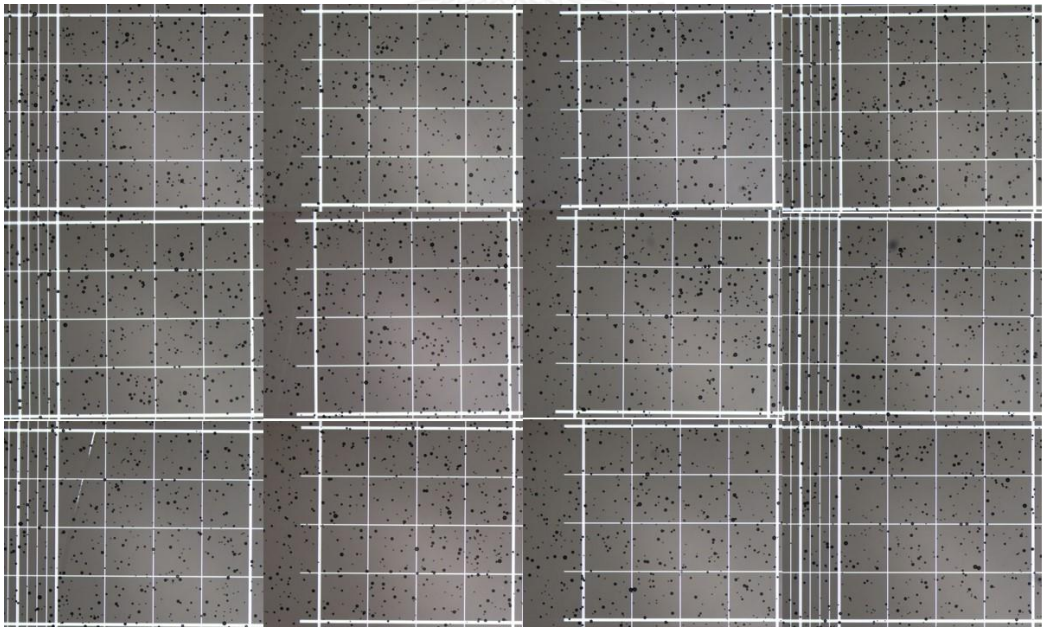

Main outlet

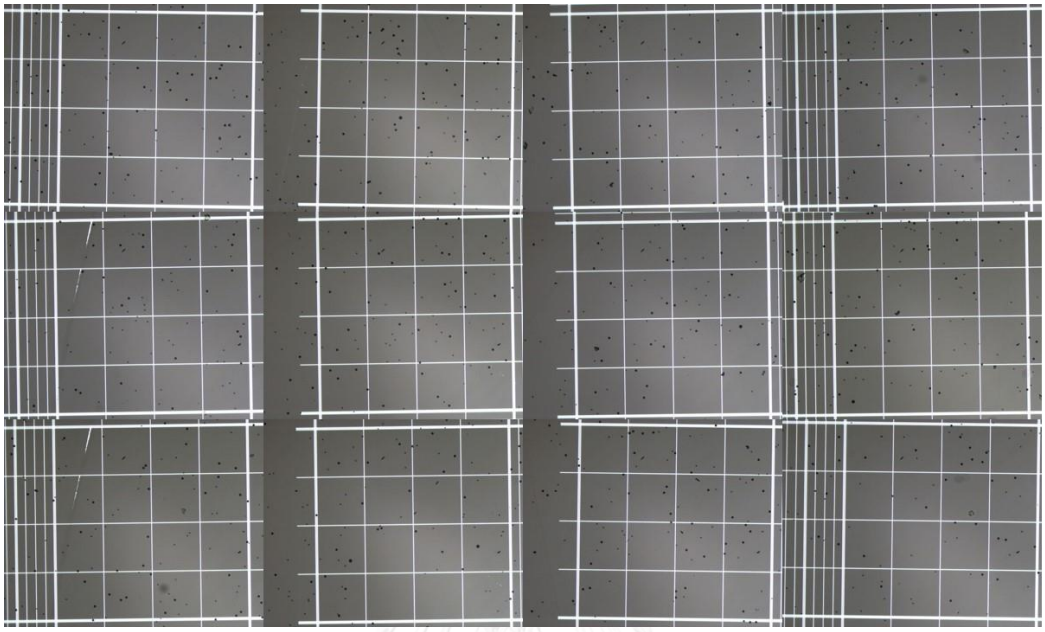

Secondary outlet

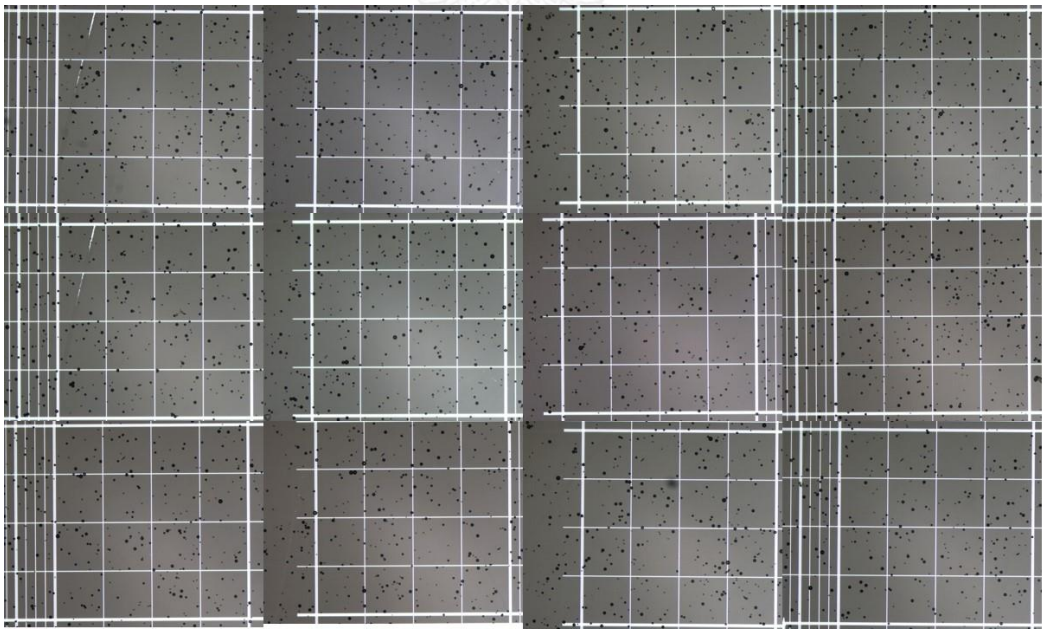

The expansion channel with 500 μm long at Re = 120

Control

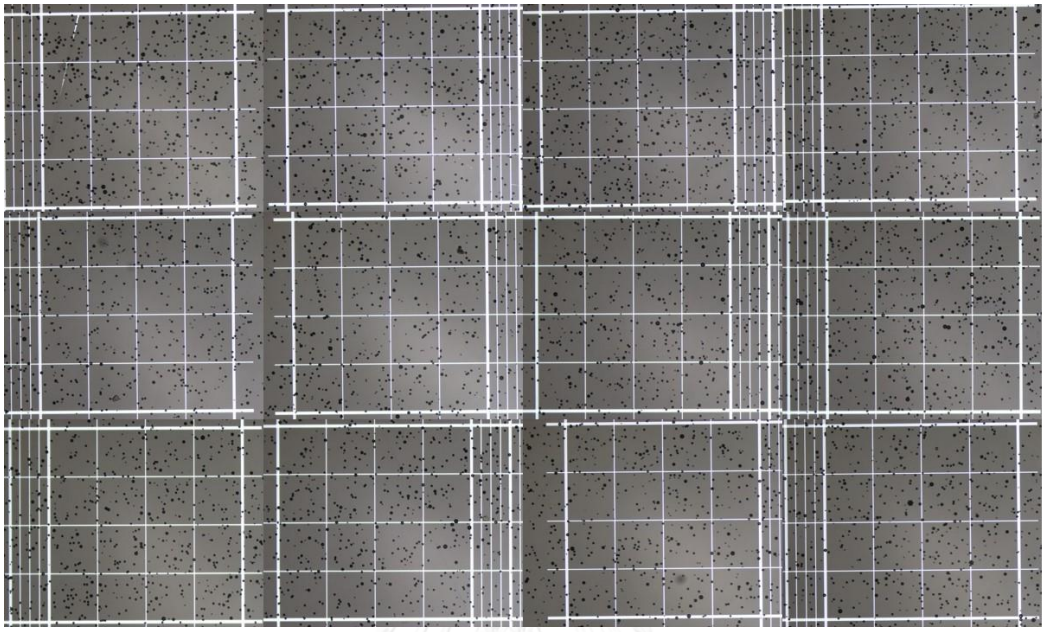

Main outlet

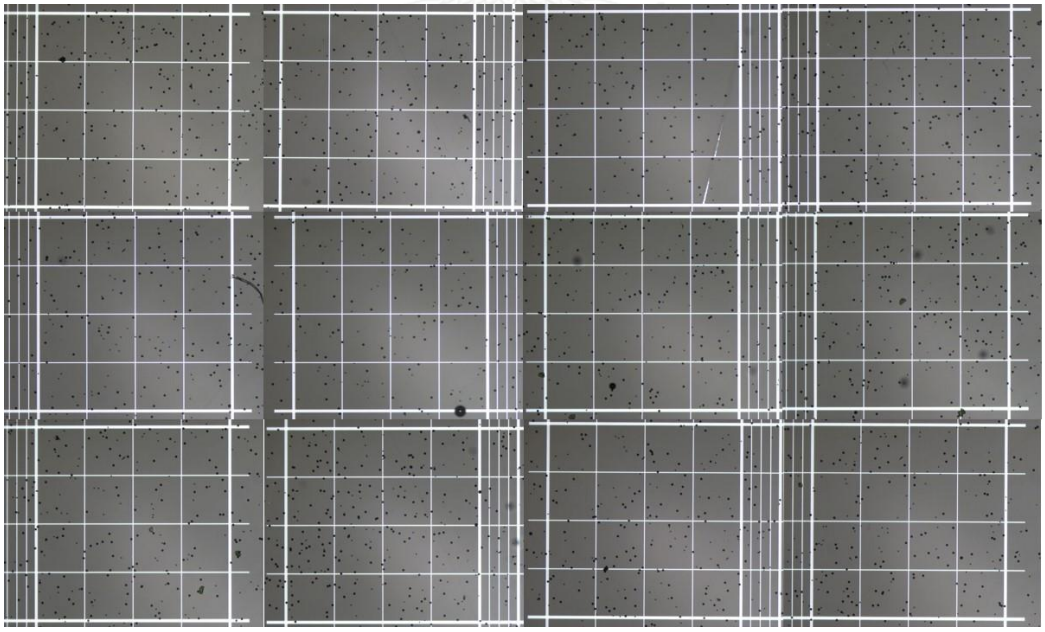

Secondary outlet

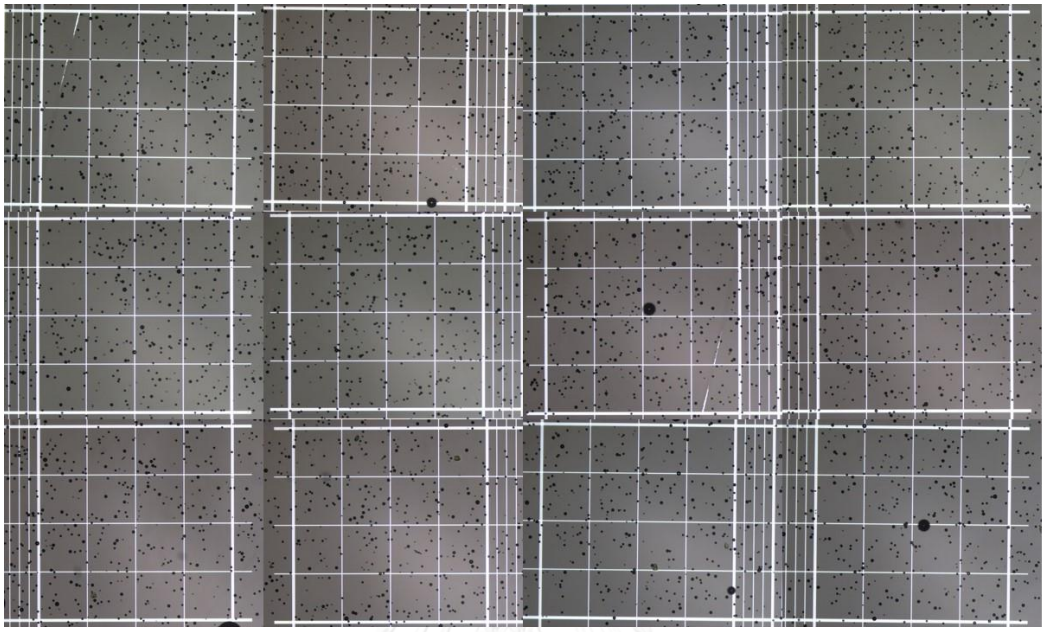

The expansion channel with 1000 μm long at Re = 40

Control

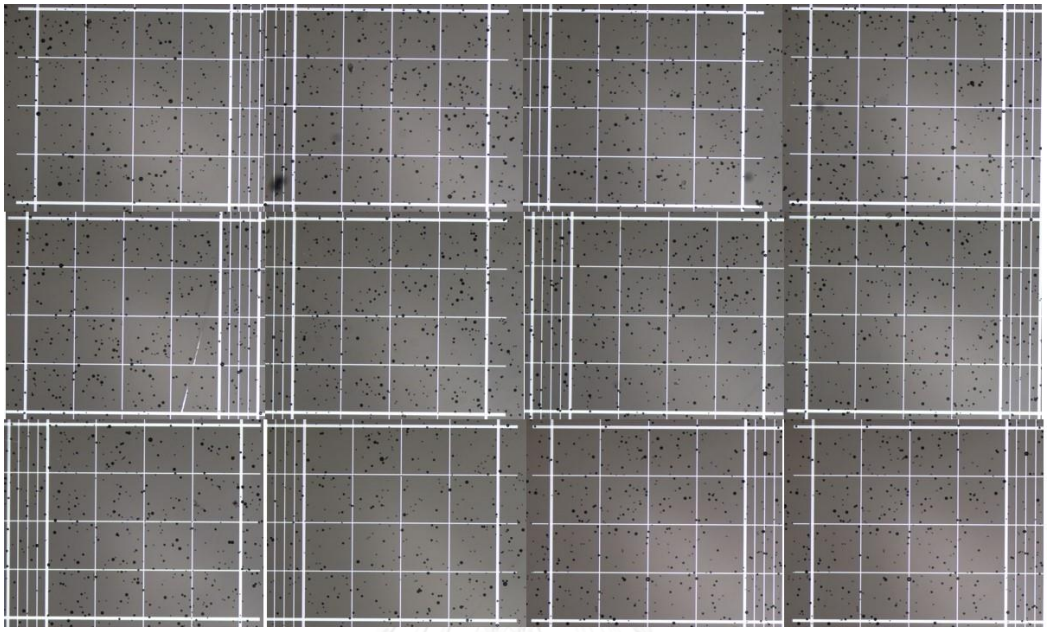

Main outlet

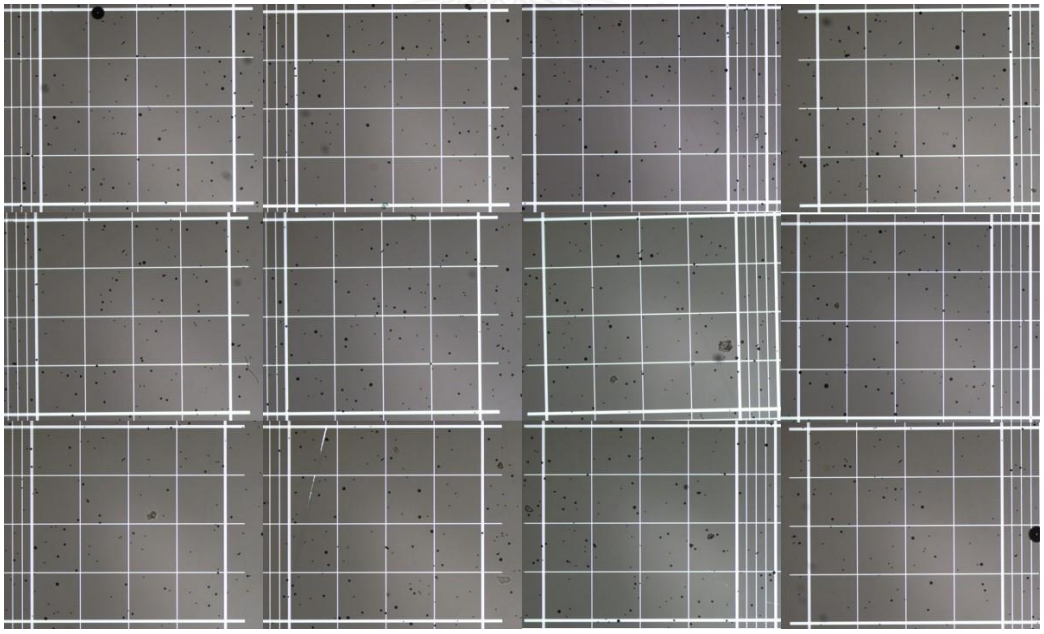

Secondary outlet

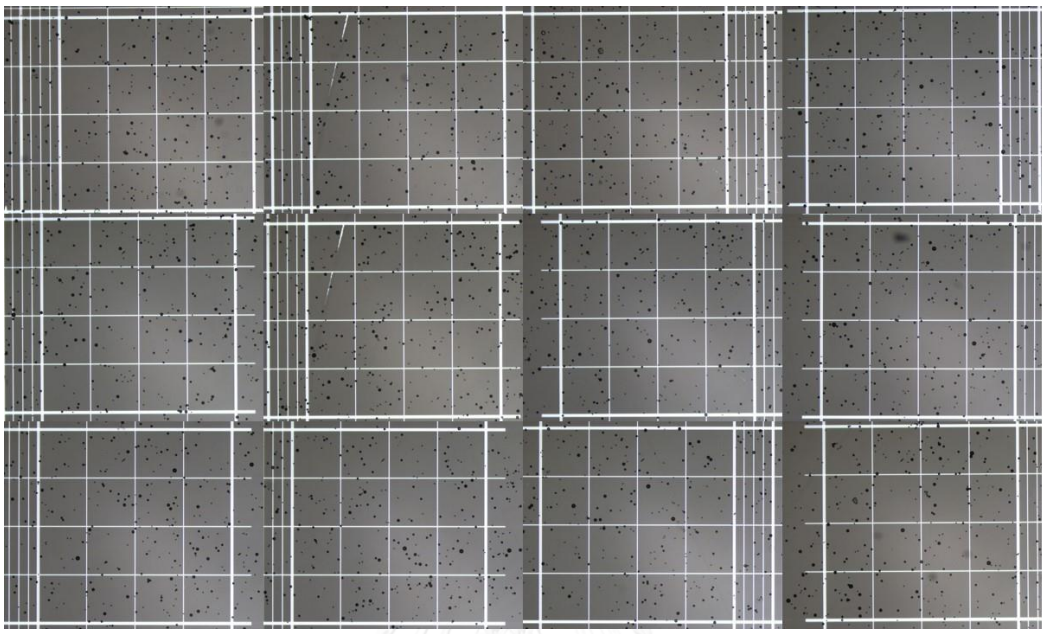

The expansion channel with 1000 μm long at Re = 60

Control

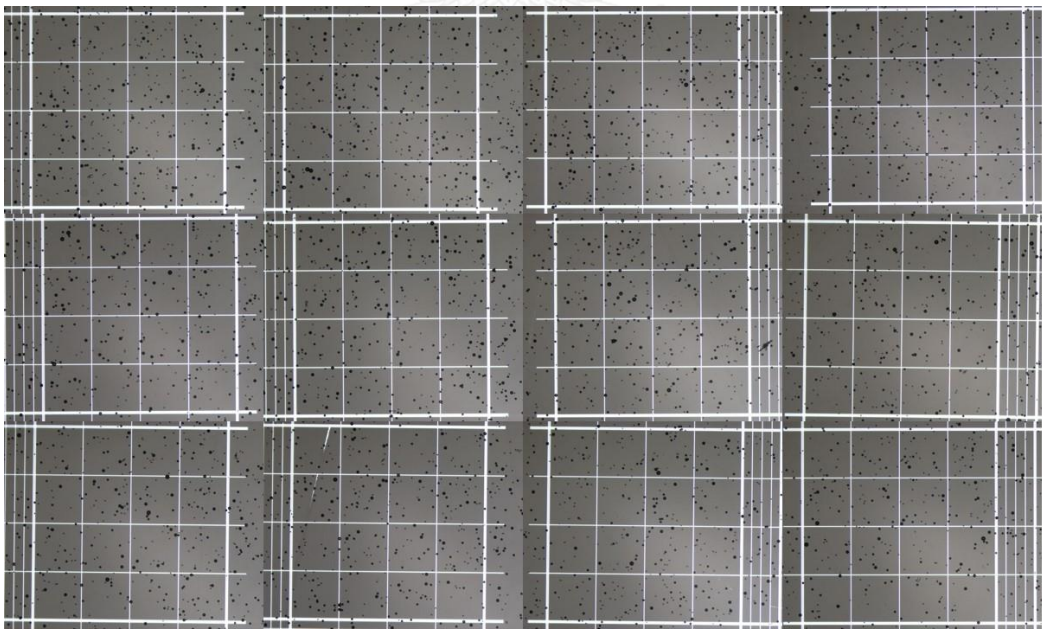

Main outlet

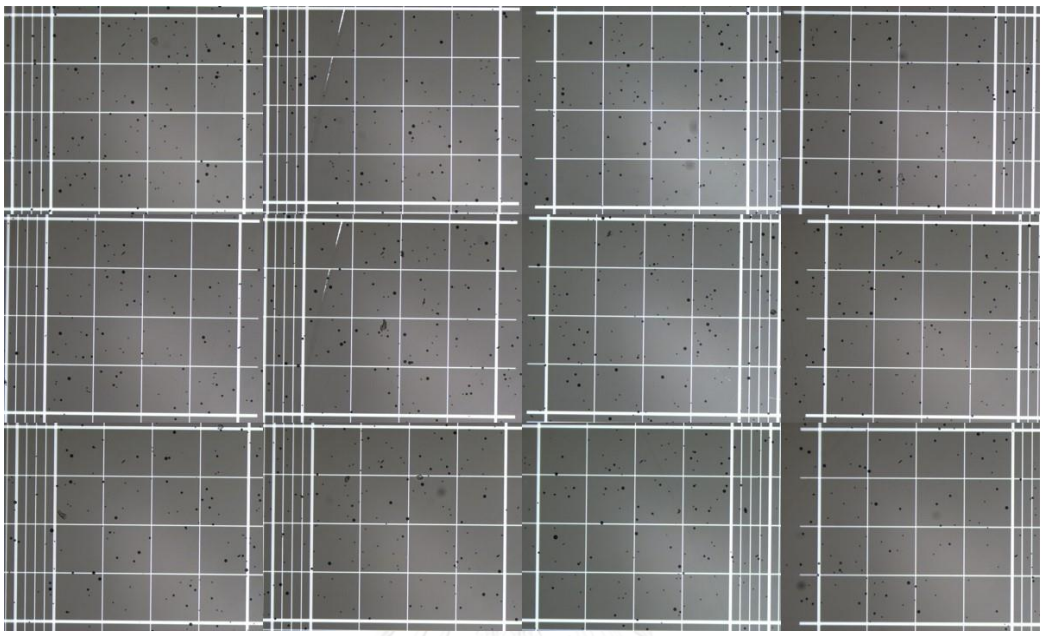

Secondary outlet

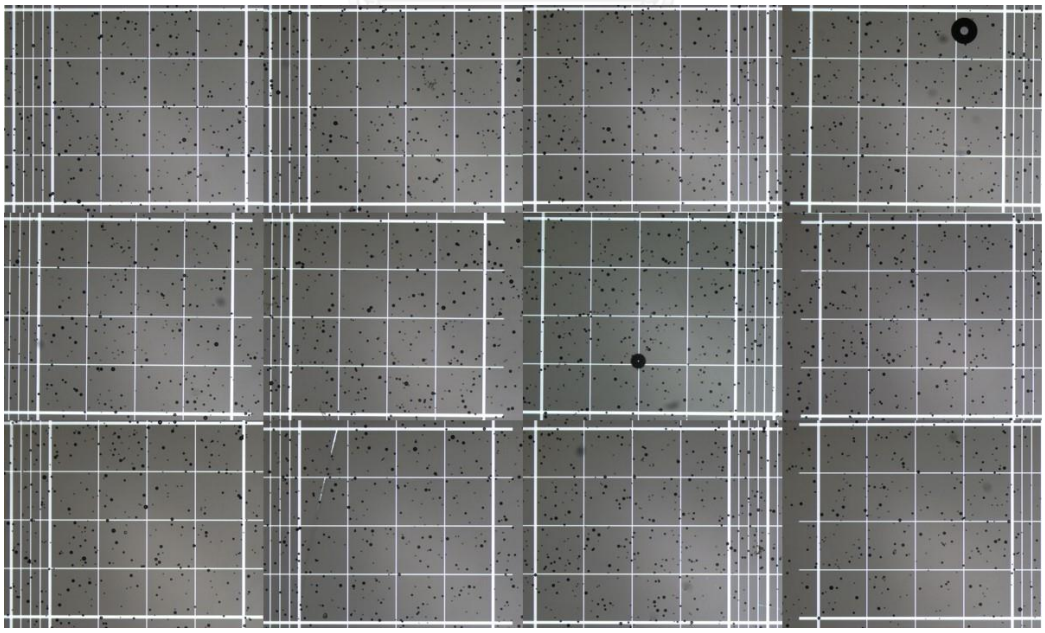

The expansion channel with 1000 μm long at Re = 80

Control

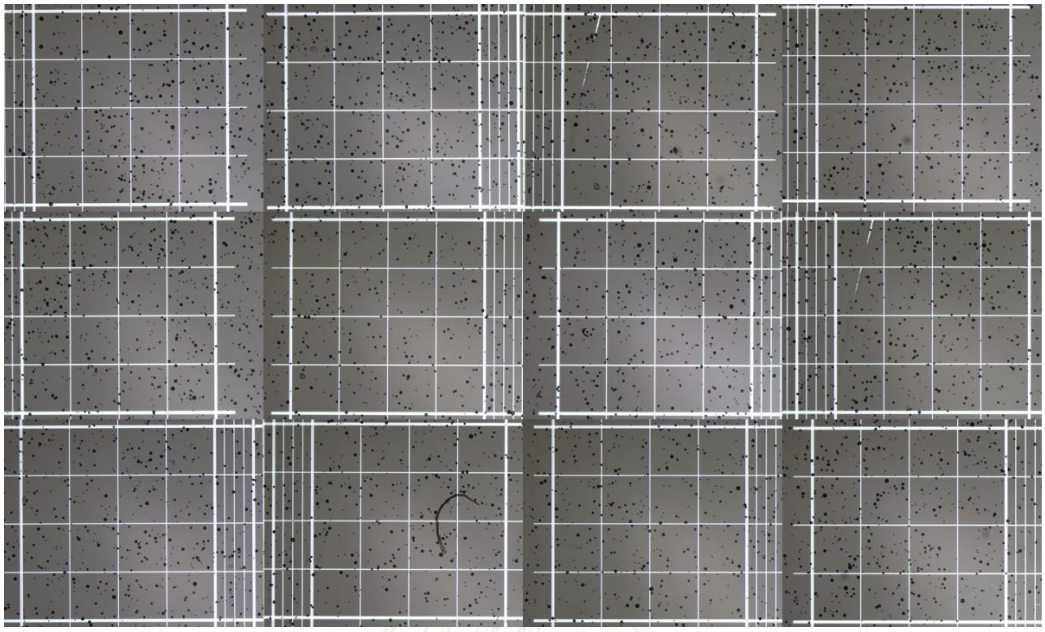

Main outlet

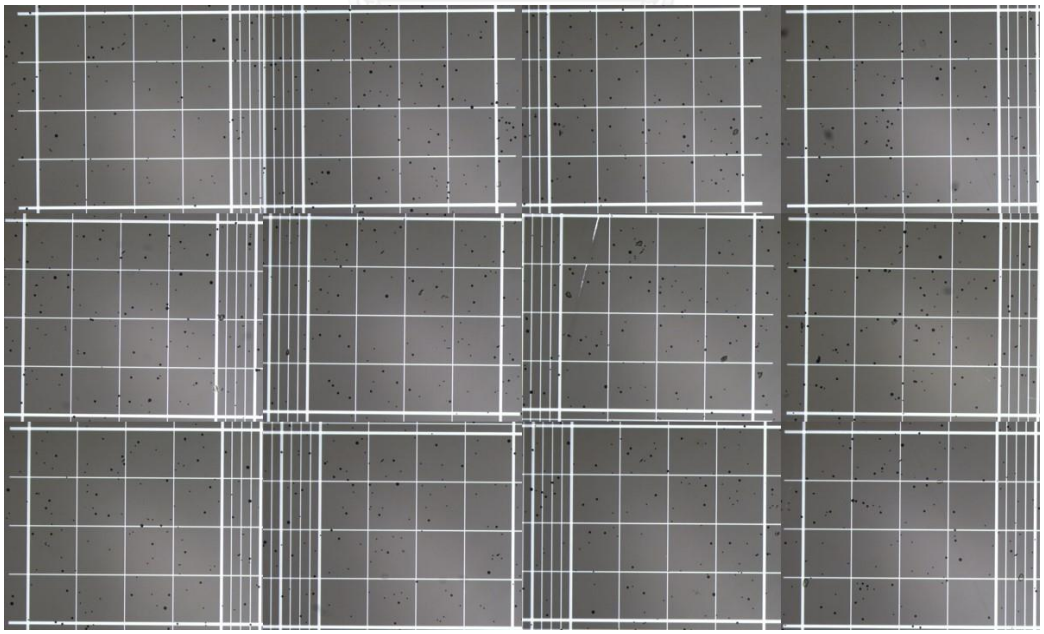

Secondary outlet

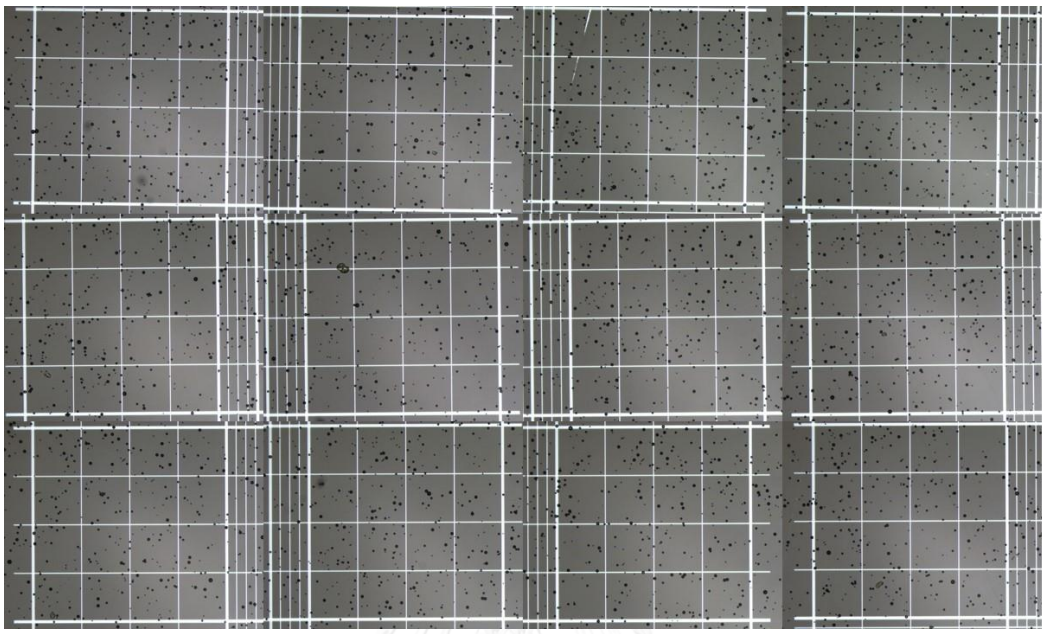

The expansion channel with 1000 μm long at Re = 100

Control

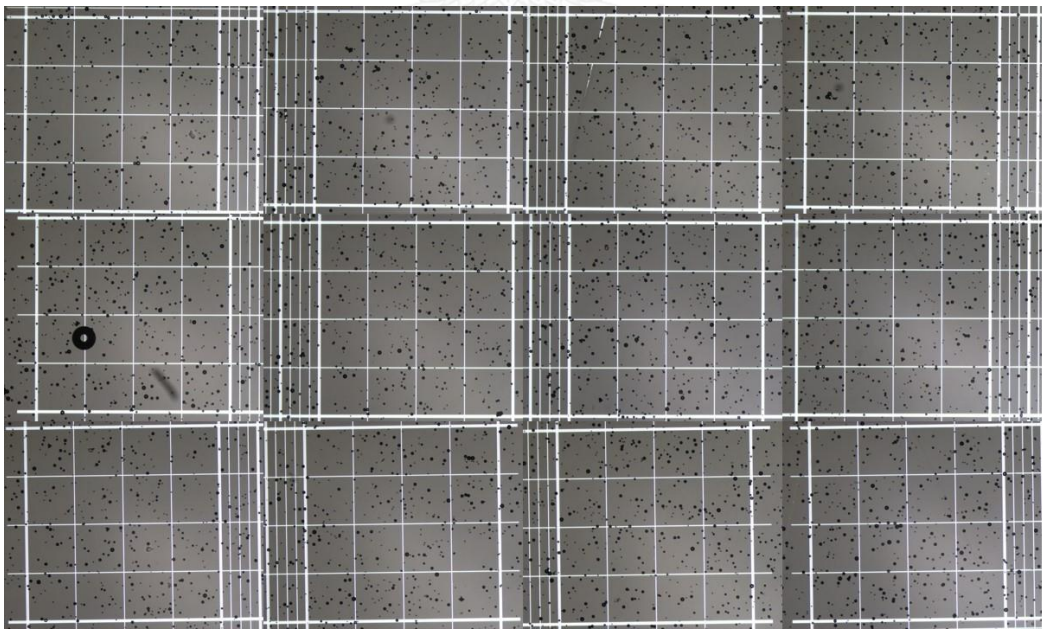

Main outlet

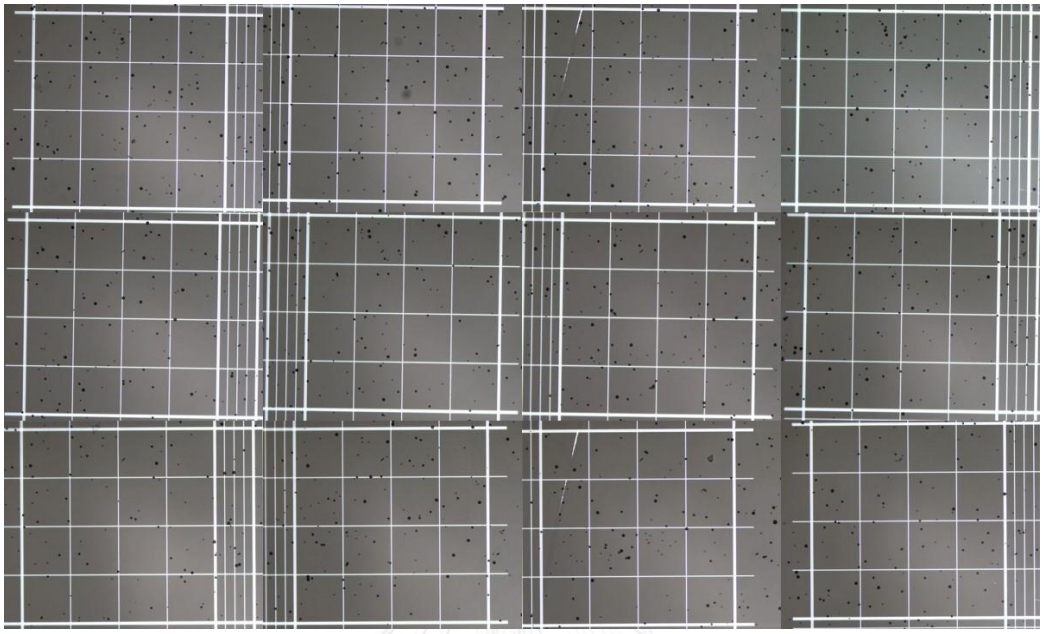

Secondary outlet

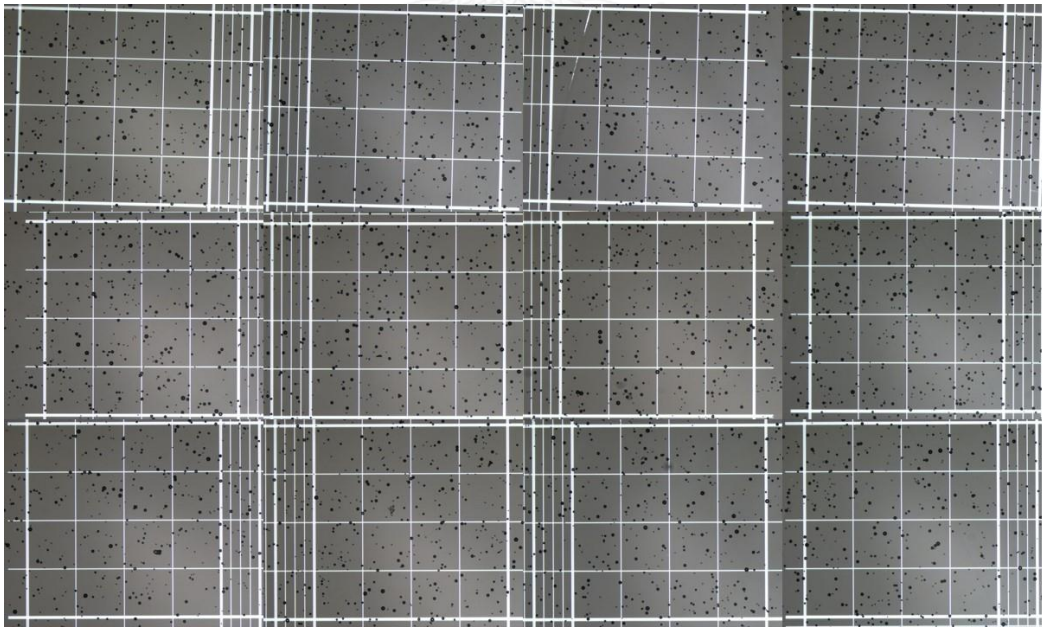

The expansion channel with 1000 μm long at Re = 120

Control

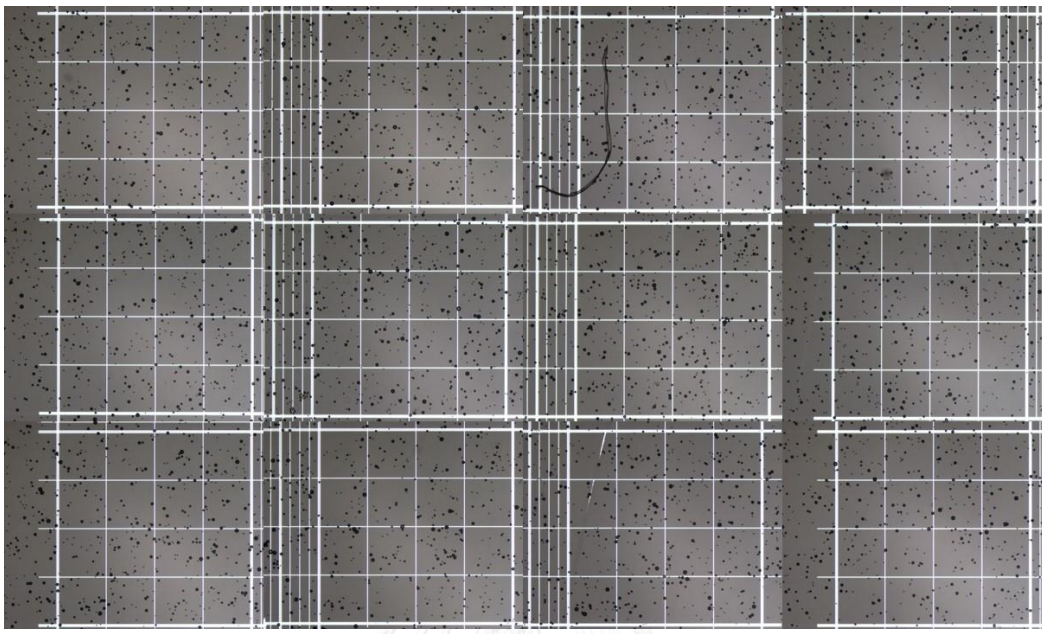

Main outlet

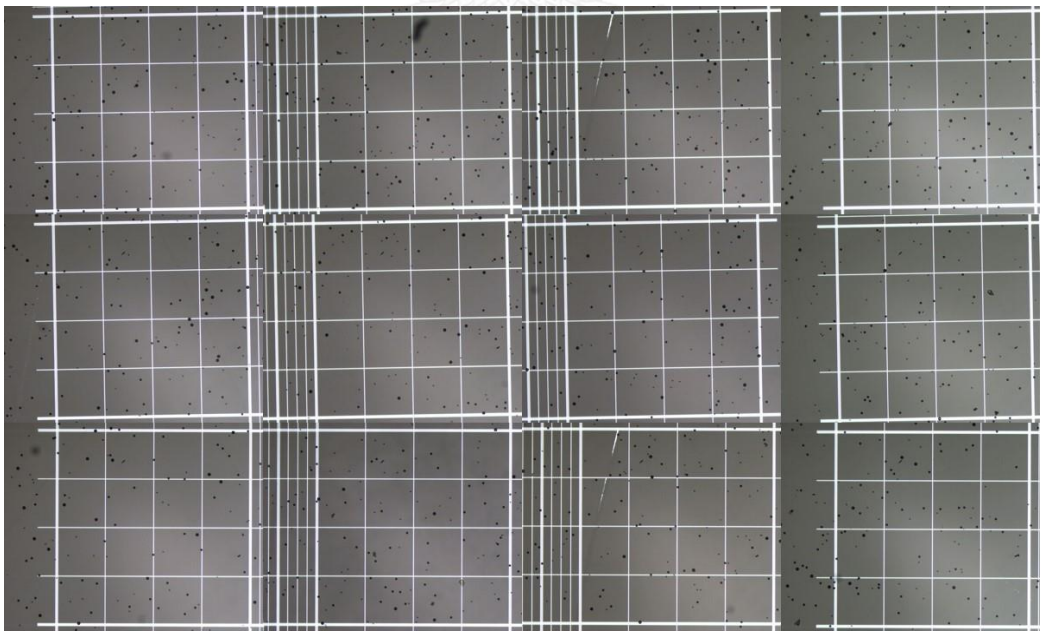

Secondary outlet

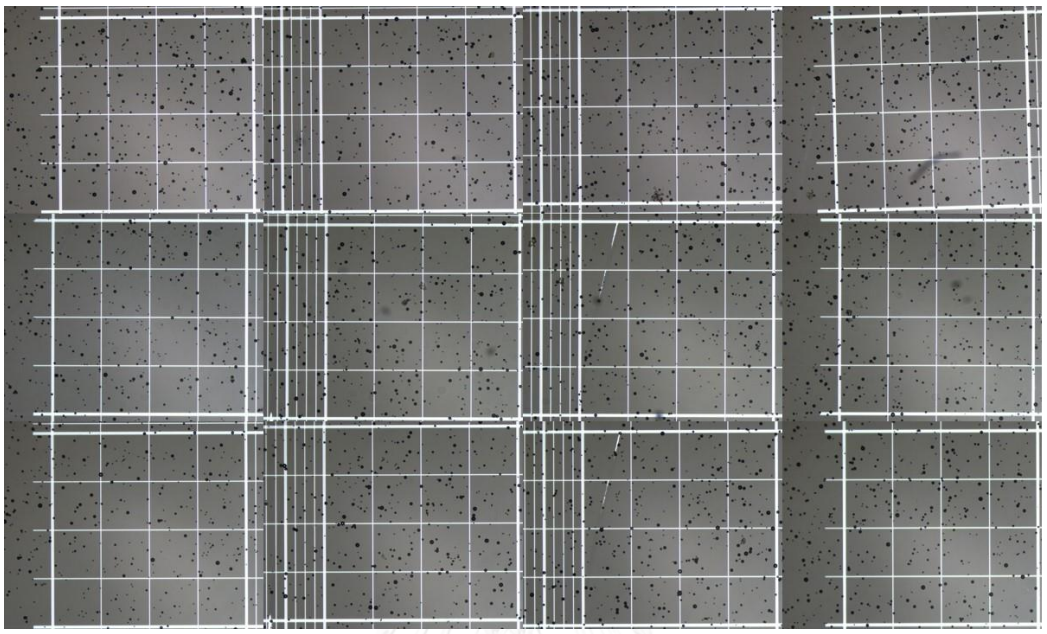

Whole blood experiments

Control

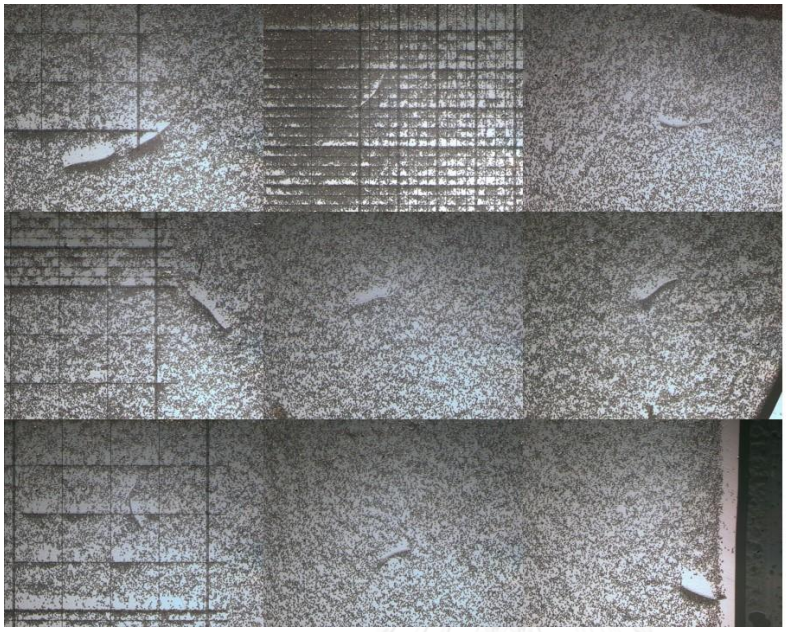

Control

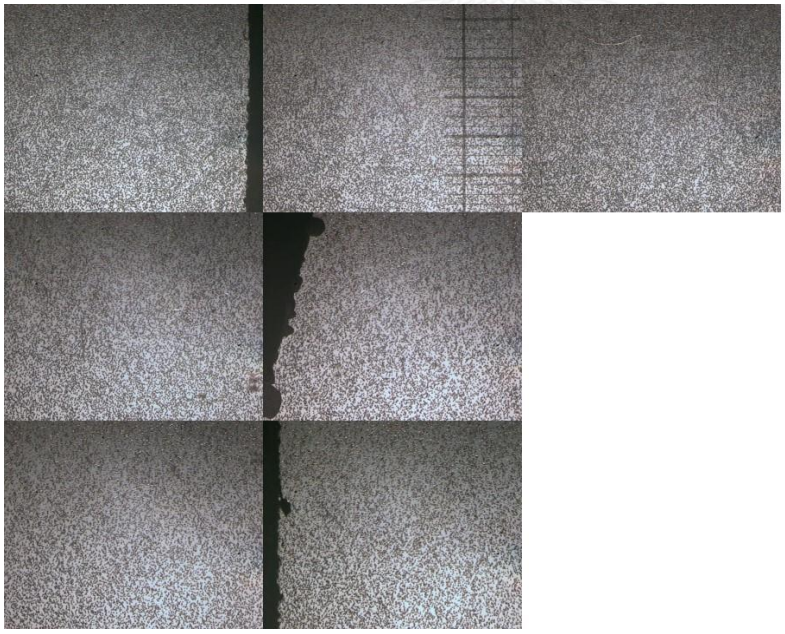

Control

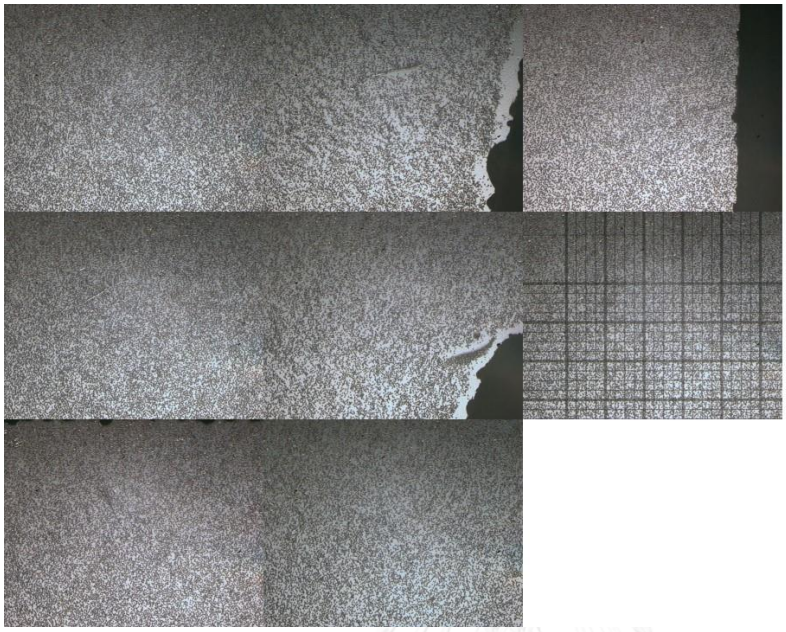

Control

Control

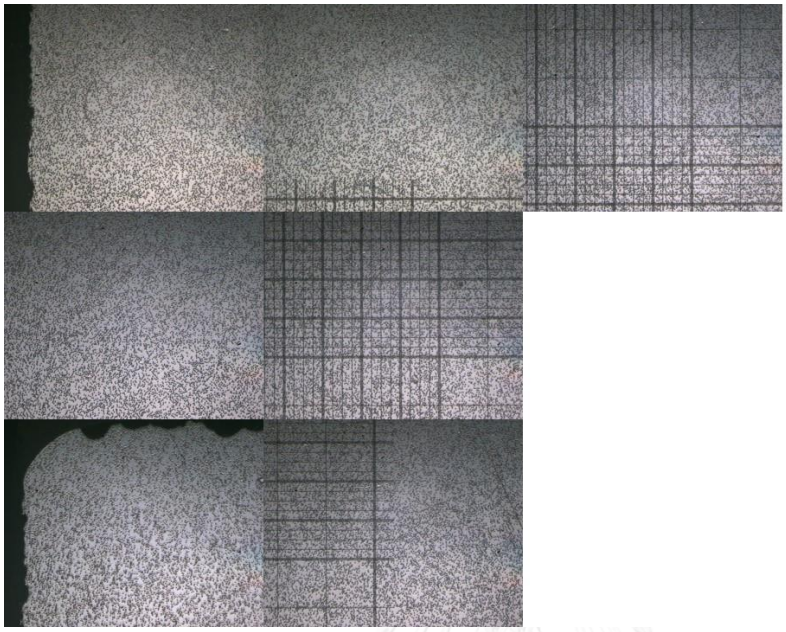

Control

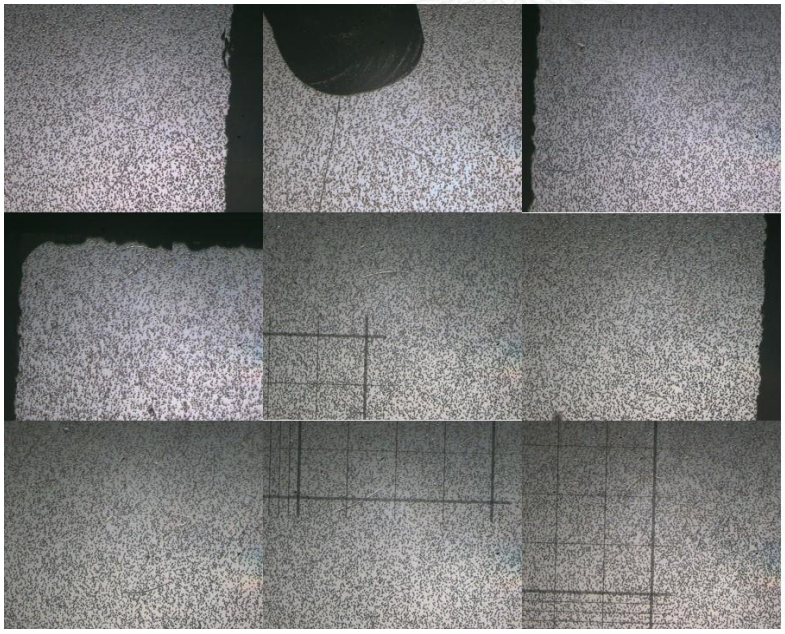

Main outlet

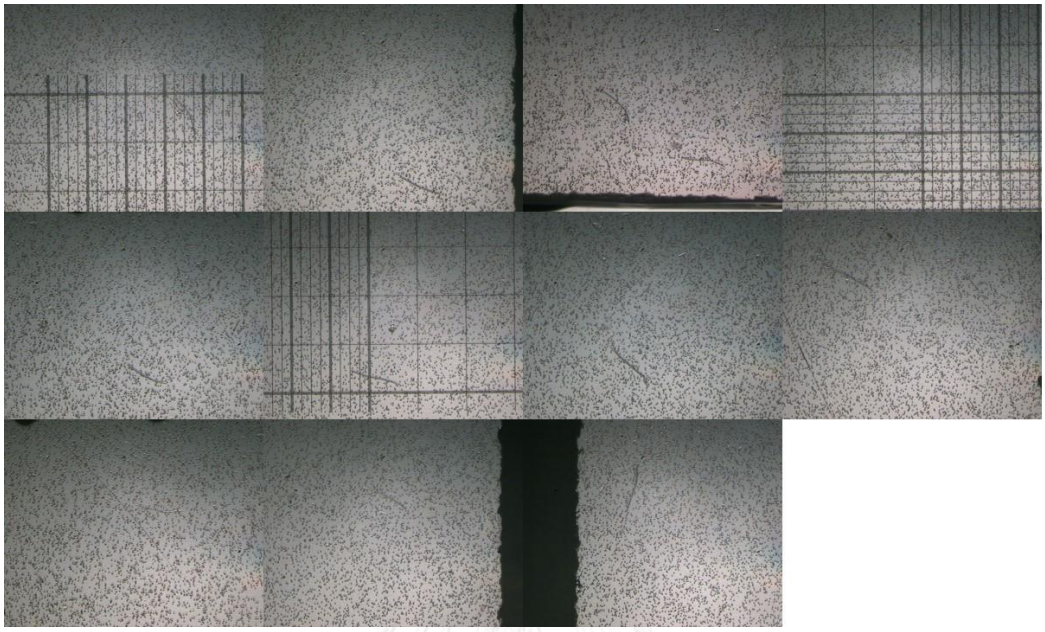

Main outlet

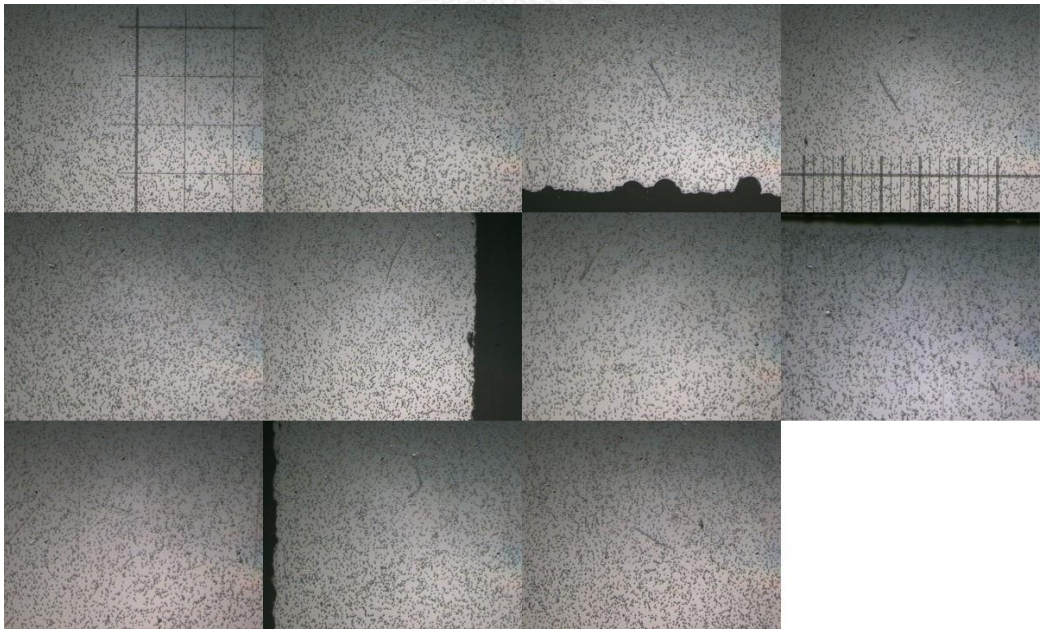

Main outlet

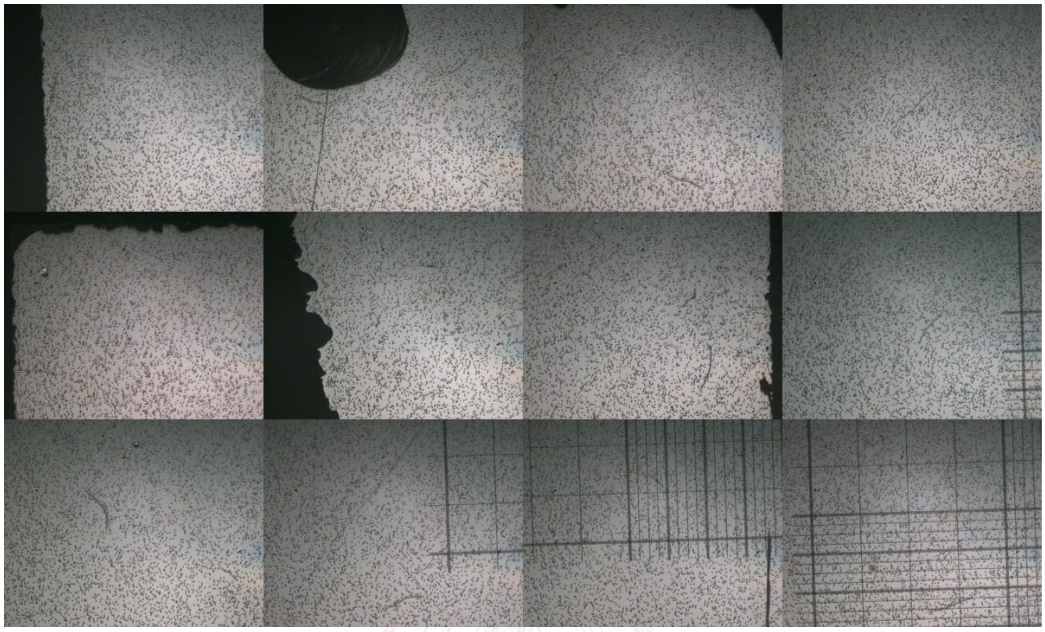

Main outlet

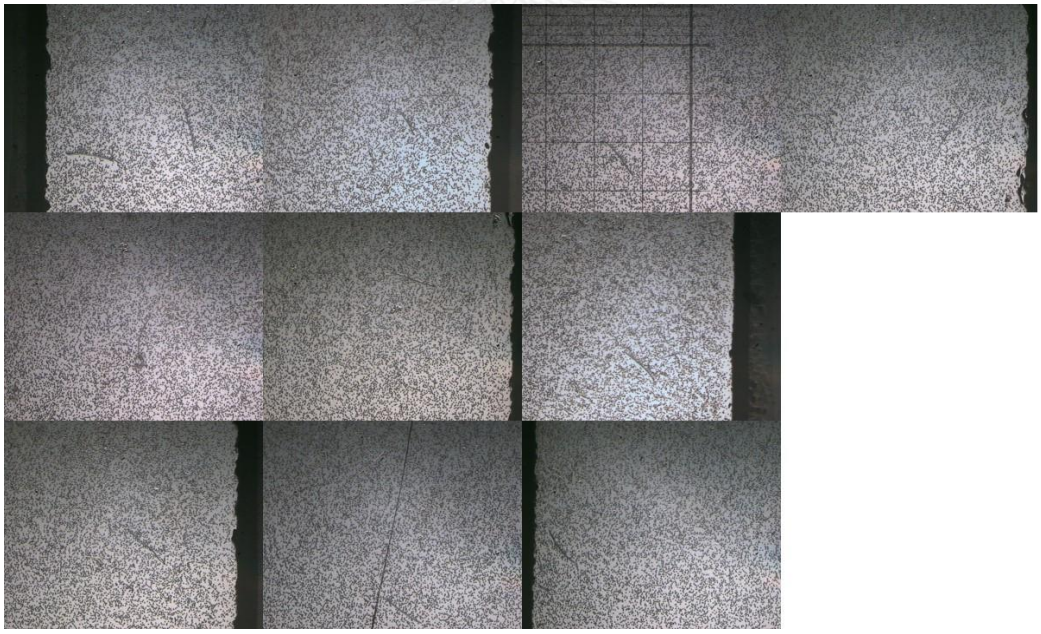

Main outlet

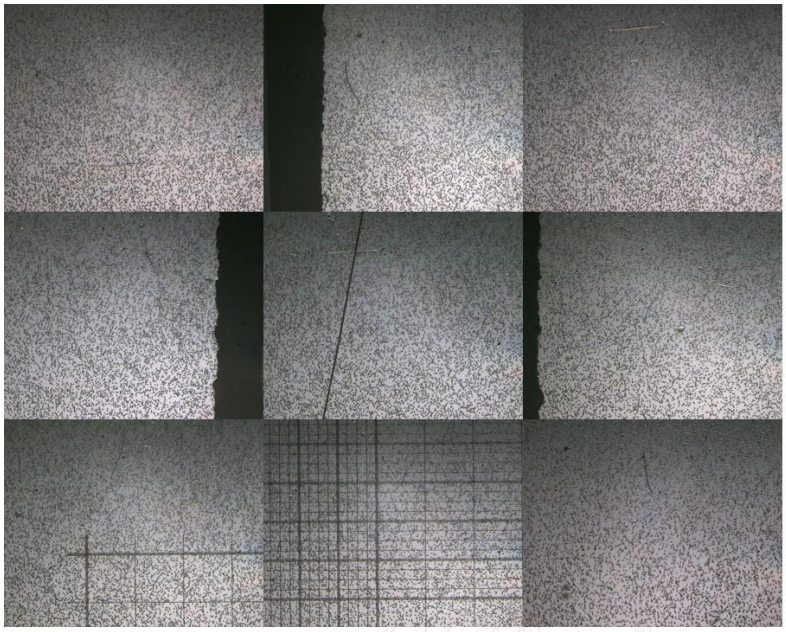

Main outlet

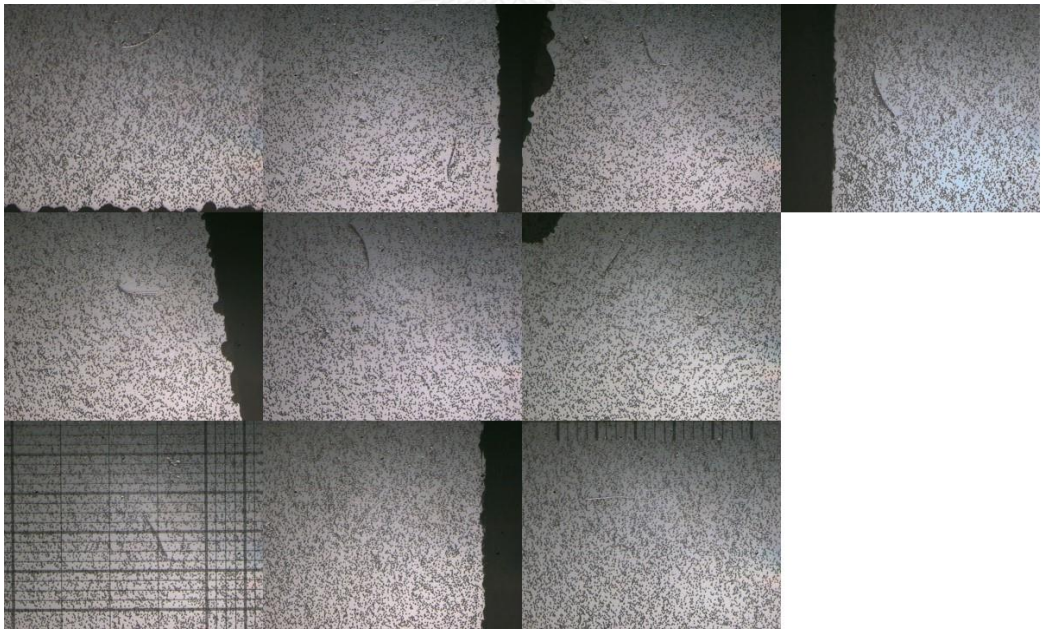

Secondary outlet

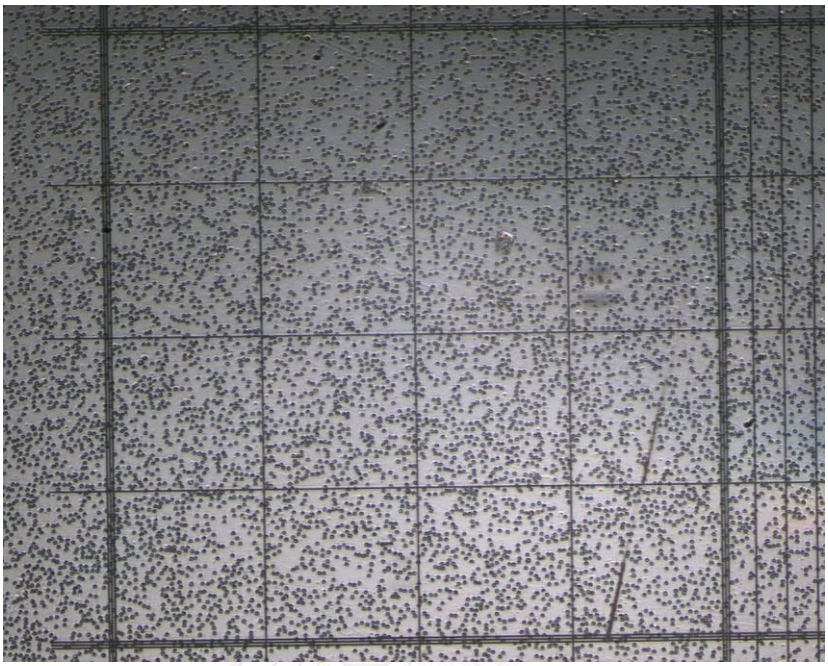

VITA

Saktip Uthongsap was born on May 27th, 1992 in Bangkok. He has one elder sister. He graduated from Saint Gabriel's College at high-school level in 2009 and Chulalongkorn University for Bachelor degree in Mechanical Engineering in 2014. After that, he continued his Master degree in Mechanical engineering at Chulalongkorn University and graduated in 2016.